

---

**EUSKAL HERRIKO UNIBERTSITATEA - UNIVERSIDAD DEL PAIS  
VASCOMATERIALEN FISIKA SAILA - DEPARTAMENTO DE FÍSICA DE  
MATERIALES**

eman ta zabal zazu



Universidad  
del País Vasco

Euskal Herriko  
Unibertsitatea

# **Design of Ancestral Enzymes for Engineering Nanobiomaterials**

**Leire Barandiaran Larrea**  
PhD Thesis

Thesis supervisors:  
**Dr. Raul Perez Jimenez**  
**Dr. David de Sancho**

2019



---

# SUMMARY

---

Nanomaterials have attracted scientific community attention as they have unique characteristics due to their increased specific surface area by volume. Two of the most interesting nanomaterials are nanocellulose and nanochitin, which are obtained from biomass, being biocompatible, biodegradable and renewable. These properties make them very promising biomaterials in biomedicine and pharmacology. But the obtention and modification of these materials still implies chemicals and processes that endanger their biocompatibility and sustainability, so a new method for their non-invasive and sustainable obtention is needed. Enzymes showed up as an alternative to nowadays methodologies for these nanomaterial engineering, nevertheless implementation of enzymes in material science is still a challenge, as enzymes need to fulfill harsh condition environments and improve their hydrolysis yields in comparison with chemical methodologies obtention yields. To obtain biocatalysts with improved performance at industrial conditions several strategies such as *de novo* enzyme design and directed evolution have

---

been implemented. But we need to improve several catalytic properties of enzymes (catalytic efficiency, pH and T range.) in a cost-efficient manner. Here we used Ancestral Sequence Reconstruction (ASR), to successfully reconstruct biomass-degrading enzymes. The reconstruction of ancestral enzymes is carried out from an extant enzyme, the one we call Query.

We have improved a set of enzymes that can hydrolyze cellulose and chitin in a wide range of conditions. The activity of these reconstructed enzymes was compared to the Query. We reconstructed a  $\beta$ -1,4 Endo xylanase and a Lytic polysaccharide monooxygenase (LPMO) to, in combination with an ancestral endoglucanase (Anc EG), boost nanocellulose obtention yields from lignocellulosic biomass, and even modifying its structure. To consolidate the capability of enzymes to obtain nanomaterials from biomass we reconstructed a chitin degrading LPMO and obtain nanochitin. In all cases, ancestral enzymes showed considerably higher specific activities than modern enzymes.

---

# LABURPENA

---

Azken hamarkadetan material berrien garapenean hobekuntza handia ekarri du nanoteknologiak, besteak beste, nanomaterialen sorreran. Azken horien artean nabarmenenak nanozelulosa eta nanokitina dira: lehena zelulosatik eratortzen da eta bigarrena kitinatik, eta biak biomasan dauden elementurik oparoenak dira. Biomasiatik eratorritako nanomaterial hauek berezi egiten dituzten ezaugarri batzuk dituzte: biobateragarritasuna eta jasangarritasuna. Lehena garrantzitsua da biomedikuntzan ezartzen diren materialekiko osagarria delako; bigarrena, hondakin organikoetatik erator daitekeelako: nanozelulosa hondakin lignozelulosikoetatik, eta nanokitina krustazeoen hondakinetatik besteak beste.

---

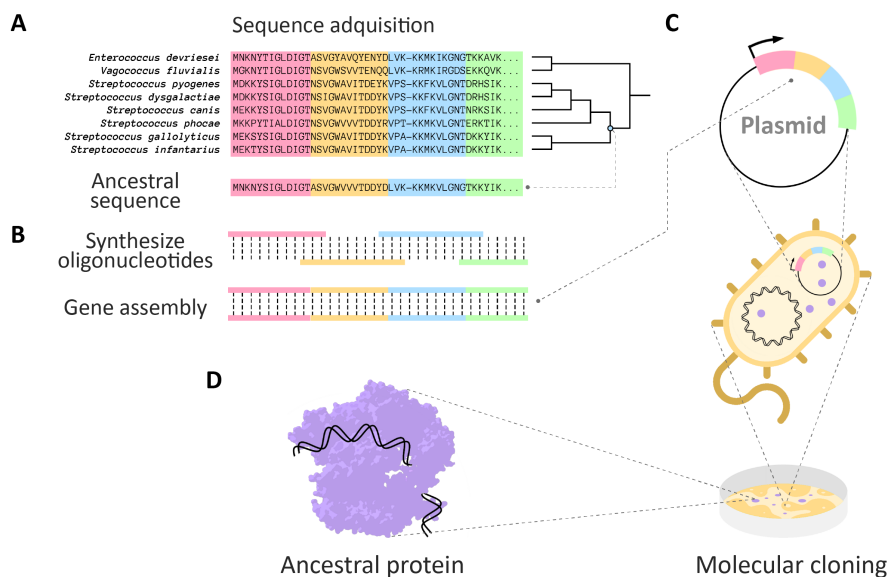
Material lignozelulosikoa hiru osagaiz osatuta dago: lignina, hemizelulosa eta zelulosa. Lehena molekula aromatikoz sortuta dagoen material rekalzitrantea da; bigarrena, pentosaz eta hexosaz sortutako polisakaridoa; eta, azkena, D-glukosaz osatutako polisakaridoa. Lehen bien artean hidrogeno loturak egin eta Van der Waals indarrak sortzen dira, zelulosa kokatzen den sare konplexu bat sortuz. Azken hau isolatu ahal izateko, ezinbestekoa da beste bi osagaietatik askatu ahal izatea.

Hondakin hauetatik nanomateriala isolatzeko orain arteko prozesuek, kimikoak erabiltzeaz gain, materialen egitura kimikoa eraldatzen dute. Ordea, materialak organikoak izaki, entzimak erabil daitezke haien hidrolisirako eta, beraz, nanomateriala lortzeko.

Entzimek izaera oso selektiboa dute eta jatorriko baldintza naturaletan bakarrik egiten dute lan. Beraz, helburua industrian lan egingo duten entzimak lortzea bada, lanerako baldintza gogor horiek jasango dituzten entzima berriak sortu behar dira. Aipatzekoa da ikergai honek duen berebiziko garrantzia. Ez zioten, ausaz, iazko Kimika Nobel saria gai hau landu zuen F. Arnoldi eman. Hala ere, orain arte garatu diren entzima bidezko metodoek (directed evolution, rational design), garestiak izateaz gain, denbora gehiegi hartzen dute eta entzimaren ezaugarrietatik bakarra hobetzen dute. Gure laborategiak, ordea, azken urteetan eboluzioa ikertzeko erabili den ARS metodoak entzima horiek berreraikitze balio dezakeela erakutsi du (1.irudia).

Metodo horrek egungo espezie askoren proteina beraren sekuentziak alderatu eta haien arteko harremana aztertzen du, zuhaitz filogenetikoak sortuz. Horrela, eta método bioinformatikoa erabiliz, espezieen arbasoen proteina-sekuentziak jakin ditzakegu. Gehien bat bakteriekin egiten dugu

lan hori, denboran are atzerago egitea ahalbidetzen digutelako, prekanbrikora iritsi arte. Garai hartako bizi-baldintzak oraingoak baino askoz ere latzagoak ziren (itsas-tenperatura 60-70 gradukoa zen, adibidez), eta beraz, espezieak extremofiloak. Halako ezaugarriak dituzten proteinak birsortu ditugu gure laborategian, biologia molekularra erabiliz, eta industria-baldintzetan lan egin dezaketela frogatu.



*1. irudia: Antzinako entzima bat eraikitzekeo burutu behar diren pausoak. A) ASR metodo bioinformatikoen bidez antzinako entzimaren sekuentzia lortu. B) Antzinako entzimaren genea sintetizatu. C) Entzimaren genea expresio bakteriar batean sartu ingenieritza genetiko teknikak erabiliz. D) Antzinako entzima laborategian purifikatu.*

Horretarako, lehenik, endoglukonasa berreraiki eta nanozelulosa laborategiko sustratu idealetatik lortu ahal izan dugu. Jarraian, sustratu

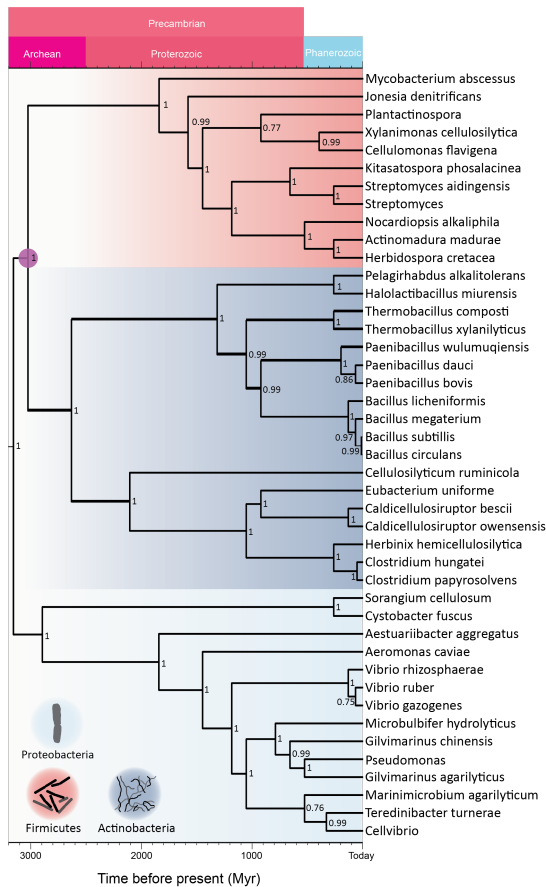
---

errealetatik, hau da hondakin izan daitezkeenetatik, nanozelulosa isolatzeko Xylanasa eta LPMO (Lytic Polyssacharide Monooxygenase) entzimen laguntza behar dugu. Xylanasari dagokionez, *Bacillus subtilisen* Endo b 1,4- xylanasatik abiatuta, 3 mila milioi urteko xylanasa bat lortu dugu. LPMOaren kasuan, *Streptomyces viridisporusen* LPMO batetik abiatuta 2.8 mila milioi urteko aitzin-entzima bat (2.irudia). Ondoren, entzima berreraiki hauen ezaugarriak karakterizatu ditugu gure laborategian, jatorrizko entzimekin konparatuz, eta antzinakoek propietate termiko, pH- eta kinetiko hobekak aurkeztu dituzte: esaterako, horietako zenbaitek aktibitatea mantentzen dute temperatura 12 gradu igota ere. Prekambriko garaiko ingurugiro baldintzekon bat eginez.

Hurrengo pausua nanozelulosa hondakin lignozelulosikoetatik lortzea izan da, BKP (Bleached Kraft Pulp) eta UBKP (Unbleached Kraft Pulp) sustratuetatik, zeintzuek, zelulosaz gain, lignina eta hemizelulosa ere baduten. Antzinako entzima berreraikiekin nanomaterial gehiago lortu dugu eta, gainera, LPMOak modu oxidatzailean lan egiten duenez, lehen aldiz nanozelulosa oxidatua lortu dugu, entzimen erabilera hutsarekin.

Amaitzeko, entzimen erabilera biomasan oparoen aurkitzen den bigarren materialarekin ere frogatu nahi izan dugu: kitinarekin. Kitina modu hierarkiko batean ordenatuta dagoen N acetyl glukosaminaz osatutako polisakarido bat da, modu hierarkiko batean ordenatzen diren zuntzak osatuz. Naturalki duen ordenazio horrek zuntz handietatik txikienetara kitina eskala txikitzen joatea ahalbidetzen digu, nanokitina lortu arte.

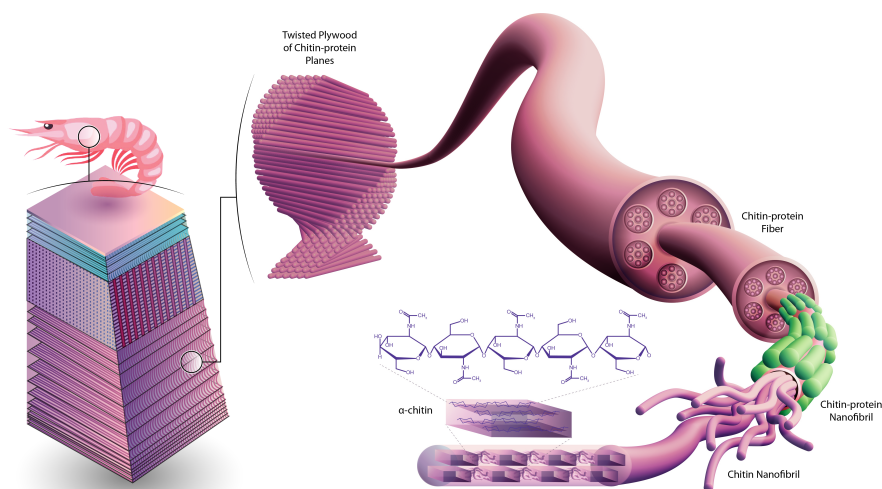




2. irudia: zuhaitz filogenetiko. Zuhaitz honetan Aktinobakteria, Firmikutes eta Proteobakteria filoen LPMO sekuentziak konparatzen ditugu zuhaitz filogenetiko lortzeko. Geroago, nodoa aukeratu eta anztinako entzima eraikiko dugu.

Industrian prozesu azido, mekaniko zein termikoen bitartez egiten da prozesu hau, nanobiomaterial honen biobateragarritasuna zalantzan jarriz. Horregatik, tesi honetan, eta aurretik egindako lana bermatzeko, kitina hidrolizatzen duen aitzin-entzima bat berreraiki dugu: 2,8 mila milioi urtetako *Bacillus thurigiensis* bakteriaren LPMO entzima. Laborategian bere aktibitatea gaur egungo bere baliokidearekin alderatu

dugu eta berreraikiak, besteetan bezala, temperatura, pH eta kinetika hobe aurkeztu du, nanokitina ekoizpena handitzearekin batera.



*3. irudia. Kltinaren egitura. Kitina, bigarren material oparoena biomasa krustazeoen exoeskeletoak aurkitzen da besteak Beste. Irudian bere ordenazio hierarkikoa nabarmentzen dugu, fibra handietatik, makrofibrak, fibra txikienera, nanofibrak.*

Lan honetan, antzin-entzimek industrian lan egiteko duten balioa azpimarratu nahi izan dugu: hondakin lignozelulosikoetatik nanozelulosa atera daitekeela erakutsi dugu, xylanasa eta LPMO entzimen antzin-berreraikitzea eginez.





---

# INDEX

---

<b><i>SUMMARY</i></b>	<b>3</b>
<b><i>LABURPENA</i></b>	<b>5</b>
<b><i>Chapter 1 Introduction</i></b>	<b>19</b>
<b><i>Objectives</i></b>	<b>43</b>
<b><i>Chapter 2: Phylogenetic analysis and ASR</i></b>	<b>47</b>
<b>2.1 Introduction</b>	<b>48</b>
<b>2.2 Theory of phylogenetic analyses</b>	<b>49</b>
2.2.1 Methods	50
<b>2.3 Experimental Phylogenetic Analysis</b>	<b>54</b>
2.3.1 Select extant sequences: Uniprot and NCBI	55
2.3.1 Multiple sequence alignment: MUSCLE	57
2.3.2 Computing a phylogenetic tree	59
2.3.1 Reconstruction of ancestral sequences	65
<b><i>Chapter 3: Experimental methods</i></b>	<b>68</b>
<b>3.1 Molecular biology</b>	<b>69</b>
3.1.1 Genetic engineering procedures	69
3.1.2 Protein production	74
3.1.3 Protein purification	76
<b>3.2 Enzymatic Characterization assays</b>	<b>80</b>
3.2.1 Xylanase characterization	81
3.2.2 LPMO characterization	85
3.2.3 Reconstructed enzymes synergy	89
3.2.4 CNC isolation and Characterization from BKP and UBKP	92
<b>3.3 New Nano biomaterial isolation</b>	<b>95</b>
3.3.1 Enzymatic nanochitin isolation	95
3.3.2 Nanochitin yields	96
<b>3.3 New Nano biomaterial characterization: CNCh</b>	<b>96</b>
3.3.2 Atomic force microscopy	96
3.3.2 Fourier-transform infrared spectroscopy	96
3.3.3 X-Ray diffraction	97
3.3.4 Solid-state cross-polarization magic angle spinning <sup>13</sup> C nuclear magnetic resonance	99
3.3.5 Thermogravimetric analysis	100
<b>4.1 Ancestral reconstruction of C-LPMO</b>	<b>105</b>

4.1.1 C-LPMO sequence analysis	110
<b>4.2 Ancestral reconstruction of Ch- LPMO</b>	<b>111</b>
4.2.1 Ch-LPMO sequence analysis	113
<b>4.3 Ancestral reconstruction of Xln</b>	<b>114</b>
4.3.1 Ancestral Xln sequence analysis	116
<b><i>Chapter 5: Xylanase production and characterization</i></b>	<b><i>118</i></b>
<b>5.1 Xylanase Production and purification</b>	<b>119</b>
<b>5.2 Arabinoxylan</b>	<b>120</b>
5.2.1 Temperature	121
5.2.2 pH	123
5.1.3 Kinetics	124
<b><i>Chapter 6:LPMO production and characterization</i></b>	<b><i>128</i></b>
<b>6.1 C-LPMO</b>	<b>129</b>
6.1.1 Production and purification	129
6.1.2 DMP Assay	130
<b>6.2 Ch-LPMO</b>	<b>133</b>
6.2.1 Production and purification	134
6.2.2 DMP Assay	134
<b><i>Chapter 7:Lignocellulosic biomass degradation with enzymatic cocktail</i></b>	<b><i>138</i></b>
<b>7.1 Lignocellulosic biomass treatment by enzymatic CK</b>	<b>139</b>
<b>7.2 Isolation and characterization of CNC from lignocellulosic biomass</b>	<b>144</b>
<b>7.3 Nanocellulose Oxidation</b>	<b>147</b>
<b><i>Chapter 8: CNCh Isolation and Characterization</i></b>	<b><i>150</i></b>
<b>8.1 Isolation of CNCh from <math>\alpha</math> chitin</b>	<b>151</b>
<b>8.2 CNCh yield by enzymatic hydrolysis</b>	<b>154</b>
<b>8.3 Characterization of CNCh</b>	<b>156</b>
8.3.1 Morphology	156
8.3.2 Physicochemical characterization	164
<b><i>Chapter 9:Discussion</i></b>	<b><i>180</i></b>
<b><i>Bibliography</i></b>	<b><i>190</i></b>
<b><i>Appendix</i></b>	<b><i>216</i></b>
<b>APPENDIX I</b>	<b>217</b>
List of Endo-1,4-beta-Xln A	217
C-LPMO	222

---

Ch-LPMO	228
<b>APPENDIX II</b>	<b>236</b>
ENDO 1,4 BETA Xln A	236
C-LPMO	236
Ch-LPMO	237
<b><i>List of Abbreviations</i></b>	<b>238</b>
<b><i>Acknowledgements</i></b>	<b>242</b>





---

# PART I



# Chapter 1 Introduction

---

In the past decades, nanotechnology has made great improvements in the development of new materials that have attracted the attention of researchers and industry. A prominent example is graphene, but many other materials such as carbon based fullerene, carbon nanotubes [1], 2D and Van der Waals materials [2], titanium nanoparticles [3], nanocomposites [4] and liquid crystals [5] [6], have also shared great interest. These materials are commonly used in many applications such as electronics [7], construction, aeronautics[8], [9], water treatment[10], and coating [11], among others. However, material scientists are facing new challenges, especially in bio-related disciplines that force them to incorporate biologically relevant materials, also in the nanoscale, that are known as nanobiomaterials. These materials have their origin in biological system and as such, often require treatment methods that also involve biosystems. Two notable examples of these materials are nanocellulose [12], [13] and nanochitin [14], [15]. Nanocellulose is obtained from cellulose and nanochitin from chitin. Luckily, cellulose and chitin are the first and second most abundant polymers on Earth,

respectively. These materials have been introduced in the past decade and active research is currently ongoing at a global level. These materials are the center of study of this thesis, where I have worked in their obtention, development and applications.

Nanobiomaterials have found an area of application in bio-related disciplines such as Biomedicine. Traditional biomedical applications have started benefiting from the use of nanomaterials in multiple areas, such as biosensors [16], [17], tissue engineering [18], [19], controlled release systems [20], drug delivery systems and nanocomposites used in implant design [21], [22]. These applications require materials with high biocompatibility and also physico-chemical properties that often need to approach living cells and tissues. This is still a challenge that can only be approached through multidisciplinary research involving biology, chemistry, physics, physiology, bioengineering and all related disciplines. The great effort required in such designs has remained a barrier that it has been overcome only in recent years.

Some of the most promising nanobiomaterials are the ones obtained from biomass due to their biocompatibility and easy tunability towards biomedical applications. The above-mentioned nanocellulose and nanochitin are currently investigated for such applications and both have been predicted to have a bright future in biomedical research. However, the obtention of these materials implies mechanical, thermal and chemical treatments that may affect not only their physico-chemical properties but also their biocompatibility, thus affecting their applications in biomedicine. This motivated us, in our laboratory, to develop a novel method for nanobiomaterial obtention based on enzyme catalysis. We use molecular evolution as the driving force for the design of enzymes with capabilities that go beyond catalysis, i.e., material transformations. In this thesis, I have contributed in developing these

methods for the design of enzymes capable of rendering nanobiomaterials such as nanocellulose and nanochitin.

The most abundantly raw material on Earth is lignocellulosic biomass from plants. Lignocellulosic biomass is composed of carbohydrate polymers (cellulose and hemicellulose), and aromatic polymer (lignin). These carbohydrate polymers contain different sugar monomers (five and six carbon sugars). Cellulose is the most abundant biopolymer; it is a linear homopolymer composed by D-glucose units bonded together by  $\beta$ -1,4-glycosidic bonds, where each unit is rotated  $180^\circ$  to the next one. The smallest unit is cellobiose, formed by two D-glucose units, with a size of 1,03 nm (Figure 1.1).

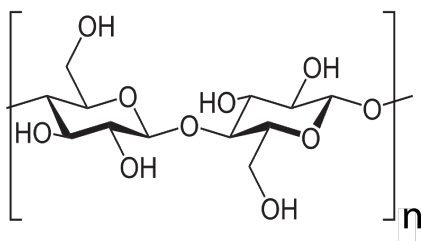


*Figure 1.1. Cellulose chemical structure. Two glucose molecules bonded together by a  $\beta$ -1,4-glycosidic bond. Glucose is the repeating unit of cellulose polymer and cellobiose is form by two D-glucose units. Each unit is rotated  $180^\circ$  to the next and has three hydroxyl groups that made the polymer very reactive.*

This monomer polymerizes forming linear cellulose chains and the hydroxyl groups, present in glucose monomers, help to form hydrogen bonds between chains. These hydrogen bonds can happen intramolecularly (between different cellulose chains), giving stiffness to cellulose, or intermolecularly, ordering chains to form a crystalline structure. Cellulose is a semi crystalline material, divided into crystalline

and amorphous fractions. The amount and orientation of inter and intramolecular hydrogen bonds vary depending on cellulose source and on the treatment used to its extraction. The native, and most abundant form of cellulose is type I cellulose, which shows a parallel organization of the chains. Cellulose II is the second most abundant polymorph, where chains have an antiparallel organization, allowing hydrogen bonds among neighbor's groups improving interlayer attraction forces.

In nature, cellulose is produced as an individual long chain that during the biosynthesis process is organized in a hierarchical structure forming the fibers. The polymeric chains are packed together through hydrogen bonding forming the elementary fibrils with a diameter of 3-5 nm and a length of 2-20 nm depending on the source [23]. At the same time, these fibers are ordered into bigger fibers by van der Waals forces and more intra and intermolecular hydrogen bonds. These microfibrils have a diameter around 30 nm and a length of several micrometers. Microfibrils are packed in larger structures called macrofibrils that together form the main cellulose fibers (Figure 1.2).

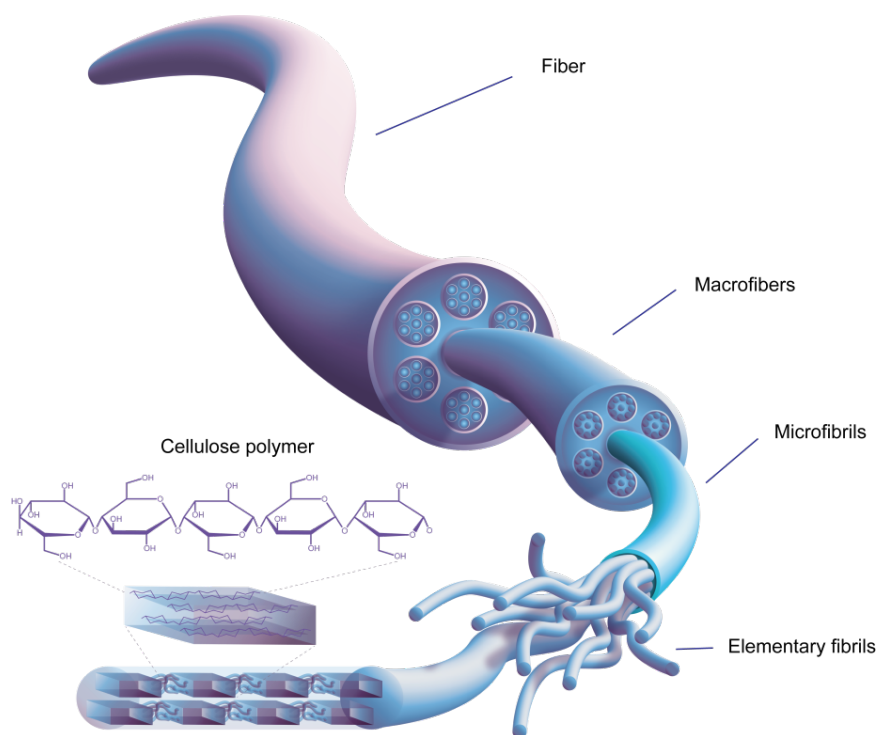


*Figure 1.2. Hierarchical cellulose structure. Cellulose polymers are packed together forming elementary fibrils. These tiny fibers are aggregated by hydrogen bonding and van der Waal forces into microfibrils and these are assembled in macrofibers; the macrofibers are the last unit that forms the main cellulose fibers.*

The hierarchical structure of cellulose from glucose chain to cellulose fibers permits a top down approach to obtain cellulose nanocrystals (CNC). Until now, the most common method to isolate CNC is by chemical treatment that includes sulfuric acid hydrolysis ( $\text{H}_2\text{SO}_4$ ) [29], [30], or 2,2,6,6-tetramethylpiperidine-1-oxyl (TEMPO) oxidation [26]. This hydrolysis is carried out in combination with thermal or mechanical pretreatments. Some works have shown the possibility of using enzymes, but always in combination with other pretreatments such as mechanical

and acid [13][27][33][34]. However, **common methods to isolate nanocellulose from cellulose are a barrier to the full implementation of nanomaterials in biotechnological applications.** Learning from nature, we propose a full enzymatic treatment to isolate not only nanocellulose from biomass but to isolate nanomaterials with the only action of enzymes.

Microorganisms, like bacteria and fungi, use enzymes for the degradation of cellulose. Cellulases are the most common enzymes used by organisms to break down the  $\beta$ -1,4-glycosidic bonds of cellulose. For the total hydrolysis of cellulose into glucose monomers three cellulases are needed: Endoglucanase (EG), which cleaves  $\beta$ -1,4-glycosidic bond randomly producing oligomers with reducing ends and preferably attacking the amorphous region of the material; Exoglucanase (CBH), which breaks down crystalline cellulose degrading the previous reducing oligomer into cellobiose units; and  $\beta$ -glucosidase (BG), which hydrolyzes cellobiose into glucose.

The recent discovery of the Lytic Polysaccharides MonoOxygenases [30] (LPMO) has attracted the attention of the lignocellulosic research community, since it has been proved that they are able to break down recalcitrant polysaccharides such as cellulose, LPMOs are produced by fungi and bacteria, and are even found in some viruses and insects [31]. LPMOs are enzymes containing a copper atom in their catalytic domain, and they have been described to produce oxidative cleavage on the glycosidic bonds. They were first studied for their activity in crystalline



chitin [32] and cellulose [33], but they also showed activity on other polymers such as hemicellulose [34] or starch [35].

The most described oxidation mechanism of LPMO to produce chain cleavage is the one made on C<sub>1</sub> or C<sub>4</sub> carbons of glucose (Figure 1.3), but in some cases it even oxidized C<sub>6</sub> [36]. C<sub>1</sub> oxidation produces soluble oligosaccharides with an aldonic acid in the reducing end and C<sub>4</sub> oxidation generates a ketoaldose in the non-reducing end [33], [37]. Since LPMO discovery, several reports of using them in combination with cellulases in biomass conversion have been published [38]–[40]. Addition of LPMO to cellulose cocktails boost their activity as LPMO helps cellulases to attack the crystalline cellulose [38].

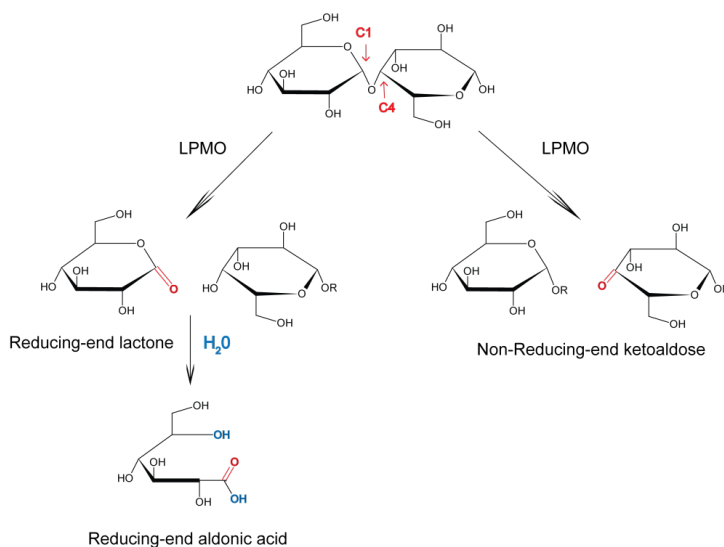


*Figure 1.3. LPMO catalytic activity. LPMO can break the cellulose polymer by oxidation of C<sub>1</sub> or C<sub>4</sub> carbon in general. C<sub>1</sub> oxidation leads to soluble oligosaccharides with an aldonic acid in the reducing end and C<sub>4</sub> oxidation produces a ketoaldose in the non-reducing end.*

Cellulose does not come alone in nature, it is embedded into a complex matrix form of lignin and hemicellulose, the other two components of lignocellulosic biomass. Hemicellulose is linked to cellulose by hydrogen bonding and covalently to lignin, giving stiffness to the lignocellulose matrix [44],[45],[43], [44]. In Figure 1.4 we see how cellulose (in blue) is trapped in a matrix of hemicellulose (in green) and lignin (in red). Cellulase and LPMO hydrolyze cellulose, but in order to get better yields of cellulose from raw materials, lignocellulosic biomass enzymes hydrolyzing lignin-hemicellulose matrix are needed [44]–[46]. In this work, we propose the degradation of hemicellulose in parallel to cellulose, to have more chances for cellulases to reach cellulose.

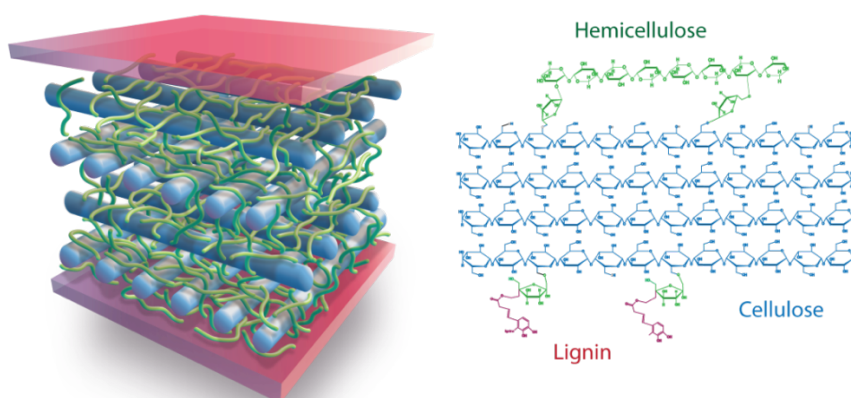


*Figure 1.4. Lignocellulosic biomass. Cellulose is located in a matrix of hemicellulose and lignin. Hemicellulose is composed by monosaccharides of 5 or 6 sugars binded together by  $\beta$ -glycosidic bond, and lignin is formed by phenylpropanoid precursors. Hemicellulose is bonded to cellulose and lignin by hydrogen and covalent bonding producing a very recalcitrant and stiff*

structure. This structure needs to be degraded in order to liberate cellulose fibers for further cellulose conversion into nanocellulose or sugars.

Hemicellulose structure consists of different carbohydrate polymers; the main polymer is xylan or glucomannan but has other sugars like xyloses, arabinoses, glucose, galactose, mannose, and sugar acids (Figure 1.5). Due to the short size of its lateral chains and its low molecular weight is easier to degrade than cellulose [38]. The hemicellulose can be extracted from biomass with sulfuric acid [47], alkaline pretreatment [48], steam explosion [49], and mechanical treatments [49], but due to its polysaccharide structure, it can also be removed by enzymatic hydrolysis. The most used enzyme is the Endo-1,4- $\beta$ -xylanase that degrades the xylan polymer into oligosaccharides by breaking the  $\beta$ -glycosidic bonds between the monomers. Xylanase is produced by bacteria or fungi [50] and has been used in biomass degradation or in paper pulp bleaching processes [51][52].

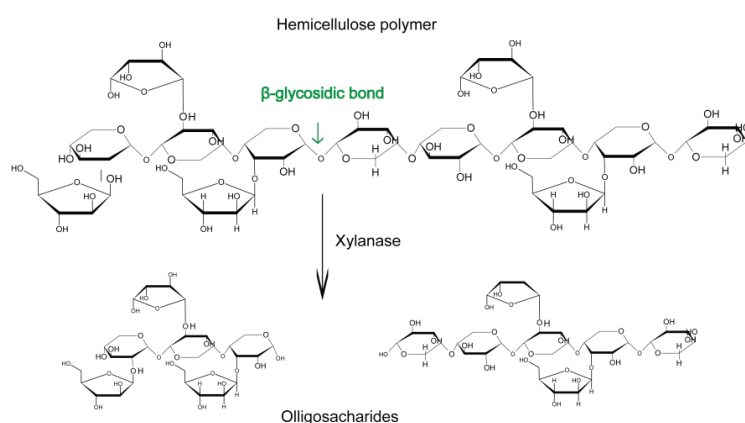


Figure 1.5. Xylanase catalytic reaction. Xylanase is able to break down the  $\beta$ -glycosidic bond between the xylan polymers and produces small oligosaccharides as product.

Lignin is the third main component of lignocellulosic biomass embedding cellulose. It is a physical barrier that protects cellulose fibers due to its structural complexity, high molecular weight, and insolubility. The linkage between lignin, cellulose, and hemicellulose are believed that inhibit the enzyme activity [53]. Chemical and physicochemical treatment can be used to disrupt lignin structure [54], [55]. There are two main families of enzymes that can depolymerize lignin too: peroxidases and laccase, produced mainly by the lignolytic white-rot fungi [56] and higher plant, but also found in bacteria [57].

In this thesis, we propose the addition of xylanase and LPMO to EG in order to hydrolyze biomass and get more accessibility to cellulose. In this way, together with other enzymes developed in our group at CIC Nanogune, we can isolate enzymatically nanomaterials from lignocellulosic biomass.

As we propose, enzymes seem to be a promising alternative for nanomaterial obtention from biomass. Nevertheless, they are adapted to their natural biological conditions, which often are far from industrial or even laboratory conditions required for biotechnological applications. These conditions often demand pH and temperature resistance that out of the reach of enzymes (Figure 1.6). This limitation has put the scope of biotechnology into enzyme engineering for industrial applications. In the past decades, researchers have focused on the improvement of enzymes properties, paying special attention to the enhancement of thermal stability, increase of specific activity, improvement of their substrate promiscuity and increase of the production rate [58]–[62].

The use of enzymes from extremophiles has been a solution for some industrial demands, producing satisfactory results, but there are situations in which even these extremophile enzymes need to be improved. Development in protein engineering research over the past decade has enable enzymes to be evolved in vitro for properties that favor the required process conditions, and also to obtain enzyme variants with altered substrate specificity or enantioselectivity [63], [64]. That is the significance of these techniques for our society, that last year (2018) Nobel Prize in chemistry was awarded to Prof. Frances Arnold for her groundbreaking contribution in protein engineering.

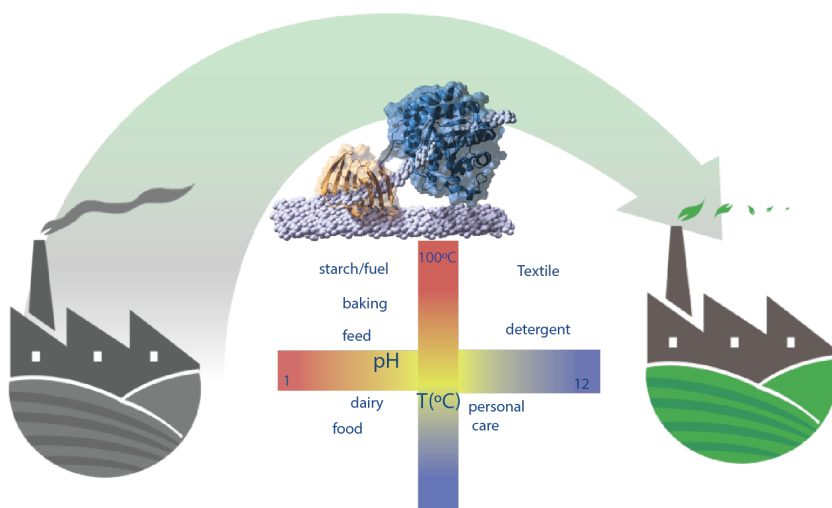


*Figure 1.6. Scheme of the industrial conditions that enzymes have to resist. In order to fulfill industrial conditions enzymes, need to be modified.*

Several strategies ranging from rational and computational design to *de novo* enzyme design and directed evolution, have been implemented to improve enzyme biocatalysis [65], [66]. Rational design involves site directed mutagenesis introducing a specific amino acid into a target gene

[67]. The structure and function of the enzyme will be determinant on the selected amino acid, but detailed structural knowledge of an enzyme is often unavailable. DNA shuffling consists on the fragmentation of gene parents, followed by some PCR (polymerase chain reaction) cycles to obtain different mutants of a gene. Error-prone PCR inserts random mutants into any piece of DNA, based on the well-founded PCR [68]. Another technique, directed evolution in vitro [66], [69] mimics the process of natural selection to evolve proteins or nucleic acids towards a user-defined condition. Directed evolution technique creates thousands of variants of the enzyme of interest with different random mutations, generating a library of mutants. These mutants are exposed to the desired conditions and the variants that best perform under these conditions are identified and selected for commercial exploitation. The likelihood of success in a directed evolution experiment is directly related to the total library size, as evaluating more mutants increases the chances of finding one with the desire properties [70]. In any case, this protocol is time and money consuming, since the generation of a mutant library and subsequent screening has to be done experimentally.

Limitations of these engineered enzymes are still a serious barrier for the chemical industry. Yet no methodology seems to be able to enhance, for instance, temperature and pH operability, the expression level or the specific activity of enzymes, all at once. In this regard, developing a strategy able to improve catalytic properties of enzymes in a cost-efficient manner may revolutionize the biotechnology and chemical industry. In our group we work using ancestral sequence reconstruction (ASR) technique, that has been used to study evolution of genes, proteins and enzymes [71]–[74], it have been proved that ancestral enzymes

display enhanced thermal and pH stability, improved activity and higher expression level, chemical promiscuity and in some cases, all of this at once [71], [74],[75]–[79].

ASR (ancestral sequence reconstruction) is based on the evolutionary theory, which states that groups of organisms change over time so that descendants differ structurally and functionally from their ancestor. Nowadays, ASR combined with biophysical and biochemical state-of-the-art techniques allows us to study and compare features of extinct proteins and genes that are otherwise inaccessible [71]–[73].

In this regard, phylogenetic methods applied to genomic information have made possible to establish evolutionary relationships among different living organisms, including the possibility of inferring the putative sequences of the genes of their already extinct ancestors [80], [81]. Since 1837, when Charles Darwin sketched an evolutionary tree, the scope of phylogeny has been to reconstruct the correct relationship between organisms and estimate the time of divergence since they share a common ancestor. This is carried out combining the phylogeny (relationship between organisms) and the time of divergence, which together form a phylogenetic tree scaled to time. This way, Ancestral sequence reconstruction allows determining the sequences of genes and proteins of ancestors from extant species [82].

The resurrection of an ancestral gene involves five steps (Figure 1.7). First, we select modern species genes of the desired gene or protein; these sequences are descended from the ancestral protein we want to reconstruct. We acquired from Internet databases. After selection we

align them, and the tree of their relationship is inferred. Phylogenetic methods such as Maximum likelihood are then used to infer the best estimate of the ancestral state for each sequence site given the present-day sequence data. Then DNA sequence for the ancestral protein is inferred. To express ancestral protein, we cloned into a plasmid that allows high-level expression, and the plasmid is then transfer to a high expression host bacterium in order to produce the ancestral protein. All these steps are explained in chapter 2 and chapter 3.

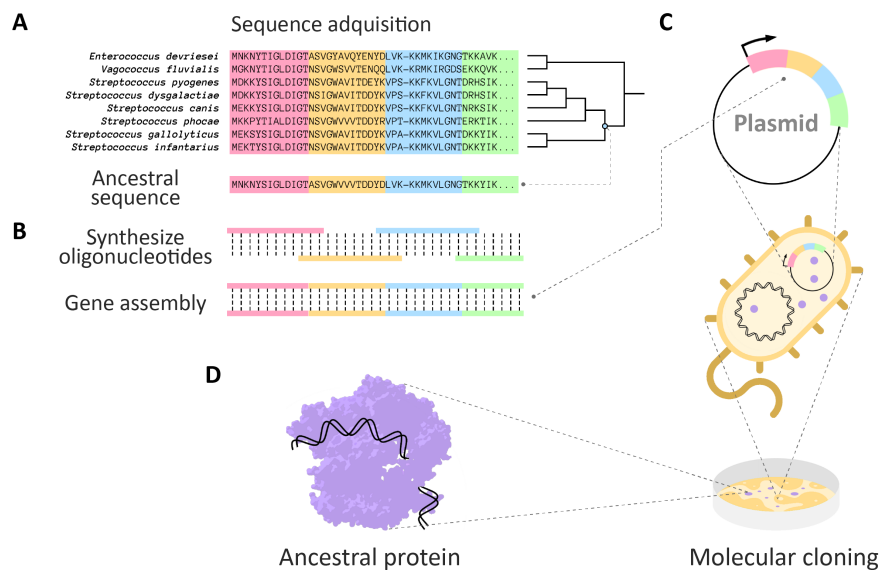


*Figure 1.7 Ancestral sequence reconstruction. (A) Amino acids sequences from extant organisms are aligned and a phylogenetic tree is inferred with bioinformatics tools, (B) Sequences from the ancestral proteins are calculated from the nodes of the tree. (C) Expression plasmid with the gen from the ancestral protein and the bacterial host for protein expression. (D) Ancestral proteins expressed from the bacterial host.*



The first ancestral protein was reconstructed in 1994 by Shindyalov et al [83]. Since then, numerous studies have used ASR, providing information about physiological and metabolic features [84] and about the environmental conditions that hosted ancestral organisms [73]. More recently, a study carried out by Perez-Jimenez et al. demonstrated the thermochemical evolution of thioredoxin enzymes covering a span between 4 to 1.4 Gyr, using single molecule force spectroscopy confirming a paleotemperature trend [74]. The deduction of the environmental conditions of different geological eras is an important application of ASR.

In our group we have implemented ASR as a biotechnological approach to improve the physico-chemical features of enzymes. Ancestral proteins and enzymes often show exceptional thermal stability, and also superior chemical properties due to the fact that our planet has been subjected to extreme environmental conditions throughout history and organisms and their molecules were adapted to these conditions. Moreover, it has been shown that ancestral enzymes are promiscuous, being able to work with lower selectivity and therefore with different types of substrates [70], [75], [84].

In our laboratory we reconstructed cellulases belonging to the different ancient species: LFCA EG (Last Firmicutes Common Ancestor), LCCA EG (Last Clostridium Common Ancestor) and LACA EG (Last Actinobacteria Common Ancestor) and compared their activity (Figure 1.8) with modern *Thermotoga maritima* EG (Tm EG) and *Bacillus subtilis* EG (Bs EG). We demonstrated that the activity of cellulase follows a trend parallel to that of the cooling trend of the ocean, highlighting the tight relation between enzymes activity and

environmental temperature[85] as reported by Robert and Chaussidon [86], who demonstrated that the temperature on ancient oceans cooled down over 30 °C during the period of 3.5-0.5 Gyr ago. The EG of the late Archean eon efficiently work in a broad range of temperatures (30-90°C), pH values (4-10) and processes different lignocellulosic substrates showing processive activity and even doubling the activity of modern enzymes in some conditions [85].

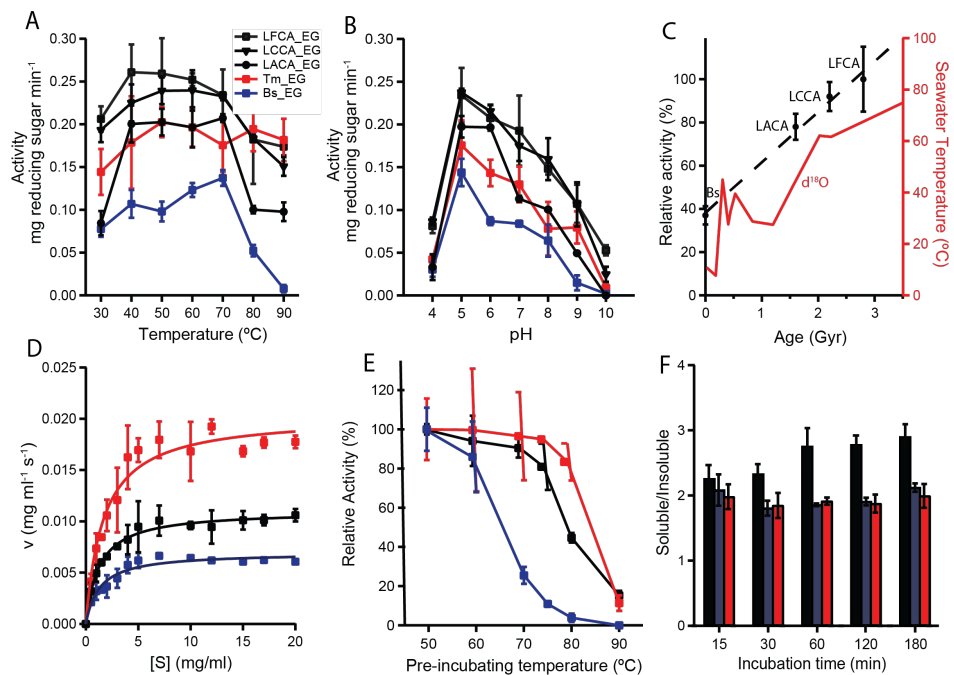


Figure 1.8. A published work of our laboratory showing A) activity assays for different ancestral endoglucanase as function of temperature: LFCA EG, LCCA EG and LACA EG against modern Tm EG and Bs EG at pH 4.8 and 5mg enzyme/g of glucan. B) EG activity as function of pH at 70 °C. C) Relative activity of the ancestral cellulases and Bs\_EG measured at 50 °C plotted vs. evolutionary time. The right axis, seawater paleotemperature trend as inferred from  $\delta^{18}\text{O}$  isotopes in seawater cherts vs. time. D) Kinetics of enzyme catalysis

*fitted to Michaelis-Menten equation. E) Pre-incubation experiments at different temperatures conducted for 30 min. F) Ratios of soluble to insoluble reducing sugars generated using PASC as a substrate by LFCA EG, Tm EG, and Bs EG, respectively.*

Ancestral enzymes seem suitable for industrial applications, but nowadays there are relatively few studies in that field. These studies have shown that ancestral enzymes not only have a great interest from an evolutionary point of view but can also have multiple applications in areas such as bioengineering and biomedicine. These include studies about thioredoxin [74], lactamases [75] or cellulases [94]. Enzymes in industry have been well established as biocatalyst in various industrial processes and can be found in various products of daily life. Nevertheless, their application in material science is still modest, as their conventional role in industry did not imply material production [87], [88]. In our group, besides **giving a biotechnological scope to ASR, we proved that ancestral enzyme features make them suitable for material production and modification.**

Using an ancestral EG, we successfully isolated CNC from cellulose (Figure 1.9). This ancestral EG degrades cellulose chains in random locations to generate oligomers with reducing ends [85]; preferably attacking the amorphous regions of the fibers. We demonstrated that enzymatically obtained CNC kept cellulose native polymorph, whereas CNC isolated with other protocols does not maintain cellulose natural polymorph [89], where glucose chains are ordered in parallel. Chemical hydrolysis of cellulase, most commonly using sulfuric acid, leaves sulfur groups attached to the CNC surface. Similarly, the TEMPO treatment

renders oxidized CNC [90]–[92]. Enzyme hydrolysis emerges as an alternative given that CNC are obtained chemically pure, although usually enzyme yields are lower in comparison to chemical methods. In figure 1.8 and 1.9 we can observe the activity and hydrolysis capabilities of a the resurrected EG, which always shows better performance that commercial EGs.

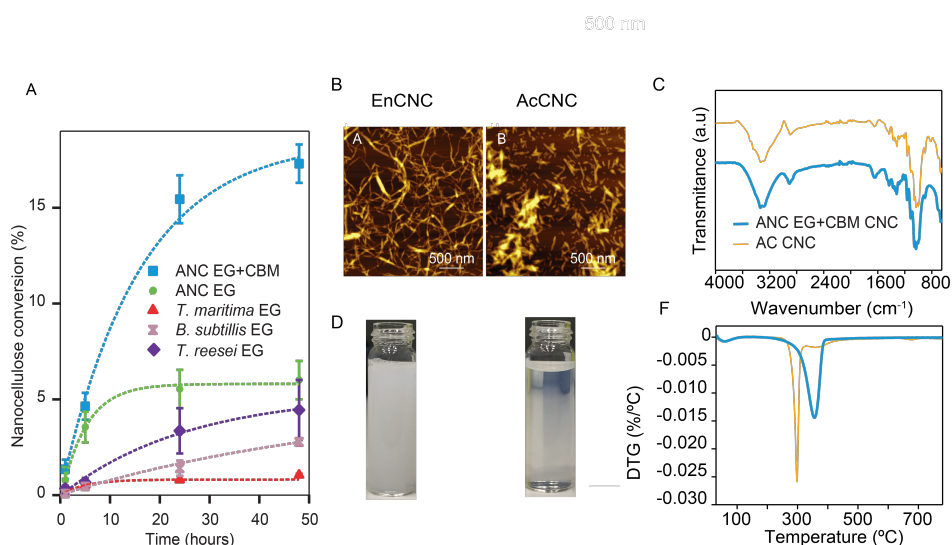


*Figure 1.9: Enzymatic isolation of CNC from filter paper using ancestral EG+CBM. A) Nanocellulose total conversion percentage using different enzymes: ANC EG+CBM, ANC EG, T maritime EG, B. subtilis EG and T. reesei EG. ANC EG+CBM shows 3 times better yields from the next enzyme after 24 hours. B) AFM images of CNC obtained using ANC EG +CBM (EnCNC) and acid (AcCNC). C) FTIR of CNC obtained by ANC EG +CBM (blue) and Acid (yellow). D) Pictures of CNC suspension in water, on the left ANC EG+CBM CNC that has a better particle dispersion on water than, on the right, AC CNC that show poor dispersion on water due to the negative charges of its surface. E) Derivative from thermogravimetric curve of CNC obtained by ANC EG+CBM has better thermo stability than CNC obtained by Acid.*

In this thesis, I consolidate the process of enzymatic isolation of nanomaterials by reconstructing an ancestral xylanase and an ancestral LPMO to help nanocellulose isolation from lignocellulosic biomass. Moreover, as LPMO is an oxidative enzyme, we think that the action of this enzyme in nanocellulose may modify its surface; hence we can obtain an oxidized CNC enzymatically without the need of chemicals such as TEMPO.

To reinforce the capability of enzymes in nanomaterial obtention, in this thesis I have used enzymes to isolate nanochitin from the second most abundant biopolymer on Earth: chitin. It is a linear homopolymer composed of acetyl -D-glucosamine linked by  $\beta$ -1,4-glycosidic bonds (Figure 1.10). It is a main component of cell walls in fungi [93], the exoskeletons of arthropods, such as crustaceans and insects [94], mollusks [9] and the scales of fish among others. It is biocompatible, biodegradable and bio absorbable, with antibacterial and wound-healing abilities and low immunogenicity [95]. Moreover, it is transparent, flexible and has high thermal and mechanical resistance. These has made of chitin and its derivatives a very valuable feedstock for industry with a broad range of applications in different fields such as food technology [96], material science [97], agriculture [98], wastewater treatment [99], drug delivery systems, tissue engineering or nanobiotechnology.

The structure of chitin can be compared to that of cellulose. But, unlike cellulose, chitin can be a source of nitrogen as well as carbon [100]. It was discovered in 1811 by French professor Henri Braconnot but it was in 1843 when Lassaigne demonstrated the presence of nitrogen on chitin [101]. So, the presence of the amyl group in the C<sub>6</sub> carbon of the sugar

ring instead of the hydroxyl group creates a bigger dipole in the molecule than in glucose, as nitrogen will be positively charged whereas the double bonded oxygen of the carboxyl is negatively charged. This dipole increases hydrogen bonding in chitin and thus, chitin strength. Therefore, chitin or chitin-combined composites resulting structures are very strong.

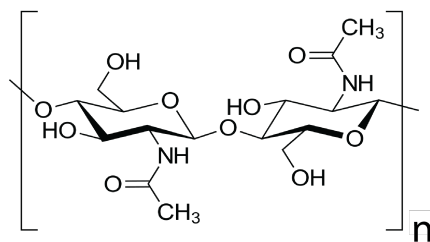


*Figure 1.10. Chitin chemical structure. b) N-Acetyl-glucosamine is the repeating unit of chitin; the second most abundant biopolymer on earth, instead of a hydroxyl group contains an amine group. Each unit is rotated 180° to the next and has three hydroxyl groups that made the polymer very reactive.*

Chitin chains are packed together by intra and inter molecular hydrogen bonding and van der Waals forces, about 18-25 chitin molecules arrange to form crystalline nanofiber structure of about 0.1-10 nm length [102]. Similarly, nanofibers form inter and intra molecular hydrogen bonds and van der Waals forces to pack them into bigger fibers that in nature are wrapped with proteins, this chitin-protein fibers are 10-100 nm long and about 20 nm diameter [103]. Chitin nanofibers are arranged into bigger fibers of about 100 nm-10  $\mu$ m length forming horizontal planes that are packed together in a twisted plywood structure (Bouligand) [104]. At the macro scale cuticles consists of three layers: endocuticle, exocuticle and

outer thin waxy layer, the epicuticle. The hierarchical chitin structure is shown in Figure 1.11.

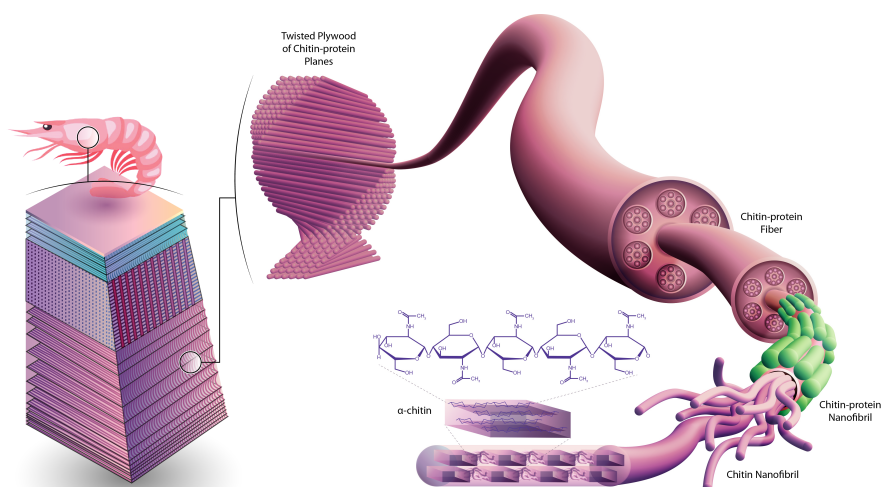


*Figure 1.11: hierarchical structure of chitin. From the N-acetyl glucosamine molecules bonded by glycosidic bonds creating chitin chains, to nanofibrils (pink), nanofibrils wrapped in protein (green), microfibrils creating horizontal planes in a twisted plywood structure. At the macroscale three cuticles consists of three layers: endocuticle, exocuticle and outer thin waxy layer, the epicuticle, from a shrimp exoskeleton.*

The hierarchical organization of chitin from N-acetyl -D-glucosamine chains to chitin fibers permit a top down approximation to obtain nanoparticles. As mentioned before, nanoparticles from biomass is focusing research attention because of its extraordinary capabilities like biocompatibility, renewability; it is sustainable, nanometer size, high

aspect ratio, flexible, electrical thermal and mechanical properties.

Chitin is predominantly present in fibrillar crystalline material. Based on X-ray diffraction data and infrared spectroscopy (FTIR) native chitin can be organized in three crystalline forms [105]:  $\alpha$ -chitin,  $\beta$ -chitin and  $\gamma$ -chitin depending on their origin.  $\alpha$ -chitin is the most abundant existing in crabs, lobsters, krill and shrimp shells, insect's cuticles, and fungal yeast cell walls. It has an antiparallel orientation of the N-acetyl-glucosamine chains, with strong intermolecular bonding, having a crystallinity higher than 80% [106].  $\beta$ -chitin, present in squid pens and tube worms [107] is the second most abundant chitin polymorph in which the molecules are arranged in parallel. Due to this molecular arrangement intermolecular interactions are weaker than those in  $\alpha$ -chitin.  $\gamma$ -chitin is the less abundant chitin polymorph in which the molecules are arranged in both parallel and anti-parallel fashion.

The amorphous domains of chitin can also be removed under certain conditions such as acidosis to give rise to crystalline nanochitin (CNCh) in bibliography is also called chitin whiskers, CHW). They can be obtained by hydrochloric hydrolysis [108], [109],[110], [111], TEMPO mediated oxidation [106], gelation, ultra-sonication [112], electro spinning [113] or mechanical grinding treatment [114]. However, HCl hydrolysis is the most common method and the others are usually carried out in combination of acid treatment [115], [116].



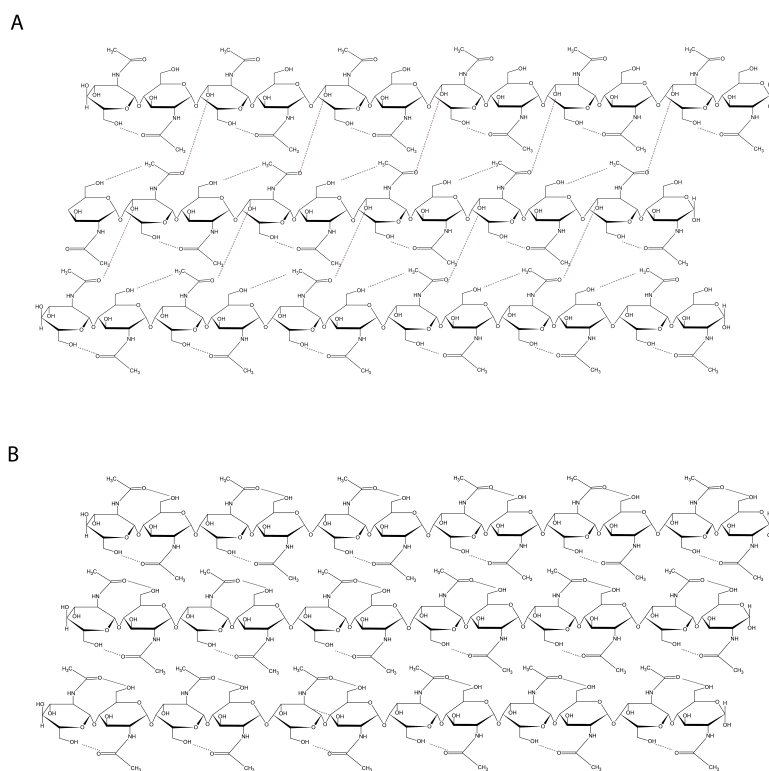


*Figure 1.8: chitin polymorphs A)  $\alpha$ -Chitin, chains are oriented antiparallel favoring intra and intermolecular bonds. B)  $\beta$ -Chitin, chains are oriented parallel.*

There are different enzymes that catalyses chitin hydrolysis. For instance, the endochitinase activity is defined as the random cleavage at internal positions in the chitin chain. The exochitinase activity is defined as the progressive action starting at the non-reducing end of chitin with release of chitobiose or N-acetyl glucosamine [117]. But, this enzyme acts in colloidal chitin and there are no reports of chitinases acting in crystalline chitin [118], [119].

CNCh has very interesting features regarding biomaterial technology, such as easy availability, nontoxicity, biodegradability, low density plus

the ones mentioned before. For this reason, they have been widely used as substitutes to inorganic nanoparticles in reinforcing polymer nanocomposites [120], In packaging for food [121], agriculture, water treatment or nanopore filter. Biomedical applications have also been reported as tissue regeneration and antibacterial material. In spite of its increasing studies about CNCh the research and development of CNCh area goes slower than CNC [116].

Organic nanoparticles such as CNC and CNCh show many advantages over traditional nanocomposites and together are being studied for multiple applications such as agriculture, medicine, tissue engineering, cellular scaffold, and conductive bio-inks. It has been reported that films cast with both nanomaterials effectively enhanced the mechanical performance of the film with high transparency and flexibility [122].

In this thesis, we will reconstruct biomass degrading enzymes in order to obtain better yield and structurally modified CNC by the only action on enzymes. Besides we will reconstruct an ancestral LPMO and, for the first time, will enzymatically isolate CNCh from chitin. We will compare the activity of all the reconstructed enzymes in this work with their modern homologous.

In order to characterize these new nanomaterials and compare them with commercially available CNC and CNCh we will use X-ray diffraction, FTIR spectroscopy, NMR and AFM to study morphology.

# Objectives

---

The main objectives of this thesis were the reconstruction of ancestral enzymes for the degradation of lignocellulosic biomass and chitin and to confirm the capability of these enzymes to isolate nanocellulose and nanochitin from biomass.

1. Reconstruction of an ancestral Endo 1,4-beta xylanase from *Bacillus subtilis* and a Lytic polysaccharide monoxygenase (LPMO) from *Streptomyces viridosporus* for the degradation of lignocellulosic biomass. Reconstruction of a LPMO from *Bacillus thurigiensis* for the degradation of chitin.
2. Characterization of the reconstructed enzymes and their extant homologous. We use molecular biology tools to first express the genes, then we purify the protein at our laboratory and finally we perform different activity assays for each enzyme.
3. Nanocellulose isolation from complex substrates from lignocellulosic biomass. Help an ancestral endoglucanase

(EG) reconstructed in our laboratory to isolate nanocellulose from complex lignocellulosic substrates by adding the reconstructed xylanase and LPMO in this work. Study the effect of an oxidative enzyme (LPMO) in the enzymatic method on the obtained nanocellulose.

4. Nanochitin isolation from  $\alpha$ -chitin using ancestral LPMO. We want to consolidate the capability of ancestral enzymes for the obtention of nanobiomaterials from different biomass substrates. The characterization of this enzymatically produced nanochitin and its comparison with a nanochitin obtained with HCl hydrolysis.

This work has been carried out to consolidate the potential of blending two different fields in nanobiomaterials engineering: Material science and Enzyme chemistry. This work was made in CIC Nanogune under the direction of Raul Pérez Jiménez and the co-direction of David de Sancho from DIPC (Donostia Physics Centre) with Nanogune findings.

---

# PART II



## **Chapter 2: Phylogenetic analysis and ASR**

---

In this chapter, I will describe the methodology to build a phylogenetic tree. Moreover, I will explain how to track the evolutionary history of genes to obtain information of extinct species using ancestral sequence reconstruction (ASR).

## 2.1 Introduction

Ancestral reconstruction is the extrapolation back in time, using statistic methods, from measured characteristics of individuals to their common ancestor. It can have non-biological applications such as the evolution of phonemes or vocabulary of ancient languages [123], oral traditions of extinct cultures [124] or ancestral marriage practices [125]. But in the context of evolutionary biology it can be used to study the evolutionary relationship among individuals, populations or species, in **phylogenetics** [126]. In this scenario, either protein or nucleic acids will be the characters to compare. All these data come from extant species that have been sequenced. In order to recover the most accurate ancestral state ASR relies on a realistic statistic model of evolution. In order to determine the route of the evolution, the genetic information already obtained through methods such as phylogenetic is used[127].

Linus Pauling and Emilie Zuckerkandl in 1963 suggested the possibility of reconstructing ancestral proteins from analyzing and comparing extant proteins. 25 years later the paleochemistry they suggested became true. Thanks to the increasing known about gene and protein sequences, more feasible statistical methods and improvements on genetic engineering techniques. This idea began in 1955, when Frederick Sanger started developing techniques for sequencing the primary structure of proteins. This achievement lead Zuckerkandl and Pauling to propose that, based on the amino acid sequence of extant proteins, it is possible to infer the phylogeny of that protein and the sequences of all the common ancestors, including the earliest point of the tree [128], [129]. But, it was in 1971 by Walter M.Fitch when the first algorithm for ancestral reconstruction



using the principles of maximum parsimony was developed [130]. Nowadays, by means of the so-called ancestral sequence reconstruction, we are able to reconstruct ancestral biological macromolecules; genes and proteins.

## **2.2 Theory of phylogenetic analyses**

To organize the diversity of life, during all the evolution, there are two main tools: taxonomy and phylogeny. Taxonomy classifies organisms in three domains (Bacteria, Achaea and Eukaryotes). Whereas phylogeny is an estimation of the organism evolutionary history where a most recent common ancestor splits to form two species.

We need to determine the route of the evolution to reconstruct an ancestor, for that, we will use the genetic information already obtained through phylogeny, constructing a phylogenetic tree. This will be a hypothetical tree or cladogram showing the order in how species are correlated between each other. In a rooted phylogenetic tree, each node with descendants represents the inferred most recent common ancestor of those descendants. The very first ancestor of the tree, and the starting point for the branches, is the last universal common ancestor (LUCA). The end of the branches or the terminal nodes are the extant species. At the end, all the species and, therefore, all the evolutionary lines converge in LUCA (Figure 2.1)

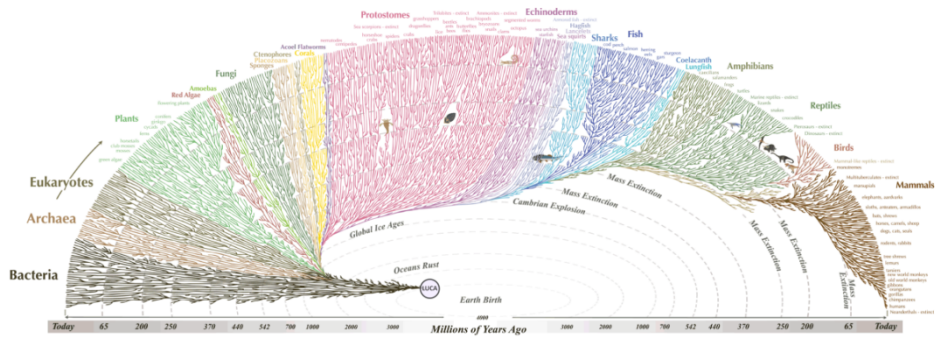


Figure 2.1. Phylogenetic tree of all the living species with a Universal Common Ancestor. This Figure wsource is Evogeneao, the tree of life.

## 2.2.1 Methods

As the computing power has grown exponentially, literature about different methods for analyzing phylogenetically structured data has also grown. First, a method to infer the tree came up: Maximum parsimony, where a set of extant sequences are used to minimize the amount of mutations that are necessary to match the available data. Since maximum parsimony method was described a lot of changes have happened. In 1975, David Sankoff added a cost to the mutation [131] optimizing the existing algorithms. In 1989, thanks to this work David. L. Swofford could develop the first phylogenetics program called PAUP [132]. At the same time, the exponential increase of the computing power made the implementation of much more complex algorithms possible, such as maximum likelihood approaches [133]–[135] or Bayesian methods [135]

The method will change depending on the question they seek to answer. Therefore, many different methods have been described.

### **2.2.1.1 Maximum parsimony**

This method attempts to reconstruct ancestral states by minimizing the number of trait changes between the ancestor and the present descendants. To infer the tree, it uses a set of extant sequences minimizing the amount of mutations that are necessary to match the available data. Due to its low computational costs and high efficiency for large datasets and when ab initio phylogenies are needed [136] this method is very useful. But, parsimony methods impose general assumptions that are not always valid such as the assumption that all character states are equally likely to occur, which is unrealistic.

### **2.2.1.2 Maximum likelihood**

The maximum likelihood approach for phylogenetic analysis seeks the tree and associated evolution model parameters that maximize the probability of producing the given set of genomes. In other words, this method assumes that the ancestral states are those, which are statistically most likely, based on the input data, the extant genomes. So, maximum likelihood provides probabilities of the sequences given a model of their evolution on a particular tree.

To use a model of evolution we need to understand that not all events are equally likely to take place. So, the more probable the sequences given the tree, the more the tree are preferred. Anyway, this does not mean that they need to happen just because they are more likely to occur. It can happen that the event with less probability occurs. In those cases, maximum parsimony may actually be more accurate because it is more willing to make large, unlikely leaps than maximum likelihood.

Maximum likelihood is really reliable in reconstructing character states. But, is not good giving accurate estimations of the stability of proteins as overestimated, since it assumes that the input proteins were the more stable and optimal [137].

In Maximum likelihood Markov process models the evolution of the sequence. In this model we assume that all mutations are independent [138] and the likelihood of the model is calculated from a sum of intermediate probabilities of the nodes for the tree. This way, in each ancestral node, the likelihood of the descendants is computed to obtain a maximum posterior probability (equation 1):

$$[1]L_x = \sum_{S_x \in \Omega} P(S_x) \left( \sum_{S_y \in \Omega} P(S_y | S_x, t_{xy}) L_y \sum_{S_z \in \Omega} P(S_z | S_x, t_{xz}) L_z \right)$$

Where node  $x$  is the ancestor of  $y$  and  $z$ .  $S_i$  represents the sequence of the  $i$ -th node,  $t_{ij}$  refers to the branch length from  $i$  to  $j$ .  $\Omega$  is the set of all the possible combinations (for example, the four nucleotides or the 20 basic amino acids). The ultimate objective of the reconstruction is to search for the best configuration in all the nodes before to obtain the maximum likelihood for their ancestor in a given tree. Therefore, the aim of an ancestral reconstruction is to find the assignment for all  $x$  internal nodes that maximizes the likelihood of the input data for the given tree.

Each descendant obtains a likelihood value. In order to find the most probable evolutionary lineage to the common ancestor two different conventions have been proposed (Figure 2.2):

- Joint reconstruction: where one can consider the probabilities of all the descendants for a certain ancestor and calculate the joint combination with the maximum likelihood.
- Marginal reconstruction: where instead of calculating the global likelihood, one can successively select the most likely ancestor for every node.

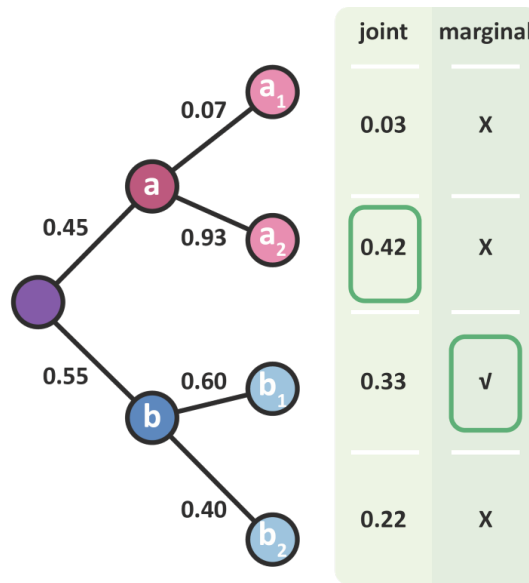


Figure 2.2. Scheme of Joint and marginal reconstructions for a phylogenetic tree. Pale pink and pale blue circles are wxtant species and dark pink and dark blue circles their extants. Purple circle is Last Universal Common Ancestor.

### 2.2.1.3 Bayesian

It is a statistical inference method in which Bayes theorem is used to seek the probability for a hypothesis in where the more information or evidence the better. It employs both the likelihood of the experimental data and a prior knowledge about the possible solutions. Thus, the aim of ancestral sequence reconstruction is to obtain the posterior probabilities

for every internal node of a known tree. Moreover, the posterior probabilities can be combined with the posterior distributions over the parameters for a given evolutionary model and the structure of all possible trees, giving the following applications of Bayes theorem (equation 2):

$$[2] P(S | D, \theta) = \frac{P(D | S, \theta) P(S | \theta)}{P(D | \theta)}$$

$\theta$  Represents the phylogenetic tree and the evolutionary model,  $S$  corresponds to the ancestral states and  $D$  is the experimental data.  $P(D | S, \theta)$  Is the likelihood of the experimental data that could be computed,  $P(S | \theta)$  refers to the prior probability of an ancestral node for a known tree and model and  $P(D | \theta)$  is the probability of a known tree and model integrated for all possible ancestral states. This formula refers to the empirical Bayes approach. This estimates the probabilities of several ancestral nodes for a given tree and model of evolution [139].

### **2.3 Experimental Phylogenetic Analysis**



Phylogenetic analysis only needs of informatics tools. Different webpages and Software's are used during the process. In this section we find a description of the process.

The reconstruction of the three ancestral lignocellulosic enzymes was carried out following the next steps: (1) Selection of the sequence of interest and its BLAST, (2) Alignment of the selected sequences, (3) Construction of the phylogenetic tree and (4) Reconstruction of the ancestral sequence.



Figure 2.3: Example of an alienation of selected sequences to construct the tree. On the right part the organisms name, ordered by taxonomy and aligned. From the alignment a phylogenetic tree is inferred with its corresponding nodes. One of these nodes will be the selected ancestral node from where the ancestral gene is inferred.

### 2.3.1 Select extant sequences: Uniprot and NCBI

The sequence of the protein of interest for the ancestral reconstruction must be in a genome or sequences databases and it is called QUERY. There are many different free online protein sequences databases but there are two that allow us to find and select other sequences having the query as a starting point: Uniprot  and NCBI  [140]. In this thesis we searched for the query at Uniprot, because it is as a catalog of proteins, with all the information ( $M_w$ , structure, function, etc...). And then, we search for homologous sequences at NCBI (BLAST, because it allows us to search for specific taxa's or exclude them besides giving a value for the query cover.

#### 2.3.1.1. BLAST

After the identification of a suitable Query at Uniprot we run a BLAST (Basic Local Alignment search Tool) in NCBI. This tool allows us to find regions of similarity between biological sequences. The program

compares protein sequences to sequence databases and calculate the statistical significance. Moreover, we can select different parameters to accurate our search (Table 2.1) after entering our query sequence.

*Table 2.1: Possible settings and their meaning for a protein BLAST at NCBI*

<b>SETTING</b>	<b>MEANING</b>
<b>Database</b>	NCBI Blast allows us to search sequences among different databases.
<b>Search set</b>	Allows to select specific taxon to only search for them or either exclude them.
<b>Algorithm</b>	BlastP compares a protein query to a protein database. A new accelerated version came up Quick BLASTP, is very fast and works best if the target percent identity is 50% or more.
<b>Max tar. Seq.</b>	Allows choosing the maximum number of aligned sequences to display.
<b>Word size</b>	The length of the seed that initiates an alignment. We choose the maximum.
<b>Expected threshold</b>	Expected number of chance matches in a random model. The bigger this value is, the more unlikely to be significant a match. For our sequences, that has between 20 and 54 KDa an E-threshold of 0.001 works.
<b>Matrix</b>	Assigns a score for aligning pairs of residues, and determines overall alignment score. We choose BLOSUM [141] matrix that is based on the frequency in which that substitution is known to occur among consensus blocks within related proteins.



Running the Blast can take several minutes depending on the complexity or length of the query sequence or the parameters we set. When it is finished, the sequences appear ordered from the one with the best score to the one with the worse score. This way, it is possible to choose sequences with **identity**  $\geq 40\%$  and **query cover**  $\geq 90\%$  easily. We select an identity equal or bigger than 40% because below this identity we consider them as different. Moreover, the query cover must be equal or bigger than 90% to ensure the selected sequences with a certain identity has it in the appropriate regions with reference to the query.

All selected sequences can be downloaded in different formats. Regarding the following steps we download them in FASTA format (a text base format for representing nucleotide or amino acid sequences).

### **2.3.1 Multiple sequence alignment: MUSCLE**

The file generated from the selected sequences of the BLAST, saved as FASTA format, can be opened in MEGA (Molecular Evolutionary a genetic Alignment), a very versatile tool for phylogenetic and molecular evolution. MEGA is software, with powerful visual tools, that can crate multiple sequence alignment, infer phylogenetic trees, estimate rates of molecular evolution, infer ancestral sequences and much more phylogeny related applications.

Over the last years, many algorithms have been developed for the multiple sequence alignment. ClustalW and MUSCLE [81], [142] are the most popular. Both, with a heuristic approach, use progressive alignment method where those with the best alignment score, are aligned first. Then progressively more distant groups of sequences are aligned until a global

alignment is obtained. Moreover, MUSCLE (integrated at MEGA software) is the fastest at aligning large sequences [143], [144] and the method we choose in this thesis for MSA.

When the FASTA format document with our sequences of interest is loaded, a non-aligned sequence map will appear at the interface. To run with MUSCLE algorithm, one should select all the sequences and click on the “align with MUSCLE” icon. A pop-up window will appear showing the different parameters that one can change before computing the algorithm (Table 2.2).

*Table 2.2: Alignment parameters at MEGA program for running MUSCLE.*

<b>PARAMETER</b>	<b>MEANING</b>
<b>Gap opening penalty</b>	By increasing this value, the gaps become less frequent in the alignment
<b>Gap extension penalty</b>	The bigger the value is, the shorter the gaps are in the alignment. Terminal gaps do not penalize.
<b>Max memory in MB</b>	The algorithm sets a computational memory upper limit by default set, the use of all the computer resource is avoided.
<b>Max interaction</b>	Sets the maximum number of permitted iterations.
<b>Clustering method</b>	Sets the clustering method used in the first two interactions.
<b>Max. Diagonal Length</b>	Maximum length of diagonal of the matrix made by aligning the sequences.

After running MUSCLE algorithm and all interactions are finished, we see an aligned sequences map on the interface. Sometimes regions of ambiguous alignment or with gaps in several sequences can be removed manually, directly at the alignment, or using GBLOCKS [145]. GBLOCKS is software that gets rid of poorly aligns positions and divergent regions of an alignment of DNA or protein sequences. Each residue shows a different color depending on its biochemical properties. If a residue is conserve in all sequences an asterisk is show on top of the residues. Finally, the alignment needs to be saved as nexus file for the following steps.

### **2.3.2 Computing a phylogenetic tree**

To construct the phylogenetic tree from the alignment we choose software that uses Bayesian analysis of molecular sequences using MCMC (Markov Chain Monte Carlo): BEAST (Bayesian Evolutionary Analysis Sampling Trees). It uses MCMC to average over tree space, this way the tree is weighted proportional to its posterior probability. Moreover, it is orientated towards rooted, time-measured phylogenies inferred using strict or relaxed molecular clock models.

From Beast package we will use BEAUti, BEAST and TREE Anotator but we need to download BEAGLE library first in order to run the program, TRACER to track the phylogenetic tree and FIG tree to draw the tree.

#### **2.3.2.1. BEAGLE**

BEAGLE is a high-performance library able to run the core calculations at the heart of most Bayesian and Maximum Likelihood phylogenetic package. With BEAGLE, processors can be used in parallel, such as those in graphics processing units (GPUs) found in many PCs.

### 2.3.2.2. BEAUti

BEAUti (Bayesian Evolutionary analysis Utility) is a graphical user interface to generate a suitable input data for BEAST (xml). Here we can design the analysis by setting the evolutionary model or options for MCMC from the aligned sequences. It has a user-friendly interface with several tabs and allows modifying these parameters.

*Table 2.3. parameters that can be changed at beauty to generate the desire best input data.*

SETTING	MEANING
<b>Partitions</b>	Allows to load sequences that were not in the initial pool and to make partitions within this pool.
<b>Taxa</b>	Clusters selected taxa into subgroups. There is the possibility to force these subgroups to be monophyletic.
<b>Tips</b>	Permits data sampling of individual taxa.
<b>Traits</b>	Sets the phenotypic trait analysis.
<b>Sites</b>	Allows selecting the substitution model and the site heterogeneity.
<b>Clocks</b>	Permit to choose the clock model the different clock models use the mutation rate of biomolecules to estimate when they

diverged.

<b>Trees</b>	Set the tree prior.
<b>States</b>	Allows reconstruction the states of all the ancestors or only certain subgroups.
<b>Priors</b>	Sets the prior distribution for the subgroups, the gamma shape parameter, the proportion of invariant sites parameter (a parameter that assumes which residues do not mutate)
<b>Operators</b>	Switches on or off the some of the parameters set in previous tags.
<b>MCMC</b>	Sets the MCMC values for phylogeny computing

---

When we have set all the parameters, we push “Generate BEAST file” button and an XML command file is generated, ready to be run in BEAST.

### **2.3.2.2 BEAST**

BEAST takes as input an XML command file and returns as output log files, files that record a sample of the states that the Markov chain encountered. Here we can analyze the evolutionary rates, divergence times, population sizes and tree topologies. An examination of this output is needed to determine whether the Markov chain has been run for long enough to obtain accurate estimates of the parameters. Tracer carries out this post-analysis. Running BEAST with a graphical user interface will open the following dialog box:

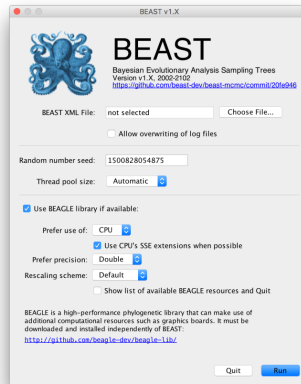


Figure 2.4. Graphical user interface (GUI) application of BEAST where .XML file is loaded in order to infer the tree.

This graphical interface is user friendly and let you set different parameters. The following table shows all the parameters that can be set at BEAST

Table 2.4. Parameters at the Grafical User Interface (GUI) used by BEAST.

PARAMETER	MEANING
<b>BEAST XML file</b>	The name of the selected BEAST XML file.
<b>Allow overwriting of log files</b>	By default, BEAST does not overwrite existing log or trees files to protect the data. .
<b>Random number seed</b>	Like all computer software, BEAST uses a pseudo-random number generator. The random numbers are used to generate the random starting tree, to propose new states in the MCMC tree and to accept or reject these proposals.
<b>Thread pool size</b>	Specifies the number of threads that BEAST will use to divide up the computation amongst cores and processors.
<b>Use BEAGLE</b>	This option and the rest of the dialog box is used to tell BEAST

**library** to use the BEAGLE library and control the options for its use.

---

Once all the parameters are set by pressing RUN button the analysis will start until completion.

### **2.3.2.3 Tracer**

Tracer is graphical interface (Figure 2.5) that allows monitoring and analyzing the MCMC output carried out in BEAST. Once the log file that corresponds to the analysis of the phylogenetic computation is opened, the name of the log file to the traces that it contains and many parameters related to MCMC analysis will appear on the left side of the interface. These parameters are pondered by their Effective Sample Sizes (ESSs). A low ESS means that the trace contained a lot of correlated samples and may not represent the posterior distribution well. It is advisable to run BEAST again until ESS reaches a value higher than 100.

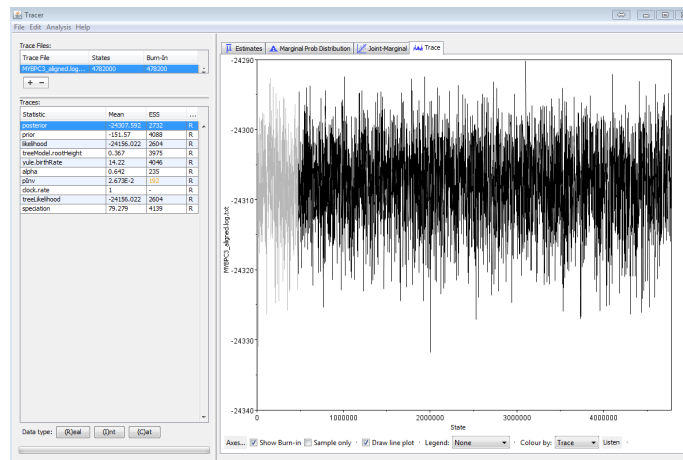


Figure 2.5. Tracer graphical interface. The evolution of posterior probability can be visualized in this picture. The data in grey is excluded for the calculation of average.

### 2.3.2.4 Treeanotator

This tool permits us to select a tree among all the trees that has been generated during the BEAST process. This tree contains the generated posterior probabilities of the nodes in the target tree. The program includes the options in Table 2.5.

Tabla 2.5: table explaining the different options for setting in TreeAnotator and their meaning.

PARAMETER	MEANING
<b>Burnin</b>	Number of samples that will be discarded at the start of the run.
<b>Posterior probability limit</b>	Specifying a limit as starting point in PAUP. They will only be calculated for the nodes that in the target tree have a bigger posterior probability than the specified.



**Target tree type** In “maximum clade credibility” the node height and rate statistics will be merge on the tree posterior probabilities on its (n-2) internal nodes. The “user target tree” option summarizes the tree statistics on a user-specified tree.

**Node heights** To set the way the node heights are summarized on the target tree.

---

### 2.3.2.5 FigTree

After the selection made by TreeAnotator among all the trees generated by Beast Fig tree gives an easy and intuitive interface to visualize and modify the phylogenetic tree. We can select between different options at the left side of the screen such as time scale, node labels, node bars, scale bar, scale axis or legend.

### 2.3.2.6 TreeGraph

With TreeGraph is possible to both visualize and edit a phylogenetic tree. Besides, it supports several (visible or invisible) annotations (e.g. support values) for every branch or node. These annotations can be imported from Nexus tree files or text files containing tabulated data (e.g. exported from a spreadsheet program).

## 2.3.1 Reconstruction of ancestral sequences

A consensus phylogenetic tree has been obtained following the previous steps. Now we have to infer the ancestral sequence from the tree.

Although there are different software for this purpose, in this thesis we

use PAML. As we mention previously, the ancestral sequences are inferred using maximum likelihood algorithm.

### **2.3.3.1. PAML**

Phylogenetic Analysis by Maximum Likelihood (PAML) is a package of programs for phylogenetic analysis. It can analyse DNA or protein sequences using maximum likelihood. To reconstruct an ancestral sequence in this thesis we use **codml** programme. To run **codml** we need a sequence data file, a tree file (in Newick format), a matrix file (usually Jones matrix) and the control file before running the programme.

We have to make sure that all the input files of the alienation (.fas) and the tree file (.tre) have the exact same sequences and names of sequences. Moreover, we have to make sure that the model we choose at Beauty to construct the tree is the same that we input in codml, in this case Jones model. Once everything is set up, we run the executable file and the program will start computing the algorithm to calculate the ancestral sequences.

When the process is over, the program creates an output file (.rst) with all the information of the process, posterior probabilities and the joint and marginal protein reconstructions. For this thesis we choose marginal

```

codeml.ctl - Notepad
File Edit Format View Help
seqfile = LPMD.fas * sequence data filename
treefile = LPMD.tre * tree structure file name
outfile = LPMD_ef_jones * main result file name

noisy = 9 * 0,1,2,3,9: how much rubbish on the screen
verbose = 3 * 0: concise; 1: detailed; 2: too much
runmode = 0 * 0: user tree; 1: semi-automatic; 2: automatic
* 3: StepwiseAddition; (4,5):PerturbationNNI; -2: pairwise

seqtype = 2 * 1:codons; 2:AAs; 3:codons-->AAs
CodonFreq = 2 * 0:1/61 each, 1:F1X4, 2:F3X4, 3:codon table

*
ndata = 10
clock = 0 * 0:no clock, 1:clock; 2:local clock; 3:CombinedAnalysis
aaDist = 0 * 0:equal, +geometric; -linear, 1-6:G1974,Miyata,c,p,v,w
aaRatefile = jones.dat * only used for aa seqs with model=empirical(_F)
* dayhoff.dat, jones.dat, wag.dat, mtmam.dat, or your own

model = 3
* models for codons:
* 0:one, 1:b, 2:2 or more dN/dS ratios for branches
* models for AAs or codon-translated AAs:
* 0:poisson, 1:proportional, 2:Empirical, 3:Empirical+F
* 6:FromCodon, 7:AAClasses, 8:REVaa, 9:REVaa(nr=189)

NSsites = 0 * 0:one w;1:neutral;2:selection; 3:discrete;4:freqs;
* 5:gamma;6:2gamma;7:beta;8:beta&w;9:beta&gamma;
* 10:beta&gamma+1; 11:beta&normal>1; 12:0&2normal>1;
* 13:3normal>0

icode = 0 * 0:universal code; 1:mammalian mt; 2-10:see below
Mgene = 0
* codon: 0:rates, 1:separate; 2:diff pi, 3:diff kapa, 4:all diff
* AA: 0:rates, 1:separate

fix_kappa = 0 * 1: kappa fixed, 0: kappa to be estimated
kappa = 2 * initial or fixed kappa
fix_omega = 0 * 1: omega or omega_1 fixed, 0: estimate
omega = .4 * initial or fixed omega, for codons or codon-based AAs

fix_alpha = 1 * 0: estimate gamma shape parameter; 1: fix it at alpha
alpha = 0. * initial or fixed alpha, 0:infinity (constant rate)
Malpha = 0 * different alphas for genes
ncatG = 8 * # of categories in dG of NSsites models

getSE = 0 * 0: don't want them, 1: want S.E.s of estimates
RateAncestor = 1 * (0,1,2): rates (alpha>0) or ancestral states (1 or 2)

```

Figure 2.6. Screenshot of control file of *codeml* in PAML. There we change our input *.Tree* and *.Fas* files in order to reconstruct nodes sequences.

```

C:\Users\Ibarandiaran\Desktop\OneDrive - Asociacion Cic Nanogune\ENZYME ...
Reading matrix from jones.dat
ntime & nrate & np: 100 0 100

np = 100
lnL0 = -14735.075979

Iterating by ming2
Initial: fx= 14735.075979
x= 0.06133 0.03911 0.09596 0.03475 0.03539 0.04412 0.01739 0.05978 0.01
671 0.03857 0.09404 0.05108 0.06929 0.08646 0.08813 0.10839 0.08520 0.0
9958 0.01988 0.06179 0.02941 0.04863 0.07317 0.04342 0.07299 0.04850 0.
08602 0.04033 0.00123 0.04104 0.09557 0.04516 0.10176 0.07390 0.05234 0.
107262 0.06472 0.08873 0.03724 0.03287 0.09244 0.08730 0.01827 0.06748
0.08251 0.03892 0.05045 0.07710 0.10767 0.02761 0.09866 0.02077 0.10663
0.01242 0.03816 0.10567 0.10795 0.04943 0.06242 0.05338 0.10420 0.09873
0.10297 0.10356 0.06867 0.01500 0.04094 0.09089 0.08168 0.09492 0.0649
6 0.10640 0.10878 0.03000 0.10522 0.02895 0.04800 0.08824 0.04817 0.087
84 0.03828 0.02297 0.01179 0.09255 0.09639 0.08246 0.03589 0.04052 0.02
439 0.06059 0.01732 0.08886 0.10495 0.06806 0.09466 0.05096 0.07656 0.0
5469 0.06208 0.05397

1 h-n-p 0.0000 0.0001 6086.9821 ++ 13164.188701 m 0.0001 105 1/100
2 h-n-p 0.0000 0.0001 1050.2195 ++ 13077.158239 m 0.0001 208

```

Figure 2.7. PAML program running the calculations for the ancestral reconstruction of our protein.

## **Chapter 3: Experimental methods**

---

This chapter explains the experimental procedures followed during this thesis. The experimental works of this thesis are divided in three different sections. The first section explains the molecular biology techniques and procedures applied for obtaining the different proteins used during this work. The second section, following the results from the first section, shows the experiments realized in order to characterize each enzyme. Finally, the third section explains the production and characterization of the nanomaterial obtained with our proteins.

It is important to note that all the experiments carried out during this work were applied equal and at the same time to the ancestral enzyme and its homologous extant one (Query).

## **3.1 Molecular biology**

To carry out this research it has been necessary to design, express and purify the ancestral sequences obtained from the ancestral reconstruction and their Query. During this section all the procedures followed, from the genetic engineering to the purification, are explained.

### **3.1.1 Genetic engineering procedures**

The genes obtained from the ancestral reconstruction step are purchase from Life Technologies, which are provided inside of the commercial plasmid and with the sequences of the genes codon-optimized for their expression in *Escherichia coli*. Besides, we need to order all the genes with specific restriction sites, that later will allow to introduce our gene in a desire expression to produce the enzyme.

#### **3.1.1.1 Commercial plasmid amplification and digestion**

The first step is to amplify the commercial plasmid containing the gene of interest. We use *E. coli* XL1-Blue competent cells (Agilent technologies) with approximately 50 ng of DNA following the protocol of Agilent Technologies. The transformation takes places in ice, in order to maintain the competent character of the cells. Then, the bacteria's are grown in SOC media (Invitrogen) for 1 h at 37C° and 250 rpm to later culture them over plates made of LB, Agar, Carbenicillin (Fisher) at 37°C. The commercial plasmid is resistant to Carbenicillin antibiotic. After letting them grow overnight, single columns are picked and grown in LB containing 0.1 µg/mL of Carbenicillin for 12-16 h at 37C° and 250

rpm. Cells were then pelleted by centrifuging them to 4000 rpm for 10 min at 4C° and plasmidic DNA is extracted from them with QIAprep© miniprep kit (QIAGEN). Finally, plasmidic DNA is eluted and stored in nuclease-free water (Fisher) and concentration is determined using the Nanodrop 200L spectrophotometer (Thermo Scientific).

When the commercial plasmid, containing our genes, is amplified the digestion is done to bind our gene sequence to the desire plasmid. All our genes have a *Bam*HI restriction site in their 5' end and a *Kpn*I site in their 3' end. These sites can be open using restriction enzymes purchase in Thermo Scientific and following the manufacturer's Fast Digest protocol. The final digestion volume is adjusted to 50 µL and incubated at 37C° for one hour. The digestion products are screened in a DNA agarose gel (1%) in TAE buffer. All DNA agarose gels are run using Bio Rad agarose electrophoresis equipment for approximately 90 min. using UV light we can observe two bands in the gel, one corresponding to the commercial plasmid and another one corresponding to our protein gene. For each gene we will have different sizes. Finally, the gene is purified with a DNA extraction kit from *Thermo Scientific* following the usual protocol. Concentrations are calculated using *Nanodrop 2000L* system.

### **3.1.1.2 Expression plasmid-protein sequence constructs ligation**

When the digestion is successfully done, the genes encoding our ancestral and query enzymes have to be ligated to a high-efficiency bacterial expression vector with compatible cohesive ends. The restriction enzymes produce cohesive ends so the insertion of the

purified gene into the plasmid was bidirectional and could produce the chimeric protein of interest. In this work, we use two different plasmids:

### **pQE80 L**

This plasmid was a kind gift from Professor Julio Fernandez’s lab at Columbia University. It contains ampicillin resistance gen for selection and the protein expression is induced with Isopropyl  $\beta$ -D-1 thiogalactopyranoside (IPTG). IPTG is a chemical compound that inhibits the suppression of the lac inhibitor in the lac operon that controls the expression of the protein of interest. The plasmid also has an N-terminal *his-tag* that attaches a 6-histidine chain to the recombinant proteins and helps the partial or total protein purification by using metal affinity resins.

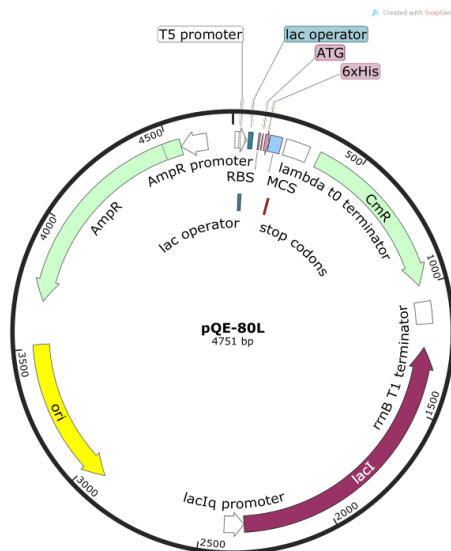
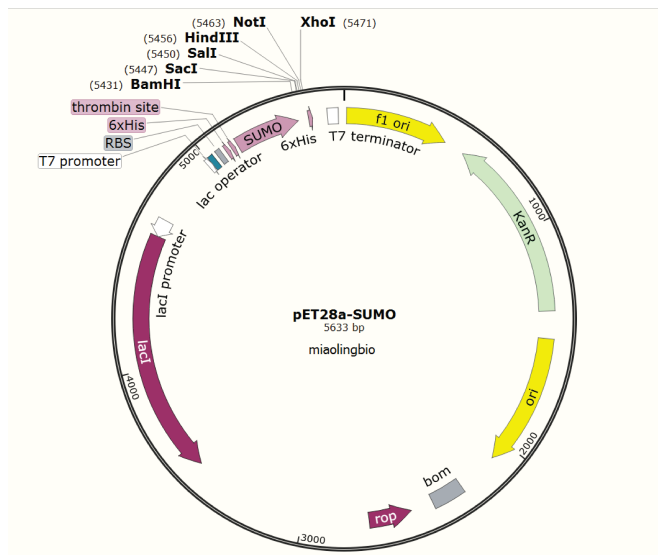


*Figure 3.1. pQE80 expression plasmid. This plasmid contains carbenicillin resistance gen for selection and a lac operator for controlling protein overexpression by IPTG.*

### pETT28a

plasmid contains kanamycin resistance gene for selection and the protein expression is induced with IPTG. This plasmid has the *his-tag* that attaches a 6-histidine chain to the recombinant proteins in the C-terminal.

Invitrogen's T4-DNA ligase protocol is used for the ligation process between the plasmids and the genes. The mol ratio between the amount of plasmid vector and gene inserts is 3:1. Ligations were incubated overnight at room temperature. Diluting the ligation with 5 times deionized water stops the process.



Figure

3.2. PET28a+ expression plasmid. This plasmid contains kanamycin resistance gene for selection and a lac operator for controlling protein overexpression by IPTG.



### **3.1.1.3 Amplification of recombinant plasmid**

We transformed *E.coli* XL1-Blue competent cells with 50 ng of DNA using the manufacturer protocol [146], the bacteria were grown in super optimal broth medium (Invitrogen) for 1 hour at 37°C and 250 rpm of agitation. The cells were plated onto LB agar plates with carbenicillin (for xylanases and endoglucanases) or kanamycin (for LPMOs) and were grown overnight at 37°C.

We took individual colonies to grow them in 5 mL of LB media with the corresponding antibiotic for 16 hours at 37°C and 250 rpm of agitation. After incubation time, cells were harvested by centrifugation at 14000 rpm, 10 minutes and at 4°C. We discarded the supernatant and plasmids were extracted from the pellets using the commercial QIAprep® miniprep kit (QIAGEN). The plasmid was eluted using miliQ water and we measured the DNA concentration using Nanodrop 200L spectrophotometer (Thermo Scientific).

### **3.1.1.4 Expression test of recombinant proteins**

Once we have our gene of interest, we transformed the construct into BL21 cells to test the protein expression, like with XL1 Blue, around 50 ng of the plasmid were used. We selected several colonies from the LB agar plates, with their corresponding antibiotic, that were grown overnight. Grew each colony in 10 mL LB media with carbenicillin or kanamycin until 0.6 O.D. Then, divide the 10 mL in two of 5 mL and to one of it we added 1 mM IPTG for protein over expression induction and the other one as a control. We let them grow overnight at 37°C and

agitation of 250 rpm. The next day we took 1 mL of both tubes to pellet the cells by centrifugation (4000 rpm, 4°C and 10 min). The supernatant was discarded, and the cells resuspended in 20 µL of extraction buffer (50 mM sodium phosphate and 300 mM NaCl at pH 7) and 20 µL of 2xSDS page sample buffer solution for the denaturalization and charging of the protein in acrylamide electrophoresis gel separation. Samples were again centrifuged for 30 minutes at 14000 rpm for separating the soluble proteins to the debris. The samples were incubated at 95°C for 5 minutes to finally run the SDS-PAGE gel to separate proteins by size. We loaded 20 µL of the samples into the polyacrylamide gels (stacking 4%, resolving 8%) and the electrophoresis was run for 1 hour and 30 minutes in a Bio-Rad electrophoresis system, at 120 V in running buffer solution (Bio-Rad). After the gels run to the end, they were cleaned in deionized water for 30 minutes. Then, the proteins are stained with Bradford solution (Thermo Scientific) for 30 minutes and washed with washing solution (10% ethanol, 10% acetic acid and 80 % miliQ water). We took an image of the gels in the Kodak image Station 4000R.

In the gel we could observe the protein overexpression in the IPTG treated samples, as an intense band. The colonies with the best expression were used for large-scale protein production.

### **3.1.2 Protein production**

The colony that showed more expression was selected for bigger production and purification. First, 1 mL of the selected inoculum without IPTG is added to 1L of LB media with 0.1% of the corresponding antibiotic. To maintain the ability of overexpression of the bacterial pLys

system we add 0.05 % of chloramphenicol. We incubated the culture at 37°C until the OD of the culture reached 0.6, in this moment we added 100 mg/mL IPTG to the culture for protein overexpression induction. We add 0.5 mM Cu<sup>2+</sup> to LPMO culture, as LPMO has a conjugated Cu<sup>2+</sup> atom [147]. We let bacteria produce the protein overnight at the specific temperature for each protein and 250 rpm. We have seen that all, ancestral and extant, proteins are expressed at the same conditions except the LPMO from *S.viridosporus* and the reconstructed ancestral one needed to be expressed at 20°C in order to have an optimum expression.

After the expression of the protein from our host bacteria we removed the medium from the bacteria by centrifugation (4000 rpm at 4°C for 30 minutes) and we collected the pellets. The pellets were resuspended in 16 mL of extraction buffer (50 mM sodium phosphate and 300 mM NaCl at pH 7), we added 160 µL of protease inhibitor (Merk Milipore) and 100 mg/mL of lysozyme (Thermo Scientific) incubating the mixture 30 minutes at 4°C with gentle agitation. We followed the lysis of the bacteria with a chemical lysis by adding 1.6 mL of 10% Triton solution (Sigma Aldrich) for the destabilization of the bacterial membrane, 80 µL of 11 mg/mL DNase I (Invitrogen) and 80 µL of 1 mg/mL RNase A (Ambion) for DNA and RNA enzymatic degradation respectively, and 160 µL of MgCl<sub>2</sub> 1M (Sigma Aldrich) to improve the DNase and RNase catalytic activities. The mixture was incubated for 10 min at 4°C with gentle agitation again. We followed the chemical lysis with a mechanical cell lysis using French press (G. Heinemann HTU DIGI-F Press). The mixture was introduced in the press chamber and lysed at 18000 psi during approximately 30 minutes. We obtained a darker solution that we centrifuged in an ultracentrifugation system (Beckman

Coulter Avanti J-26 XOI) at 33000 G at 4°C for 90 minutes to separate the soluble proteins from the debris.

The pellet was discarded and the soluble proteins in the supernatant were mixed with His Trap column cobalt or nickel affinity resins (thermo Scientific) for 1 hour at 4°C with gentle agitation. The pQE-80L and pET28 a+ plasmids have a His Tag that gives to the expressed protein a 6 histidine tag that has affinity to His Trap columns, making our protein to bind them. After the incubation of our protein of interest with the resin we washed the resin with the attached protein 3 times with extraction buffer. We place the resin in a proper column with a filter to appropriately elude our protein from the resin. For that, we use an elution buffer containing imidazole (50 mM sodium phosphate and 300 mM NaCl at pH 7 and 150 mM Imidazole).

### **3.1.3 Protein purification**

All the proteins were purified using a similar protocol, with small changes regarding the stability of each protein.

#### **3.1.3.1 Xylanase purification**

Both xylanases, the ancestral and the query, were expressed as explained in section 3.1.2. The Protein expression at the host bacteria was made at 37°C overnight. After the expression of the protein and lysis of the bacteria we bind our protein to a His trap cobalt column. Both xylanases contain a His tag composed of 6 consecutive histidines in the N terminus of the construct, which poses the ability to specifically bind to the cobalt

affinity column. This binding was later eluted with elution buffer containing imidazole (50 mM sodium phosphate and 300 mM NaCl at pH 7 and 150 mM Imidazole). We eluted in fractions of 0.5 mL and measure the protein concentration on the Nanodrop at A280, we eluted until the protein concentration decrease considerably. Fractions containing the mayor protein concentration were mixed and the others discarded.

We followed the purification by using a ÄKTA pure fast protein liquid chromatography (FPLC) system (GE Healthcare) with a Superdex 200 column of 30 cm in diameter (GE Healthcare). In this step we separate proteins in terms of sizes and using the most appropriate buffer for our proteins. In the case of xylanase we used phosphate buffer 50 mM at pH 7. Fractions are collected in terms of their UV absorption, above 100 mAU. The fractions of the peak appearing

We followed the purification by using a ÄKTA pure fast protein liquid chromatography (FPLC) system (GE Healthcare) with a Superdex 200 column of 30 cm in diameter (GE Healthcare). In this step we separate proteins in terms of sizes and using the most appropriate buffer for our proteins. In the case of xylanase we used phosphate buffer 50 mM at pH 7. Fractions are collected in terms of their UV absorption, above 100 mAU. The fractions of the peak appearing after 80 minutes of elution are the ones containing pure xylanase.

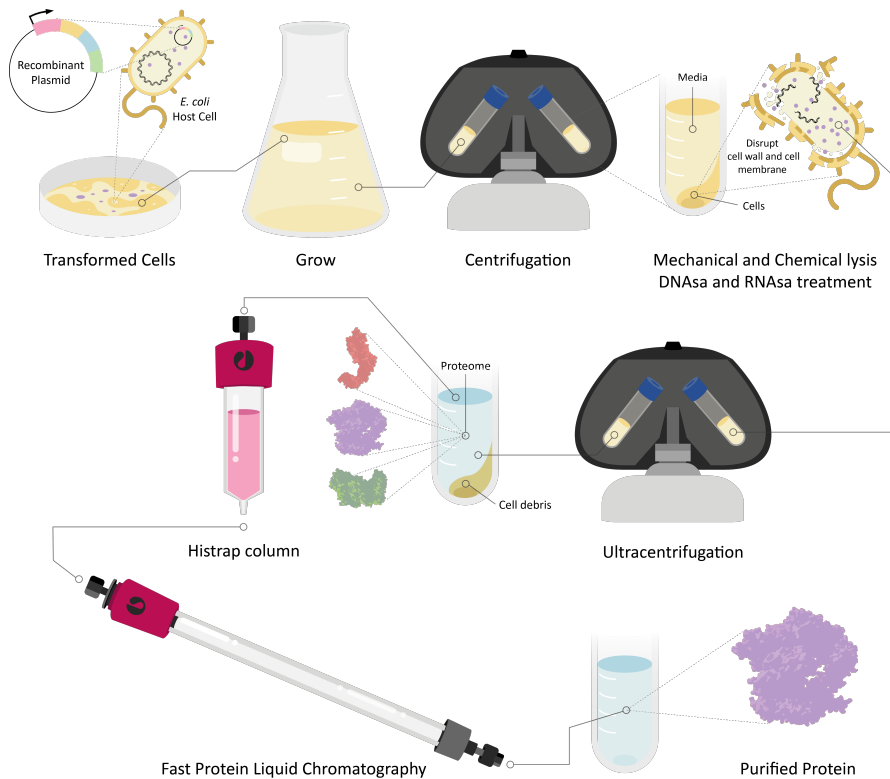


*Figure 3.3. Overview of protein purification protocol in our laboratory, the expression plasmids pQE80 or pT28A+ with the cloned genes, were transformed in the competent E.coli BL21 bacteria. The bacteria were grown in 1L of LB media overnight at 37°C and 250 rpm agitation. The bacteria were separated from the culture medium using centrifugation and then pellets were resuspended in extraction buffer. Then, bacterial cells were put down to chemical and mechanical lysis to disrupt the bacterial membrane to liberate the proteins. Soluble proteins were separated by ultracentrifugation and were mixed to a trap column as first purification step. To conclude the purification we used a size exclusion chromatography step to obtain purified proteins.*

### **3.1.3.2 C- LPMO purification**

Both LPMOs, the ancestral and the query, were expressed as explained in section 3.1.2. The expression of the protein from the host bacterium was made at 37 °C overnight. After the expression of the protein and lysis of it from the bacteria we bind our protein to a His trap Nickel column. Both LPMOs contain a His tag composed of 6 consecutive histidines in the C terminus of the construct, which poses the ability to specifically bind to the cobalt affinity column. Elution is made as specified in section 3.1.3.2.

Purification by using an ÄKTA pure fast protein liquid chromatography (FPLC) system (GE Healthcare) with a Superdex 200 column of 30 cm in diameter (GE Healthcare) was done using Acetate buffer 50 mM at pH 4. Fractions are collected in terms of their UV absorption, above 100 mAU. The fractions of the peak appearing after 85 minutes of elution are the ones containing pure LPMOs.

### **3.1.3.3 Ch-LPMO purification**

Both LPMOs, the ancestral and the query, were expressed as explained in section 3.1.2. But this time the expression of the protein from the host bacterium was made at 20 °C overnight. After the expression of the protein and lysis of the bacteria we bind our protein to a His trap Nickel column. Both LPMOs contain a His tag composed of 6 consecutive histidines in the C terminus of the construct, which poses the ability to specifically bind to the cobalt affinity column. Elution is made as specified in section 3.1.3.2.

Purification by using an ÄKTA pure fast protein liquid chromatography (FPLC) system (GE Healthcare) with a Superdex 200 column of 30 cm in diameter (GE Healthcare) was done using acetate buffer 50 mM at pH 4. Fractions are collected in terms of their UV absorption, above 100 mAU. The fractions of the peak appearing after 85 minutes of elution are the ones containing pure LPMOs.

### **3.1.3.3 Endoglucanase purification**

We used two Endoglucanases (EG); a *B.subtilis* EG and Ancestral EG (Anc EG), reconstructed in our laboratory. The purification of endoglucase was carried out first by temperature. We incubated the supernatant after the centrifugation of the last step of the lysis. The incubation is made at 50 °C for 30 minutes. In this step, proteins that are not thermostable precipitate. These proteins are discarded as pellet after centrifugation (4000 rpm, 4°C and 20 minutes). The remaining purification steps are made as specified in section 3.1.3.2

## **3.2 Enzymatic Characterization assays**

Each protein has its own specific activity, in this part of the chapter I will explain the activity they perform and the biocatalytic characterization assays we did in our laboratory. In one hand we characterized all proteins separately (each ancestor with their query) and in the other hand we have characterized their ability to work in combination: the synergy between our reconstructed enzymes. In the first step we characterize the proteins that have been reconstructed in this work whereas in the second part we use the reconstructed enzymes in this thesis and a reconstructed endoglucanase on a previous thesis in our laboratory.



### 3.2.1 Xylanase characterization

Xylanases (EC.3.2.1.8) is a class of enzymes that degrade the linear polysaccharide Xylan into Xylose. So, Endo  $\beta$ -1, 4- xylanase are mainly responsible for the hydrolysis of  $\beta$ -1, 4- bonds in plant Xylan, the main component of hemicellulose [148]–[150] (Figure. 3.4).

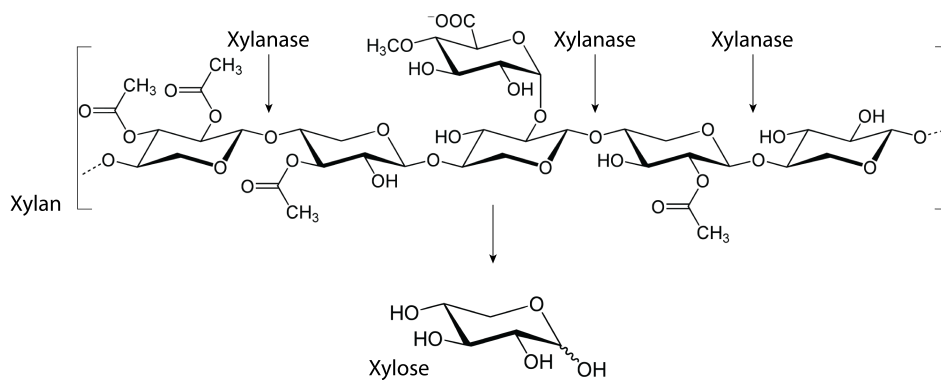


Figure 3.4.  $\beta$ -1,4- xylanase cleaving reaction to xylose. This enzyme cleaves  $\beta$ -1,4- bonds randomly, resulting in reduced xyloses.

The most commonly used method for the measurement of xylanase activity is commercial enzyme preparation is the 3,5-dinitrosalicylic acid (DNS) reducing sugar method [151] using Wheat Arabinoxylan (Megazymes) as substrate. Besides, in order to proof the promiscuity of our reconstructed xylanase we measure the kinetics of the ancestral xylanase and the *B.subtilis* xylanase with carboxymethylcellulose (CMC).

### 3.2.1.1 Wheat Arabinoxylan assays

We use commercial Wheat Arabinoxylan (Megazymes) to characterize Anc Xln and *Bt* Xln. Enzymatic hydrolysis with the substrate produces reduced xyloses. These reduced xyloses react with 3,5-dinitrosalicylic acid (DNS) that turns colour from pale yellow to brown. This colorimetric change allows us to determine the quantity of reducing sugars cleaved during the hydrolysis reaction. In this assay we prepared the reactants and substrate following commercial instructions, but modify the assay performance in order to characterize different features.

1% arabinoxylase solution was made adding 1 g of commercial wheat arabinoxylan to 90 mL of 100 mM sodium acetate buffer (pH 4.5) and dissolved by stirring at approximately 50°C for 10 minutes on a magnetic stirrer hot plate. Volume was adjusted to 100 mL using 100 mM sodium acetate buffer (pH 4.5). Solution was stored in a well-sealed Duran bottle at room temperature.

Different characterization assays were performed following the same steps and concentrations, unless the assay had specific requirements. In order to have a significant colorimetric signal the enzyme substrate ratio used in the reactions was 5 mg of xylanase for 1 g of substrate.

The hydrolysis were carried out using 450  $\mu$ L of 1% arabinoxylan, which made 0.0045 g of substrate, and 50  $\mu$ L of enzyme solution, with a total xylanase concentration of 0.0225 mg, to maintain the enzyme substrate ratio of 5 mg enzyme per gram of substrate. The substrate dilutions together with the enzyme are incubated at the desired conditions for 15 minutes prior 750  $\mu$ L of DNS were added to stop reaction. After DNS

reactant was added and the solutions were placed in a boiling water bath and boiled for 15 minutes. DNS reaction was stopped placing the boiled tubes in ice for at least 5 minutes and finally tubes colour intensity was measured at 540 nm using Nanodrop 200L spectrophotometer (Thermo Scientific). A reagent blank with the substrate and an enzyme blank were made for each condition and experiment.

Calibration curve was made using commercial xylose (Sigma Aldrich) standards at different concentrations in 500  $\mu$ L total volume and following the same procedure as for the blank and samples. Using this method we have characterize different features of the Xylanase.

#### **3.2.1.1.1 Temperature assay**

Thermo stability of the xylanases with arabinoxylan was measured by first preincubating the enzyme to the desire temperature for 5 minutes and then followed the hydrolysis reaction and reducing sugars measurement as explained in section 3.2.1.1.

#### **3.2.1.1.2 pH stability assay**

To characterize the pH stability of the xylanases we prepared arabinoxylan substrate 1% with different pH buffers ranging from pH 4 to pH 10. The hydrolysis reactions were carried out as explained in section 3.2.1.1. A substrate blank at each pH was made in order to avoid substrate degradation interference because of different pH buffers.

#### **3.2.1.1.3 $T_{60}$ Assay**

Enzymes were preincubated at 60 °C 0,5,10,15,20 and 25 minutes. After preincubation time they were place in ice for 10 minutes and 10 minutes

at room temperature. Preincubated xylanases were characterized by hydrolysis reaction as explained in section 3.2.1.1

#### **3.2.1.1.4 T<sub>50</sub> Assay**

Enzymes were preincubated at different temperatures from 40°C until activity decreased. After preincubation time they were placed in ice for 10 minutes and 10 minutes at room temperature. Preincubated xylanases were characterized by hydrolysis reaction as explained in section 3.2.1.1.

#### **3.2.1.1.5 Kinetics**

Different arabinoxylose concentration samples were prepared from 0.4 mM xylose to 40 mM xylose. 450 µL of each solution were used to measure the kinetic parameters. Reactions were performed as explained in section 3.2.1.1.

#### **3.2.1.2 CMC assays**

This assay is specific for measuring endoglucanases activity we wanted to see whether our enzyme could cleave randomly beta 1-4 glucosidic bonds in substrates that are not their own specific ones. Water-soluble derivatives of cellulose such CMC and hydroxyethylcellulose (HEC) are commonly used to characterize beta 1,4-glucosidic bonds cleavage [152], [153]. The reaction of hydrolysis can be determined in different ways determining the reducing sugars: using colorimetric measurements or measuring the viscosity. We determined the colorimetric change in order to characterize reducing sugar changes. This method requires 0.5 mg of absolute glucose released under the reaction condition [154]. The reducing sugars concentrations are finally measured by the DNS method.

An enzyme and reactive with substrate blanks are made together with the samples.

### **3.2.1.1.5 Kinetics**

We prepared different substrate concentrations by diluting CMC in 50 mM and pH 5 citrate buffer. Ranging concentrations from 0.005 mg/mL to 40 mg/mL, 250  $\mu$ L of CMC at different concentration were hydrolysed using 50  $\mu$ L of enzyme dilution containing a final concentration of 5 mg. The reaction was placed for 90 minutes and stopped by adding 750  $\mu$ L of DNS reagent. The mixture of the samples together with the DNS was placed in a boiling water bath and boiled for 15 minutes. DNS reaction was stopped placing the boiled tubes in ice for at least 5 minutes and finally tubes colour intensity was measured at 540 nm using Nanodrop 200L spectrophotometer (Thermo Scientific). A reagent blank with the substrate at all the used concentrations and an enzyme blank were made. A calibration curve was made by using different D-glucose concentrations and following the same conditions as the samples.

### **3.2.2 LPMO characterization**

C-LPMO and its Query Sv LPMO and Ch-LPMO) and its query Bt LPMO were characterized using a colorimetric assay to rapidly determine the activity. This assay is based on the recently discovered peroxidase activity of LPMO using 2,6 dimethoxyphenol (2,6-DMP) as chromogenic substrate. The enzymatic assay consists of 1 mM 2,6-DMP as chromogenic substrate, 100  $\mu$ M H<sub>2</sub>O<sub>2</sub> as co-substrate and an adequate

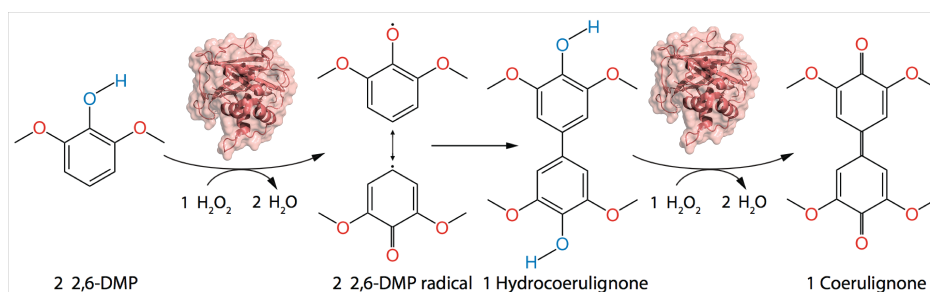


*Figure 3.5. 2,6-DMP oxidation: LPMO catalyses the oxidation of 2,6-DMP to the corresponding phenoxy radical at the presence of  $\text{H}_2\text{O}_2$  as co-substrate. 2,6-DMP that generates the 2,6-DMP radical reduces the active site Cu (II). Two formed 2,6-DMP radicals dimerize rapidly to form the molecule call hydrocoerulignone, which by action of the LPMO is converted to coerulignone.*

concentration of LPMO in a suitable buffer. The high molar absorption coefficient of the formed product coerulignone ( $\epsilon_{469}=53,200 \text{ M}^{-1} \text{ cm}^{-1}$ ) makes the assay sensitive allowing performing reliable activity measurements of LPMO [155].

The reaction of the LPMO with 2,6-DMP has to be in presence of  $\text{H}_2\text{O}_2$  as cosubstrate, which outperforms oxygen as cosubstrate. This reaction depends on the initial reduction of the active site copper from its Cu (II) state to Cu (I). 2,6-DMP and  $\text{H}_2\text{O}_2$  are converted to 2,6-phenoxy radicals and water. Next, two 2,6-DMP phenoxy radicals dimerize and form hydrocoerulignone, which is again oxidized by LPMO forming the final Chromogenic product coerulignone (Figure 3.6).



Figure 3.6. Spectrophotometer EPOCH 2 plate reader from BioTek.

Unless otherwise specified, all the reactions were performed in 96- well plates mixing 166  $\mu\text{L}$  of 100 mM phosphate buffer pH 8, 20  $\mu\text{L}$  of 10 mM DMP (final concentration of 1mM) and 4  $\mu\text{L}$  of 5mM  $\text{H}_2\text{O}_2$  (final concentration of 0,1 mM). Finally we add 10  $\mu\text{L}$  of enzyme dilution at a suitable concentration to each well, in a final volume of 200  $\mu\text{L}$  per well. Plates were orbital mixed and reaction was follow at 50°C. Activity was calculated measuring the increase of absorbance at 469 nm for 5 minutes using the molar absorption coefficient of coerulignone ( $\epsilon_{469}=53,200 \text{ M}^{-1} \text{ cm}^{-1}$ ) to calculate the peroxidase activity of LPMO.

### 3.2.2.1 DMP Kinetic assay

The Michaelis-Menten constant ( $K_m$ ) was calculated changing DMP concentration in each well from 0.05 to 4 mM. The catalytic constant ( $K_{cat}$ ) was determined from  $V_{max}$  and enzyme concentration. Reaction was carried out as explained in section 3.2.2. The enzymatic

concentration for all the substrate concentration was 0.15 mg per each well (Figure 3.7).



*Figure 3.7. Example of a kinetic assay of DMP. The less substrate concentration the lighter orange we see. The experiment was carried out from 0.05 mM to 4 mM DMP.*

### **3.2.2.2 DMP temperature assay**

To study the resistance of the LPMO to the temperature we designed a new experiment based on the DMP assay (section 3.2.2). As DMP is a substrate sensible to high temperatures we could not carry out the reaction at high temperatures. We preincubated the LPMO enzymes to the targeted temperatures for 5 minutes in a 1.5 mL eppendorf in a thermo mixer and then place them in ice for 5 minutes. The reaction was carried out at a 96 well plate (thermo fisher). 169,5  $\mu$ L 100 mM phosphate buffer pH 8, 20  $\mu$ L 10 mM DMP as a chromogenic substrate that makes a final concentration of 1mM, 0.5  $\mu$ L of 5 mM H<sub>2</sub>O<sub>2</sub> and 10  $\mu$ L of enzyme dissolution with adequate enzyme concentration making a final volume of 200  $\mu$ L. Absorbance at 469 nm was measured during 30 minutes at Epoch 2 spectrophotometer (Figure 3.7).



### **3.2.2.3 DMP pH assay**

pH profile of the LPMO's was performed using DMP assay, as DMP uses H<sub>2</sub>O<sub>2</sub> as a cofactor. pH profile for the activity of the all LPMO's was made at a 96 well plate (thermo fisher) following the steps in 3.2.2.2. The pH of the reaction was the pH of the buffer (169,5 µL out of 200 µL). Different pH buffer dissolutions were prepared from pH 3 to pH 10: 100 mM citric acid for pH 3-5, 100 mM phosphate buffer for pH 6-7, 100 mM carbonate buffer for pH 8 and 100 mM Boric acid for 9-10.

### **3.2.3 Reconstructed enzymes synergy**

To test the synergy between our ancestral enzymes comparing with the nowadays enzymes we designed an assay in were we studied the activity of the enzymes in lignocellulosic complex substrates. For that, we used 0,4 grams of pulps kindly provided from ENCE: One Unbleached Kraft pulp (UBKP) and other Bleached Kraft pulp (BKP) (Figure 3.8). Before the enzymatic hydrolysis we milled the substrates with 1mm grinder to facility the enzyme activity.

These two substrates are what we called non-ideal substrates. We used them as reference of lignocellulosic materials that we can found in lignocellulosic waste. UBKP contains lignin, hemicellulose and cellulose, and BKP contains hemicellulose and cellulose.

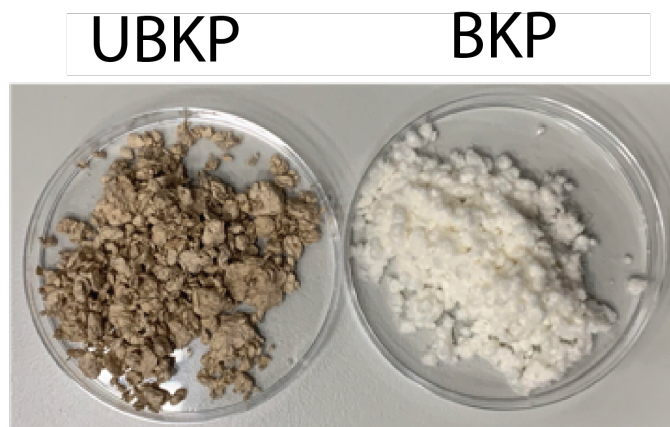


*Figure 3.8: Non-ideal lignocellulosic substrates used for synergy test in our laboratory. On the left side, Unbleached Kraft Pulp (UBKP) a paper pulp that contains the main three components of lignocellulosic biomass (lignin, hemicellulose and cellulose). On the right side, Bleached Kraft Pulp (BKP) a pulp after a bleaching process to remove lignin, it is mainly composed of hemicellulose and cellulose.*

For the comparison of different enzyme contribution in this hydrolysis we used different enzymatic ratios always maintaining the ratio of 5 total enzyme mg per gram of substrate. The ratios we used were: EG+CBM alone, EG+CBM + Xln (ratio 4:1), EG+CBM + LPMO (ratio 3:1), EG+CBM + Xln+ LPMO (ratio 3:1:1). As a control we used the queries in the same raitios. When C-LPMO was in the cocktail we added 2 mM of ascorbic acid (Sigma Aldrich) as electron donor. The hydrolysis was then incubated at 50°C in agitation and water for 24 hours. We stopped the reaction by placing the Erlenmeyer in ice. Then we took a sample to calculate reducing sugars yield. EG reacts with cellulose, Xln with hemicellulose and C-LPMO with both.

Reducing sugars yield was measured by 3,5- dinitrosalicilic acid (DNS) [B 163,164], similar to section 3.2.1.1 but with some changes. Again, we used this method to quantify the reducing sugars produced during the enzymatic hydrolysis with a colorimetric measurement. We took 1 mL from each reaction and we added 3 mL of DNS reagent. Then, we boiled the solution for 5 minutes in a boiling water bath and cooled the boiled samples in ice for 10 minutes. Finally, we added 20 mL of miliQ water and measured the absorbance at 540 nm in a Nanodrop 200L spectrophotometer (Thermo Scientific). We used a glucose standard curve to calculate the reducing sugars concentrations in the different hydrolysis samples (mg/mL). We prepared standards from 0.05 mg/mL glucose to 2 mg/mL and follow the same procedure that with the samples.

We prepared a substrate blank and all the enzyme ratios blanks, with ascorbic acid when needed, at each experiment. The blank were treated same to the samples and their absorbance was rested to the samples. Once we calculated the reducing sugar concentration we used the equation [1] or [2] to calculate the total reducing sugar conversion. The formulas are the same, but the concentration of the products sensible to the hydrolysed was different depending on the substrate and the enzymes we used.

$$[1] (\%) = \frac{\text{Reducing sugars (mg/mL)} \times 0,9}{\text{Initial cellulose concentration}} \times 100$$

$$[2] (\%) = \frac{\text{Reducing sugars (mg/mL)} \times 0,9}{\text{Initial cellulose and hemicellulose concentration}} \times 100$$

Where the factor 0,9 was to transform polysaccharides to monosaccharide's considering the water uptake during the hydrolysis.

### **3.2.4 CNC isolation and Characterization from BKP and UBKP**

0,4 grams of BKP and UBKP substrates were milled with a 1 mm grinder previous hydrolysis to facility the enzyme activity. For this hydrolysis we used enzymatic treatments with 5 mg of total protein per gram of substrate: we used ANC EG+CBM (Anc EG to abbreviate) alone and ANC EG+ C-LPMO (ratio 4:1). As a control for the ancestral enzymes we used the queries enzymes from the reconstruction trees, the EG (Q EG) and *Sv* LPMO from *S. viridiosporus*. we added 2 mM ascorbic acid (Sigma Aldrich) as electron donor fro LPMO activity. The hydrolysis was incubated at 50 °C in agitation and water for 24 hours. We stopped the reaction by placing the hydrolysis on ice and sonication the mixtures with a micro tip sonicator UPH100H Ultrasonic Processor (Hielscher) for 25 min at 75%. The nanocellulose was isolated by a gradual centrifugation steps and concentrated by ultracentrifugation at 33000 G for 1 hour. The pellets were resuspended in water and could be lyophilized in a Telstar Lyoquest for physicochemical characterization by freeze-drying for 24 hours. This process was optimized in a previous work in our laboratory [89].

#### **3.2.4.1 Atomic force microscopy of CNC**

The morphology of the nanoparticles obtained with enzymatic hydrolysis was studied with atomic forces microscopy (AFM) (Figure 3.9). This is a type of scanning probe microscopy (SPM), with demonstrated resolution

on the order of fractions and nanometre. It has more than 1000 times better diffraction limit than optical microscopes. A tip that is attached to a cantilever scans our sample. Information is gathered by the interaction between the tip and the sample, these interactions are attractive repulsion forces between them. Each time that there is an attractive or repulsive force between the tip and the sample the cantilever deflects, these phenomena allows us to map the deflections of the cantilever in each point of the sample. Images were captured at room temperature, in tapping mode, using Nanoscope V scanning probe microscope (Multimode 8 Bruker Digital instruments) with an integrated force generated by cantilever/silicon probes. The applied resonance frequency was 320 kHz. The cantilever had a tip radius of 5-10 m and was 125  $\mu\text{m}$  long. Samples were prepared by spin –coating (Spincoater P6700) at 2000 rpm for 130 seconds by casting a droplet of nanocellulose suspension on mica substrate. AFM height and phase mages were collected at the same time at all the samples.

Image frame were of 3x5  $\mu\text{m}$  for all samples, in there fibbers from different sizes could be distinguished. The length of 100 nanoparticles was measured to calculate the average length. The diameter and the aspect ratio (Length/Diameter) .

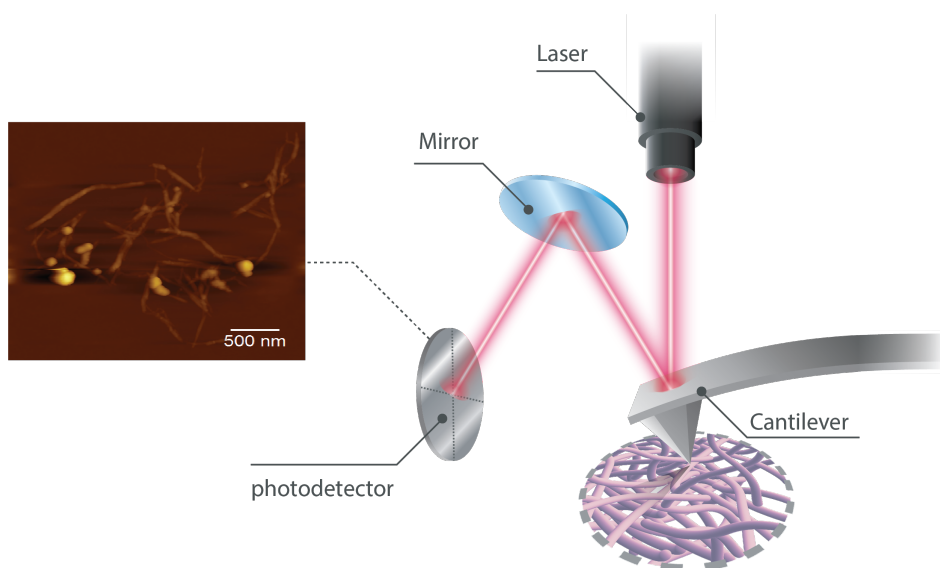


*Figure 3.9. Atomic force microscopy (AFM). This technique uses the interaction between the tip and the sample attractive-repulsion forces to create a deflection in the tip and permits to infer the images by mapping the deflections in each point of the sample.*

### **3.2.4.2 Fourier-transform infrared spectroscopy of CNC**

This technique was used to analyse the characteristic functional groups of cellulose and nanocellulose. This technique allows us to measure the changes that happen in a reflected IR beam when it contacts the sample. The IR we used in our measurements is a Nicolet Nexus spectrometer provided with a MKII Golden Gate accessory (Specac) with a diamond crystal at a nominal incidence angle of  $45^\circ$  and ZnSe lens. Spectra were measured in attenuated reflection (ATR) mode between 4000 and  $650\text{ cm}^{-1}$ , with averaging 32 scans and a resolution of  $4\text{ cm}^{-1}\text{ s}^{-1}$ .

### **3.3 New Nano biomaterial isolation**

In this section I will explain both how we isolated nanochitin (CNCh) from commercial  $\alpha$ -chitin (Sigma Aldrich) and how we characterized it. For the first time, we show how it is possible to isolate CNCh from recalcitrant commercial alpha chitin by using only enzymes. More accurately, Ch-LPMO .

#### **3.3.1 Enzymatic nanochitin isolation**

We used 1.6 grams of commercial chitin (Sigma Aldrich) for the isolation of nanochitin. As they have flake shapes there was no need to chopped or pre-treated them. We made the reaction in 200 mL of water by using 10 mg of C-LPMO and Sv LPMO per gram of substrate. The hydrolysis reaction was incubated at 50°C in agitation for different times (12, 24, 48 and 72 hours). We stopped the reaction placing the reaction on ice. Later, and in order to avoid nanochitin aggregation, the mixtures were sonicated with a micro tip sonicator UPH100H Ultrasonic Processor (Hielscher) for 25 minutes at 75%. The nanochitin was isolated by gradual centrifugation steps and concentrated by ultracentrifugation at 33000 G for 1 hour. The pellets were resuspended in water and could be lyophilized in a Telstar Lyoquest for physicochemical characterization by freeze-drying for 24 hours.

### 3.3.2 Nanochitin yields

The total nanochitin conversion was calculated by weighting the freeze-dried nanochitin from each hydrolysis and we calculated the yield by terms of equation 3.

$$[3] \text{ Nanochitin yield (\%)} = \frac{\text{nanochitin mass}}{\text{initial chitin mass}} \times 100$$

## 3.3 New Nano biomaterial characterization: CNCh

Nanochitin isolated by enzymatic treatment (En CNCh) with both ancestral and nowadays enzymes and nanochitin produced by acid hydrolysis from University of the Basque country (Ac CNCh) were analysed with different physicochemical techniques.

### 3.3.2 Atomic force microscopy

To study the morphology of the nanoparticles obtained with enzymatic hydrolysis and acid processes we used atomic force microscopy (AFM). We follow the same protocol that in section 3.2.4.1.

### 3.3.2 Fourier-transform infrared spectroscopy

This technique was used to analyse the characteristic functional groups of Chitin and nanochitin. We follow the same protocol that in section 3.2.4.2. In Figure 3.10 we show the characteristic peaks of  $\alpha$ -Chitin.



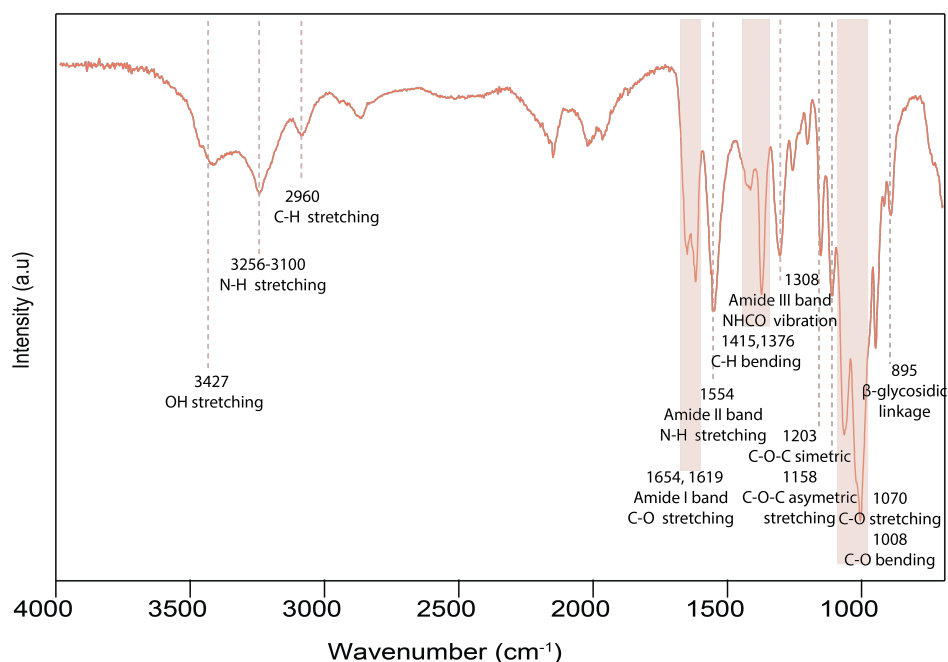


Figure 3.10. FTIR spectrum from  $\alpha$ -chitin. Typical spectrum from a chitin sample with the characteristics chitin functional groups measured in a range from 4000 to 650  $\text{cm}^{-1}$ .

### 3.3.3 X-Ray diffraction

In order to analyse the crystalline structure and crystallinity of CNCh, we use X-ray diffraction (XRD). This technique is based on the constructive interference of monochromatic X-rays and crystalline structures on the samples. X-ray powder diffraction patterns were collected using a Philips X'pert PRO automatic diffractometer operating at 40 kV and 40 mA, in theta-theta configuration, a secondary monochromator with  $\text{CuK } \alpha$  radiation ( $\lambda=1.5418 \text{ \AA}$ ) and PIXcel solid-state detector (active length in  $2\theta$   $3.347^\circ$ ). Data were collected from 5 to  $80^\circ$   $2\theta$  (step size 0.026 and time per step 80 seconds) at room temperature. A fixed divergence and

antiscattering slit giving constant volume of sample illumination were used.

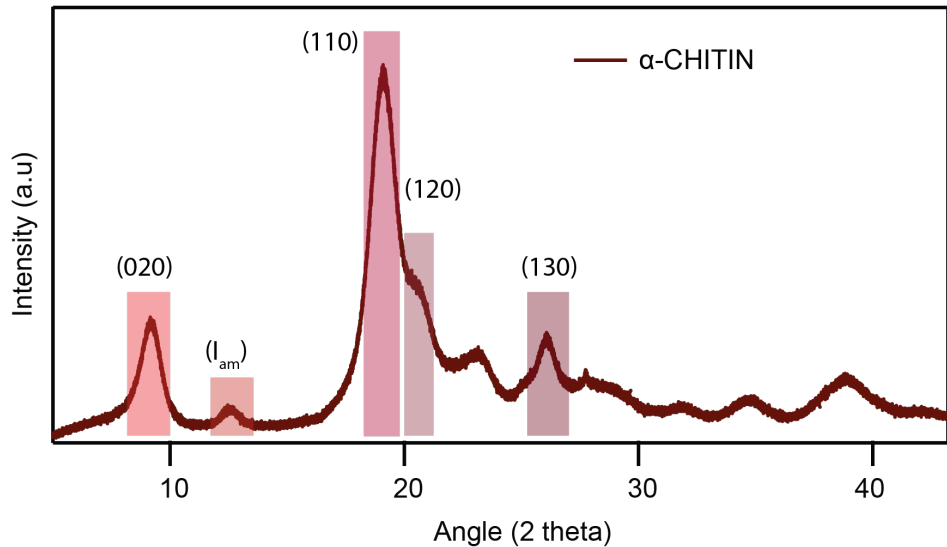


Figure 3.11. XRD spectrum from  $\alpha$ -chitin. Typical spectrum from chitin crystalline structure peaks. We note the crystalline planes that they represent.

The data collected was both analysed as raw data and a diffractogram. Crystallinity index (CI%) was calculated using Segal equation (Equation 4):

$$[4] \text{ Crystallinity index (\%)} = \frac{I_{200} - I_{am}}{I_{200}} \times 100$$

Where  $I_{200}$  is the intensity of the cellulose crystalline peak and  $I_{am}$  is the intensity of the amorphous peak. In Figure 3.11 we show an X-ray spectrogram of  $\alpha$ -Chitin.

### 3.3.4 Solid-state cross-polarization magic angle spinning $^{13}\text{C}$ nuclear magnetic resonance

The chitin functional groups were verified with solid-state cross polarization magic angle spinning  $^{13}\text{C}$  nuclear magnetic resonance CP/MAS  $^{13}\text{C}$  isotropic chemical shift, the contributions of aromatic and aliphatic groups. These groups contribute in different ranges: Aliphatic groups are placed in the range from 0 to 90 ppm and aromatic groups from 110 to 160 ppm. In the range of 160 to 185 we can find peaks corresponding to carboxylic acid derivatives.  $^{13}\text{C}$  CP/MAS NMR spectra were recorded on a 400 MHz BRUKER system equipped with a 4mm MASDVT TRIPLE resonance HYX MAS probe. Larmor frequencies were between 400,17 MHz and 100,63 MHz for  $^1\text{H}$  and  $^{13}\text{C}$  nuclei, respectively. Chemical shifts were reported relative to the signals of  $^{13}\text{C}$  nuclei in glycine. Relaxation delay of the sample was 5 seconds and rotation frequency was 12 KHz with 2K scans. Polarization transfer was achieved with RAMP cross-polarization (ramp on proton channel) with 5 ms contact time. High-power SPINAL 64 heteronuclear proton decoupling was applied during acquisition.

From the chitin NMR spectrum peaks (Figure 3.12) corresponding to each carbon from chitin polymer are observed. Peaks from 0 to 40 ppm correspond to alkyl groups, in this case to the  $\text{CH}_3$ . The peak around 55 ppm correspond to  $\text{C}_2$ , peaks between 60 and 70 correspond to  $\text{C}_6$  of the primary alcohol group. The peak between 70 and 80 ppm are assigned to carbons  $\text{C}_3$ ,  $\text{C}_5$  and  $\text{C}_4$ . Between 100 and 110 ppm we find the anomeric  $\text{C}_1$  carbon peak, and finally around 170 and 180 ppm we have the carboxyl group C

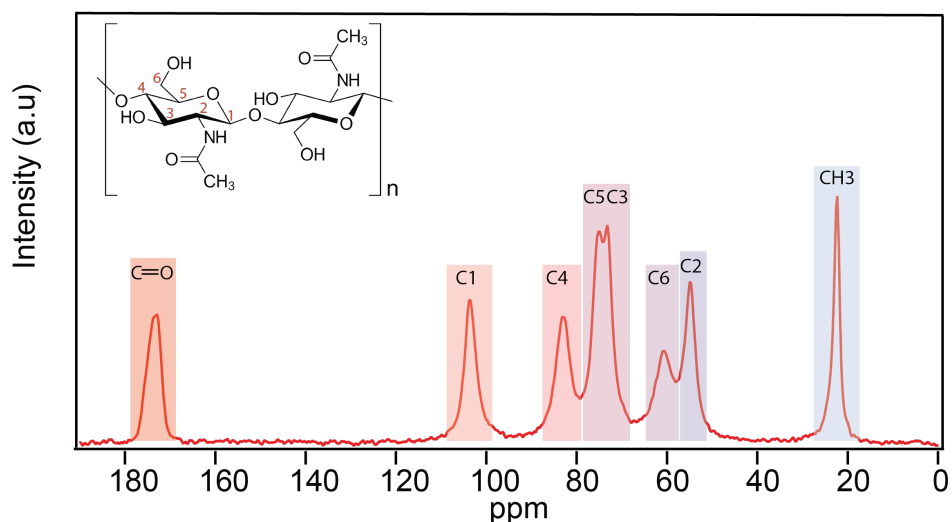
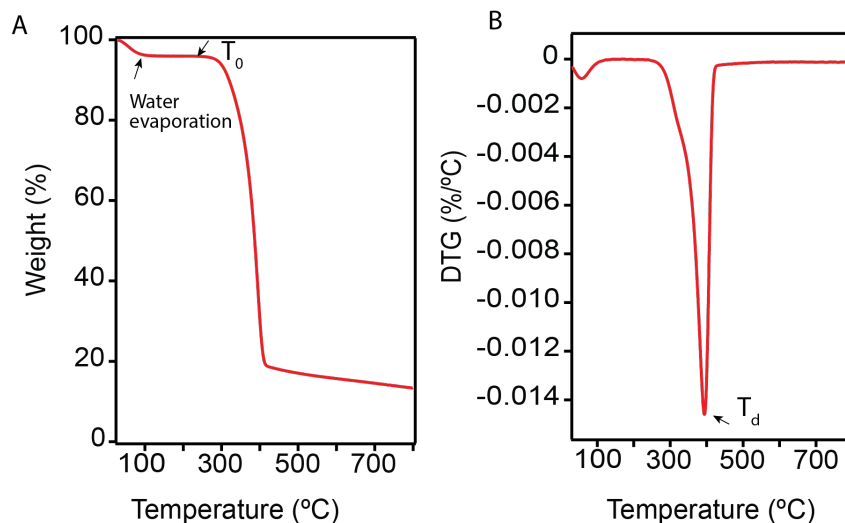


Figure 3.12. CP/MAS  $^{13}\text{C}$  NMR spectra of  $\alpha$ -chitin. At the NMR spectra different carbons from the chitin polymer can be observe. Peaks in the range of 0-40ppm correspond to primary, secondary or tertiary alkyl. Peaks in the range of 60 and 70 ppm usually correspond to C6 of the primary alcohol group. Peaks in the range of 70 and 80 ppm are assigned to C<sub>2</sub>, C<sub>3</sub> and C<sub>5</sub>. Peaks from 80 to 95 ppm are the ones corresponding to C<sub>4</sub> and between 100 and 110 ppm to the C<sub>1</sub> anomeric carbon. Finally the peak between 175 and 180 ppm correspond to the carboxyl C in the acetyl group

### 3.3.5 Thermogravimetric analysis

To determine the thermal stability of chitin samples we used thermogravimetric analysis (TGA). This technique measures the weight of the samples in a microbalance during a heating scan. This way, we follow the degradation process of the material. The analysis was carried

put using TGA/ADTA 85 Mettler Toledo equipment. 10 mg of all the samples were used and heated from 30°C to 800°C in a nitrogen atmosphere at scanning rate of 10°C/minute.



*Figure 3.12: (A) Weigh loss with temperature (B) DTG curves from commercial alpha chitin. The early weight loss, indicated in figure (A) is due to water evaporation absorbed by the chitin. The  $T_0$  is the loss of the 5 % of the weight and the  $T_d$  is the minimum of the peak in the derivative curve.*

The initial degradation temperature ( $T_0$ ) is described as the loss of 5% of the weight of the total sample and the maximum degradation temperature ( $T_d$ ) is the minimum of the degradation peak in the derivative of thermogravimetric curves (DTG).

---

# PART III

---

Capítulos 4, 5, 6, 7 y 8 sujetos a confidencialidad por la autora

---



---

# PART IV

---

## Chapter 9: Discussion

---

The aim of this thesis was to reconstruct ancestral enzymes with improved activity ranges, in terms of pH and temperature, for nanomaterial obtaining from biomass. First, we reconstructed a bacterial endo 1,4- $\beta$ -xylanase and a bacterial LPMO to help an Anc EG, reconstructed in our laboratory; these enzymes are able to produce nanocellulose from lignocellulosic biomass. Moreover, to consolidate the capability of ancestral enzymes for the obtention of nanomaterials we reconstructed another bacterial LPMO to hydrolyze chitin and compare the activities of the reconstructed enzymes with their homologous extant ones.

Reconstructed enzymes (table 9.1) showed identities equal or higher than 60% with their Queries, this means that they have enough mutations to act differently but still having the same catalytic activity.

*Table 9.1: Ancestral enzymes reconstructed in this work, their geological time, their Query, identity with the query and number of aminoacid mutated.*

Enzyme	Age (My)	Query	Identity	Mutations
Anc Xln	2.97	<i>Bacillus subtilis</i>	88%	25
C-LPMO	3.077	<i>Bacillus thurigiensis</i>	60%	71
Ch-LPMO	3.077	<i>Streptomyces viridisporus</i>	63%	69

The catalytic pocket is conserved in all reconstructed nodes, which means that the changes in activity we observed could be due to enzyme-substrate interaction. However, an ancestral node of Ch-LPMO tree showed an interesting mutation in its catalytic pocket were, instead of having a Valine (V), characteristic amino acid present in chitin hydrolyzing LPMOs, has a Leucine (L) (Figure 9.1 A), characteristic aminoacid present in cellulose hydrolyzing LPMOs [212], and it shares more common amino acids with cellulose hydrolyzing LPMO. The sequence belongs to Last Actinobacteria Common ancestor (LACA) node, the youngest bacterial filum in Ch-LPMO tree, which may indicate that LPMO evolved from degrading chitin to cellulose. There are some fossil evidences of chitin present in the first branched organisms 500 million years ago [213] and in multicellular organic-walled microfifrils around 900 million years ago [214], before cellulose appear in plant cell walls (cita), suggesting that our 900 mya reconstructed LACA Ch-LPMO could be on its transition to live with chitin structured organisms

to cellulose structures organisms, right before Cambrian explosion, when modern marine ecosystem started [212].



Figure 9.1. Ch-LPMO alignment A) Ancestral Ch-LPMO sequences from different nodes and Bt LPMO sequence alignment, from node 54 (LACA) mutations B) Alignment of reconstructed ancestral C-LPMO and St LPMO and reconstructed ancestral Ch-LPMO and Bt LPMO.

Reconstructed enzymes were from the Hadean and the Archeon eons where ocean temperature has been estimated to be around 60-70°C [71], [73], [215], [216], so bacteria living in that environment were extremophiles. Ancestral enzymes displayed this thermophile phenotype by showing increased activity in a range of temperatures and better thermal stability. Moreover, ancestral enzymes enhanced other properties such as pH, chemical promiscuity or higher expression rates. Several strategies have been proposed as protein engineering to improve enzymes activity for industrial applications, but none of them is capable of improving activity in different aspects at the same time. This proves

that ASR is an effective method to improve enzymes for industrial applications.

Reconstructed enzymes in this work improved several features regarding their Queries. Thermal stability was better in the three reconstructed enzymes: Ancestral xylanase showed more than 50% activity between 30-62°C whereas query xylanase from 40-60°C; Anc C-LPMO and Q C-LPMO had their optimal temperature at 70°C, but Anc C-LPMO showed 2.5 times higher activity; same for Anc Ch-LPMO that showed almost 2 times better activity than Q Ch-LPMO at their optimal temperature, 70°C. Reconstructed enzymes had same pH profiles than their extant homologous but showing higher activities in all pH-s for Anc Xln, and in basic pHs for the LPMOs. With REAL substrates, not laboratory substrates, they showed better activities and synergy than the queries. From these real subtracted we can obtain valuable nanomaterials, and here we proved that our reconstructed enzymes were more efficient in the obtention of nanomaterials from biomass than their queries.

Material science is predominantly an engineering discipline; where building blocks are intentionally assemble to achieve materials with desire properties, on the contrary, enzymes have been studied by biochemistry discipline, that provide exceptional features such as substrate specificity, rate acceleration, region-, chemo, and stereo selectivity within catalyzed reactions, so enzymes in industry are used to obtain chemically valuable products. **Here we combined the unique properties of both, materials and enzymes in a synergistic way leading to advance materials production and modification,** this integration of material and enzyme science is used in many fields such as

---

grafting coating of material, biosynthesis of materials, biodegradation of materials, immobilization of enzymes, biosensor... [217] (Figure 9.2) .

Ancestral enzymes effectively obtained nanomaterials from biomass. CNC and CNCh obtention from biomass is a promising application to these enzymes. These nanomaterials are natural, biocompatible, and biodegradable and can be obtained from waste. Besides their natural characteristics, their nano size give raise to great potential applications in biomedicine.

Our group successfully used an ancestral EG to obtain nanocellulose from cellulose and in this work, we have confirmed that the use of ancestral enzymes in material science develops unique and functional materials. Ancestral enzymes produced higher yields of CNC and CNCh than their modern homologues, but the most novel contribution of this work is not only that we obtain nanocellulose and nanochitin enzymatically from non ideal substrates, but **we are able, for the first time, to enzymatically oxidized these CNC and CNCh with a single enzymatic treatment: LPMO**. Reconstructed LPMOs in this work have, C-LPMO and Ch-LPMO, hydrolyze in an oxidative cleavage cellulose and chitin respectively.

Oxidation of these two nanoparticles surface is very important in material engineering to selectively modify these nanoparticles surfaces. Carboxyl groups are very reactive, and a functional group can be attached or substitute to the carboxyl group placing the desire functional group in these surfaces

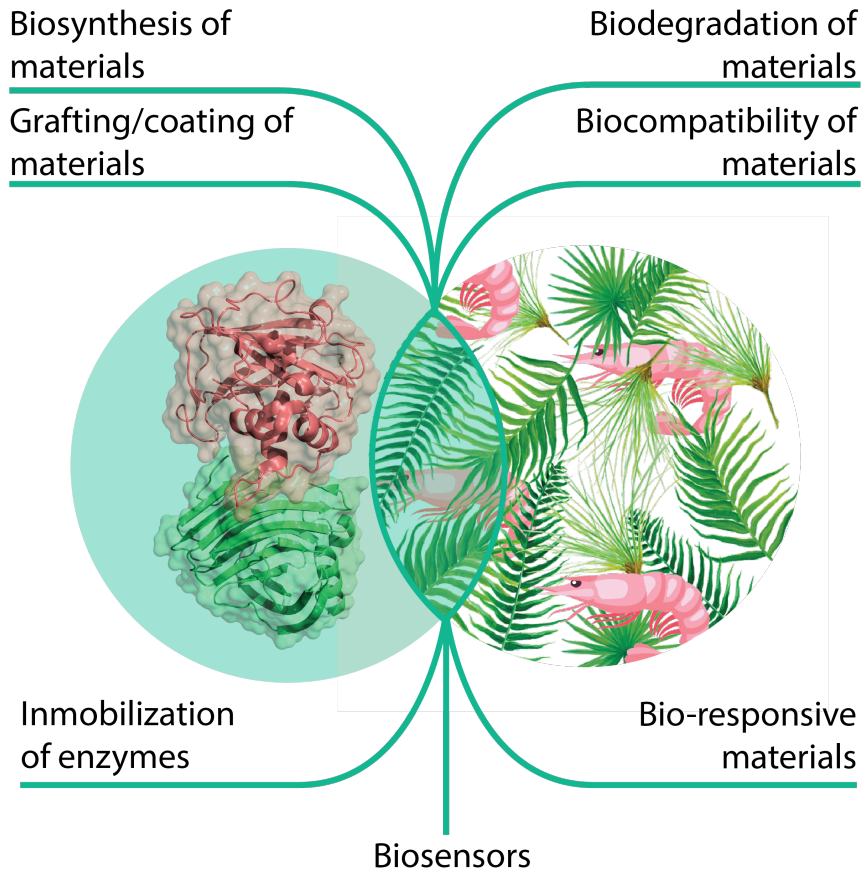


Figure 9.2: Fields of enzymes application in material science. In the Figure as an example the two most abundantly row materials on earth: lignocellulosic biomass and chitin.

.The enzymatic functionalization of these nanomaterials opens a new range of applications, as the biocompatibility and non-toxicity of the material is directly linked to its production protocol. For example, in pharmacology or biomedicine, where target drugs can be placed in these ends; or wrap treatments in a biocompatible CNC or CNCh films. We demonstrate that LPMO hydrolysis oxidizes nanocellulose and nanochitin as TEMPO, a chemical used in industry to oxidized materials,



do it [106]. Although cellulose C<sub>6</sub> carbon is oxidized like TEMPO, chitin, that has also an acetyl group in C<sub>2</sub>, showed two oxidized carbons. This has not been reported with TEMPO or other chemical mediation. Regarding RMN spectra (Figure 9.3), we think that LPMO acts oxidizing both C<sub>6</sub> and C<sub>2</sub> from nanochitin, demonstrating ancestral LPMO promiscuity towards different carbon oxidation from a polysaccharide chain, in comparison with the extant homologous.

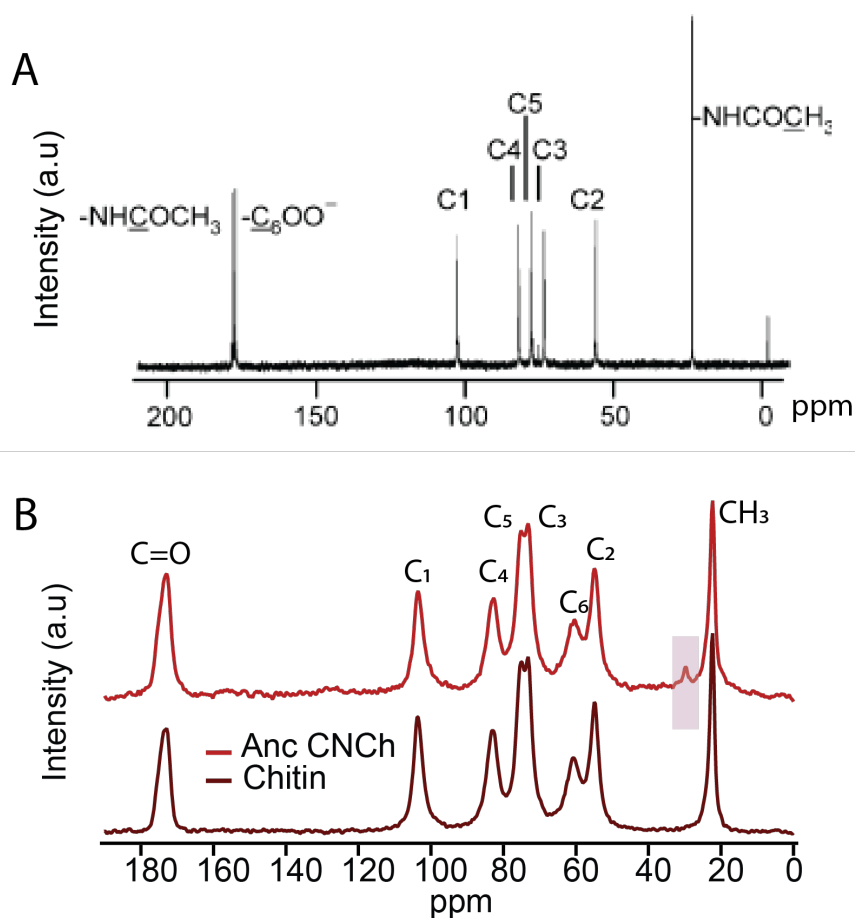


Figure 9.3 CP/MAS <sup>13</sup>C NMR A) TEMPO oxidized CNCh from literature [206] and, B)  $\alpha$ -chitin (marron) and Ch-LPMO oxidized CNCh (red).

Our enzymatic treatment of the materials is made with water, avoiding further dialysis processes to purify the nanomaterial and avoiding salts from the buffer to be attached to the nanomaterial surface. In addition, enzymes, as biomolecules, are biocompatible so the biocompatibility of the enzymatically engineered nanomaterials is preserved after treatment.

Reconstructed enzymes with not an oxidative cleavage are able of isolating nanomaterials from biomass preserving the native structure of the material. This was showed in a previous work in our group were Anc EG+CBM produced CNC with native cellulose polymorph from pure cellulose filter paper. Here we reconstructed an Endo 1,4-beta xylanase to degrade hemicellulose and help Anc EG+CBM isolate CNC. Ancestral enzymes showed better synergic work than modern enzymes, by obtaining higher reducing sugars and CNC conversion yields. Obtained CNC with EG+CBM and Anc Xln preserved cellulose native structure, the addition of the C-LPMO to the enzymatic cocktail boost the enzymatic reducing sugars and CNC conversion yields and produced an oxidized CNCs. It is therefore reasonable to think that native structure of chitin can be preserved using a chitinase to produce CNCh. In this work, we tried with a commercial chitinase that did not react with the recalcitrant chitin; in consequence it would be interesting to reconstruct an ancestral chitinase as we have seen that ancestral enzymes are more active with recalcitrant substrates. There are also enzymes for the deacetylation of chitin called chitin deacetylase, these combined with chitinases could produces for instance nanochitosan crystals that due to the lack of acetyl group would be CNC like but hydrophobic.

*Table 9.2: This table show the enzyme combination have been used in our laboratory, with which substrate and after the hydrolysis the structure of the nanomaterial.*

ENZYME	SUBSTRATE	CNC/CNCh STRUCTURE
EG	Cellulose	Native
EG+Xln	Cellulose	Native
EG+Xln+C-LPMO	Cellulose	Oxidized
Ch-LPMO	Chitin	Oxidized

In this work we show that different combination of enzymes produces nanomaterials with different structures (Table 9.2) so **we can have CNC and CNCh “a la carte” with the only use of enzymes.** This opens a new world to engineer nanomaterials with different features and biocompatible. According to our data, reconstructed enzymes are fundamental in these processes as they nanomaterial productions yields (table 9.3).

*Table 9.3: conversion yield in % of CNC from two UBKP and BKP substrates for enzymatic cocktail (CK) of EG+Xln+LPMO. We compare the yield difference for ancestral and modern proteins.*

SUBSTRATE	Conversion yield of enzymatic CK	
	Ancestral	Modern
UBKP	15%	11.5%
BKP	16%	12%

Nanochitin conversion is also more efficient with ancestral Ch-LPMO than with modern Bt LPMO obtaining 5 mg of CNCh and 2 mg of CNCh respectively. This means that ancestral LPMO is two folds efficient with recalcitrant chitin as substrate.

In this work we have successfully enhanced activities in terms of pH, T, expression levels and promiscuity of three enzymes using Ancestral Reconstruction method, a method that commonly is used in paleoenzymology studies. Moreover, these biomass degrading enzymes isolate CNC and CNCh from biomass more effectively than their extant homologous. On top of that, C-LPMO enzyme oxidized CNC and CNCh, opening a fully sustainable and biocompatible path to engineer nanobiomaterials for further biomedical applications.

# Bibliography

---

- [1] K. Kostarelos, A. Bianco, and M. Prato, “Promises, facts and challenges for carbon nanotubes in imaging and therapeutics,” *Nat. Nanotechnol.*, vol. 4, no. 10, pp. 627–633, 2009.
- [2] K. F. Mak, J. Shan, and D. C. Ralph, “Probing and controlling magnetic states in 2D layered magnetic materials,” *Nat. Rev. Phys.*, 2019.
- [3] M. N. Mustafa, S. Shafie, M. H. Wahid, and Y. Sulaiman, “Light scattering effect of polyvinyl- alcohol / titanium dioxide nanofibers in the dye-sensitized solar cell,” *Sci. Rep.*, pp. 1–8, 2019.
- [4] M. R. Begley, D. S. Gianola, and T. R. Ray, “Bridging functional nanocomposites to robust macroscale devices,” *Science (80-. )*, vol. 364, no. 6447, 2019.
- [5] C. Hong, T. T. Tang, C. Y. Hung, R. P. Pan, and W. Fang, “Liquid crystal alignment in nanoporous anodic aluminum oxide layer for LCD panel applications,” *Nanotechnology*, vol. 21, no. 28, 2010.
- [6] I. Dierking, “Nanoscience with liquid crystals,” *Liq. Cryst. Today*, vol. 26, no. 3, pp. 63–65, 2017.
- [7] A. Kamyshny and S. Magdassi, “Conductive nanomaterials for printed electronics,” *Small*, vol. 10, no. 17, pp. 3515–3535, 2014.
- [8] M. Joshi and U. Chatterjee, *Polymer nanocomposite*. Elsevier Ltd, 2016.
- [9] J. Kumirska *et al.*, “Application of spectroscopic methods for structural analysis of chitin and chitosan,” *Mar. Drugs*, vol. 8, no.

- 5, pp. 1567–1636, 2010.
- [10] C. Santhosh, V. Velmurugan, G. Jacob, S. K. Jeong, A. N. Grace, and A. Bhatnagar, “Role of nanomaterials in water treatment applications: A review,” *Chem. Eng. J.*, vol. 306, pp. 1116–1137, 2016.
- [11] K. Gajanan and S. N. Tijare, “Applications of nanomaterials,” *Mater. Today Proc.*, vol. 5, no. 1, pp. 1093–1096, 2018.
- [12] N. Lin and A. Dufresne, “Nanocellulose in biomedicine: Current status and future prospect,” *Eur. Polym. J.*, vol. 59, no. July, pp. 302–325, 2014.
- [13] A. Dufresne, “Nanocellulose: A new ageless bionanomaterial,” *Mater. Today*, vol. 16, no. 6, pp. 220–227, 2013.
- [14] N. Angulakshmi, S. Thomas, K. S. Nahm, M. M. Stephan, and N. N. Elizabeth, “Electrochemical and mechanical properties of nanochitin-incorporated PVDF-HFP-based polymer electrolytes for lithium batteries,” *Ionics (Kiel)*, vol. 17, no. 5, pp. 407–414, 2011.
- [15] J. G. Torres-Rendon *et al.*, “Bioactive gyroid scaffolds formed by sacrificial templating of nanocellulose and nanochitin hydrogels as instructive platforms for biomimetic tissue engineering,” *Adv. Mater.*, vol. 27, no. 19, pp. 2989–2995, 2015.
- [16] K. Kerman, M. Saito, E. Tamiya, S. Yamamura, and Y. Takamura, “Nanomaterial-based electrochemical biosensors for medical applications,” *TrAC - Trends Anal. Chem.*, vol. 27, no. 7, pp. 585–592, 2008.
- [17] M. Keerthi, G. Boopathy, S.-M. Chen, T.-W. Chen, and B.-S. Lou, “A core-shell molybdenum nanoparticles entrapped f-MWCNTs hybrid nanostructured material based non-enzymatic biosensor for electrochemical detection of dopamine neurotransmitter in biological samples,” *Sci. Rep.*, vol. 9, no. 1, pp. 1–12, 2019.

- [18] Y. S. Zhang and A. Khademhosseini, “Advances in engineering hydrogels,” *Science (80-. )*, vol. 356, no. 6337, 2017.
- [19] G. A. A. Saracino, D. Cigognini, D. Silva, A. Caprini, and F. Gelain, “Nanomaterials design and tests for neural tissue engineering,” *Chem. Soc. Rev.*, vol. 42, no. 1, pp. 225–262, 2013.
- [20] G. Wunner *et al.*, “Certain Critical Field Strength, the  $3 \Sigma$ ,” vol. 337, no. July, pp. 303–305, 2012.
- [21] R. Aversa, R. V. V. Petrescu, R. Sorrentino, F. I. T. Petrescu, and A. Apicella, “Hybrid ceramo-polymeric nanocomposite for biomimetic scaffolds design and preparation,” *Am. J. Eng. Appl. Sci.*, vol. 9, no. 4, pp. 1096–1105, 2016.
- [22] R. A. Hule and D. J. Pochan, “Polymer nanocomposites for biomedical applications,” *MRS Bull.*, vol. 32, no. 4, pp. 354–358, 2007.
- [23] B. J. Biol *et al.*, “, B. J. Biol. 14. BENDICH, A. ., RUSSELL,” no. 101, 1953.
- [24] R. A. Khan *et al.*, “Production and properties of nanocellulose-reinforced methylcellulose-based biodegradable films,” *J. Agric. Food Chem.*, vol. 58, no. 13, pp. 7878–7885, 2010.
- [25] S. P. Mishra, A. S. Manent, B. Chabot, and C. Daneault, “Production of nanocellulose from native cellulose - Various options utilizing ultrasound,” *BioResources*, vol. 7, no. 1, pp. 422–435, 2012.
- [26] Y. Zhou, T. Saito, L. Bergström, and A. Isogai, “Acid-Free Preparation of Cellulose Nanocrystals by TEMPO Oxidation and Subsequent Cavitation,” *Biomacromolecules*, vol. 19, no. 2, pp. 633–639, 2018.
- [27] M. Martelli-Tosi, M. D. S. Torricillas, M. A. Martins, O. B. G. De Assis, and D. R. Tapia-Blácido, “Using Commercial Enzymes to Produce Cellulose Nanofibers from Soybean Straw,” *J.*

- Nanomater.*, vol. 2016, 2016.
- [28] J. Y. Zhu, R. Sabo, and X. Luo, “Integrated production of nano-fibrillated cellulose and cellulosic biofuel (ethanol) by enzymatic fractionation of wood fibers,” *Green Chem.*, vol. 13, no. 5, pp. 1339–1344, 2011.
- [29] Z. Karim, S. Afrin, Q. Husain, and R. Danish, “Necessity of enzymatic hydrolysis for production and functionalization of nanocelluloses,” *Crit. Rev. Biotechnol.*, vol. 37, no. 3, pp. 355–370, 2017.
- [30] P. K. Busk and L. Lange, “Classification of fungal and bacterial lytic polysaccharide monooxygenases,” *BMC Genomics*, vol. 16, no. 1, pp. 1–13, 2015.
- [31] E. Chiu *et al.*, “Structural basis for the enhancement of virulence by viral spindles and their in vivo crystallization,” *Proc. Natl. Acad. Sci. U. S. A.*, vol. 112, no. 13, pp. 3973–3978, 2015.
- [32] G. Vaaje-Kolstad *et al.*, “An oxidative enzyme boosting the enzymatic conversion of recalcitrant polysaccharides,” *Science (80-. )*, vol. 330, no. 6001, pp. 219–222, 2010.
- [33] R. J. Quinlan *et al.*, “Source : Proceedings of the National Academy of Sciences of the United States of America , Vol .,” 2015.
- [34] R. J. Quinlan *et al.*, “Insights into the oxidative degradation of cellulose by a copper metalloenzyme that exploits biomass components,” *Proc. Natl. Acad. Sci. U. S. A.*, vol. 108, no. 37, pp. 15079–15084, 2011.
- [35] L. Lo Leggio *et al.*, “Structure and boosting activity of a starch-degrading lytic polysaccharide monooxygenase,” *Nat. Commun.*, vol. 6, 2015.
- [36] C. M. Phillips, W. T. Beeson, J. H. Cate, and M. A. Marletta, “Cellobiose dehydrogenase and a copper-dependent



- polysaccharide monooxygenase potentiate cellulose degradation by *Neurospora crassa*,” *ACS Chem. Biol.*, vol. 6, no. 12, pp. 1399–1406, 2011.
- [37] W. T. Beeson, C. M. Phillips, J. H. D. Cate, and M. A. Marletta, “Oxidative cleavage of cellulose by fungal copper-dependent polysaccharide monooxygenases,” *J. Am. Chem. Soc.*, vol. 134, no. 2, pp. 890–892, 2012.
- [38] Y. Arfi, M. Shamshoum, I. Rogachev, Y. Peleg, and E. A. Bayer, “Integration of bacterial lytic polysaccharide monooxygenases into designer cellulosomes promotes enhanced cellulose degradation,” *Proc. Natl. Acad. Sci. U. S. A.*, vol. 111, no. 25, pp. 9109–9114, 2014.
- [39] G. Müller, P. Chylenski, B. Bissaro, V. G. H. Eijsink, and S. J. Horn, “The impact of hydrogen peroxide supply on LPMO activity and overall saccharification efficiency of a commercial cellulase cocktail,” *Biotechnol. Biofuels*, vol. 11, no. 1, pp. 1–17, 2018.
- [40] David Cannella, Chia-wen C Hsieh, Claus Felby, and Henning Jørgensen, “Production and effect of aldonic acids during enzymatic hydrolysis of lignocellulose at high dry matter content,” *Biotechnol. Biofuels*, vol. 5, no. 26, pp. 1–10, 2012.
- [41] S. P. S. Chundawat, G. T. Beckham, M. E. Himmel, and B. E. Dale, “Deconstruction of Lignocellulosic Biomass to Fuels and Chemicals,” *Annu. Rev. Chem. Biomol. Eng.*, vol. 2, no. 1, pp. 121–145, 2011.
- [42] N. C. Carpita and D. M. Gibeaut, “Structural models of primary cell walls in flowering plants: Consistency of molecular structure with the physical properties of the walls during growth,” *Plant J.*, vol. 3, no. 1, pp. 1–30, 1993.
- [43] H. Ishizaki and K. Hasumi, *Ethanol Production from Biomass*. Elsevier, 2013.

- [44] N. Xu *et al.*, “Biomethane Production From Lignocellulose: Biomass Recalcitrance and Its Impacts on Anaerobic Digestion,” *Front. Bioeng. Biotechnol.*, vol. 7, no. August, pp. 1–12, 2019.
- [45] L. Viikari, M. Alapuranen, T. Puranen, J. Vehmaanperä, and M. Siika-Aho, “Thermostable enzymes in lignocellulose hydrolysis,” *Adv. Biochem. Eng. Biotechnol.*, vol. 108, no. June, pp. 121–145, 2007.
- [46] P. M. D. Jaramillo, H. A. R. Gomes, A. V Monclaro, C. O. G. Silva, and E. X. F. Filho, “Section 2 Production of recombinant peptides Chapter 6 Lignocellulose □ degrading enzymes : An overview of the global market.”
- [47] D. M. Reimer, “The fine line of patient consent.,” *J. Am. Assoc. Nurse Anesth.*, vol. 43, no. 1, pp. 57–58, 1975.
- [48] Y. S. Cheng, Y. Zheng, C. W. Yu, T. M. Dooley, B. M. Jenkins, and J. S. Vandergheynst, “Evaluation of high solids alkaline pretreatment of rice straw,” *Appl. Biochem. Biotechnol.*, vol. 162, no. 6, pp. 1768–1784, 2010.
- [49] M. W. Easson *et al.*, “The application of ultrasound in the enzymatic hydrolysis of switchgrass,” *Appl. Biochem. Biotechnol.*, vol. 165, no. 5–6, pp. 1322–1331, 2011.
- [50] K. K. Wong, L. U. Tan, and J. N. Saddler, “Multiplicity of beta-1,4-xylanase in microorganisms: functions and applications.,” *Microbiol. Rev.*, vol. 52, no. 3, pp. 305–317, 1988.
- [51] A. M. Madlala, S. Bissoon, S. Singh, and L. Christov, “Xylanase-induced reduction of chlorine dioxide consumption during elemental chlorine-free bleaching of different pulp types,” *Biotechnol. Lett.*, vol. 23, no. 5, pp. 345–351, 2001.
- [52] B. Battan, J. Sharma, S. S. Dhiman, and R. C. Kuhad, “Enhanced production of cellulase-free thermostable xylanase by *Bacillus pumilus* ASH and its potential application in paper industry,” *Enzyme Microb. Technol.*, vol. 41, no. 6–7, pp. 733–739, 2007.

- [53] L. Laureano-Perez, F. Teymouri, H. Alizadeh, and B. E. Dale, "Understanding Factors that Limit Enzymatic Hydrolysis of Biomass," *Twenty-Sixth Symp. Biotechnol. Fuels Chem.*, vol. 121, pp. 1081–1099, 2009.
- [54] N. Sathitsuksanoh *et al.*, "Lignin fate and characterization during ionic liquid biomass pretreatment for renewable chemicals and fuels production," *Green Chem.*, vol. 16, no. 3, pp. 1236–1247, 2014.
- [55] K. Öhgren, R. Bura, J. Saddler, and G. Zacchi, "Effect of hemicellulose and lignin removal on enzymatic hydrolysis of steam pretreated corn stover," *Bioresour. Technol.*, vol. 98, no. 13, pp. 2503–2510, 2007.
- [56] M. Heinzkill, L. Bech, T. Halkier, P. Schneider, and T. Anke, "Characterization of laccases and peroxidases from wood-rotting fungi (family Coprinaceae)," *Appl. Environ. Microbiol.*, vol. 64, no. 5, pp. 1601–1606, 1998.
- [57] M. E. Arias, M. Arenas, J. Rodríguez, J. Soliveri, A. S. Ball, and M. Hernández, "Kraft pulp biobleaching and mediated oxidation of a nonphenolic substrate by laccase from *Streptomyces cyaneus* CECT 3335," *Appl. Environ. Microbiol.*, vol. 69, no. 4, pp. 1953–1958, 2003.
- [58] X. F. Zhang, G. Y. Yang, Y. Zhang, Y. Xie, S. G. Withers, and Y. Feng, "A general and efficient strategy for generating the stable enzymes," *Sci. Rep.*, vol. 6, no. May, pp. 1–12, 2016.
- [59] S. C. Dodani, G. Kiss, J. K. B. Cahn, Y. Su, V. S. Pande, and F. H. Arnold, "Discovery of a regioselectivity switch in nitrating P450s guided by molecular dynamics simulations and Markov models," *Nat. Chem.*, vol. 8, no. 5, pp. 419–425, 2016.
- [60] A. J. Burton, A. R. Thomson, W. M. Dawson, R. L. Brady, and D. N. Woolfson, "Installing hydrolytic activity into a completely de novo protein framework," *Nat. Chem.*, vol. 8, no. 9, pp. 837–844,

- 2016.
- [61] M. R. Smith, E. Khera, and F. Wen, “Engineering novel and improved biocatalysts by cell surface display,” *Ind. Eng. Chem. Res.*, vol. 54, no. 16, pp. 4021–4032, 2015.
- [62] X. Duan, J. Chen, and J. Wu, “Improving the thermostability and catalytic efficiency of *Bacillus deramificans* pullulanase by site-directed mutagenesis,” *Appl. Environ. Microbiol.*, vol. 79, no. 13, pp. 4072–4077, 2013.
- [63] E. G. Hibbert *et al.*, “Directed evolution of biocatalytic processes,” *Biomol. Eng.*, vol. 22, no. 1–3, pp. 11–19, 2005.
- [64] P. A. Dalby, “Optimising enzyme function by directed evolution,” *Curr. Opin. Struct. Biol.*, vol. 13, no. 4, pp. 500–505, 2003.
- [65] M. Anbar, O. Gul, R. Lamed, U. O. Sezerman, and E. A. Bayer, “Improved thermostability of *Clostridium thermocellum* endoglucanase Cel8A by using consensus-guided mutagenesis,” *Appl. Environ. Microbiol.*, vol. 78, no. 9, pp. 3458–3464, 2012.
- [66] P. Molina-Espeja, J. Viña-Gonzalez, B. J. Gomez-Fernandez, J. Martin-Diaz, E. Garcia-Ruiz, and M. Alcalde, “Beyond the outer limits of nature by directed evolution,” *Biotechnol. Adv.*, vol. 34, no. 5, pp. 754–767, 2016.
- [67] O. F. Brandenburg, K. Chen, and F. H. Arnold, “Directed Evolution of a Cytochrome P450 Carbene Transferase for Selective Functionalization of Cyclic Compounds,” *J. Am. Chem. Soc.*, vol. 141, no. 22, pp. 8989–8995, 2019.
- [68] B. K. Tischer, G. Smith, and N. Osterrieder, “En Passant: A Two Step Markerless REd Recombination System,” vol. 634, no. 7, pp. 421–430, 2010.
- [69] S. Lutz, “Beyond directed evolution-semi-rational protein engineering and design,” *Curr. Opin. Biotechnol.*, vol. 21, no. 6, pp. 734–743, 2010.

- [70] P. A. Dalby, "Strategy and success for the directed evolution of enzymes," *Curr. Opin. Struct. Biol.*, vol. 21, no. 4, pp. 473–480, 2011.
- [71] E. A. Gaucher, S. Govindarajan, and O. K. Ganesh, "Palaeotemperature trend for Precambrian life inferred from resurrected proteins," *Nature*, vol. 451, no. 7179, pp. 704–707, 2008.
- [72] M. J. Harms and J. W. Thornton, "Historical contingency and its biophysical basis in glucocorticoid receptor evolution," *Nature*, vol. 512, no. 7513, pp. 203–207, 2014.
- [73] V. Nguyen *et al.*, "10.1126@Science.Aah3717," *Science (80-. )*, vol. 3717, no. December, 2016.
- [74] R. Perez-Jimenez *et al.*, "Single-molecule paleoenzymology probes the chemistry of resurrected enzymes," *Nat. Struct. Mol. Biol.*, vol. 18, no. 5, pp. 592–596, 2011.
- [75] V. A. Risso, J. A. Gavira, D. F. Mejia-Carmona, E. A. Gaucher, and J. M. Sanchez-Ruiz, "Hyperstability and substrate promiscuity in laboratory resurrections of precambrian  $\beta$ -lactamases," *J. Am. Chem. Soc.*, vol. 135, no. 8, pp. 2899–2902, 2013.
- [76] M. G. Plach, B. Reisinger, R. Sterner, and R. Merkl, "Long-Term Persistence of Bi-functionality Contributes to the Robustness of Microbial Life through Exaptation," *PLoS Genet.*, vol. 12, no. 1, pp. 1–14, 2016.
- [77] G. N. Eick, J. K. Colucci, M. J. Harms, E. A. Ortlund, and J. W. Thornton, "Evolution of Minimal Specificity and Promiscuity in Steroid Hormone Receptors," *PLoS Genet.*, vol. 8, no. 11, 2012.
- [78] T. Devamani *et al.*, "Catalytic Promiscuity of Ancestral Esterases and Hydroxynitrile Lyases," *J. Am. Chem. Soc.*, vol. 138, no. 3, pp. 1046–1056, 2016.
- [79] M. Alcalde, "When directed evolution met ancestral enzyme

- resurrection,” *Microb. Biotechnol.*, vol. 10, no. 1, pp. 22–24, 2017.
- [80] B. G. Hall, “Simple and accurate estimation of ancestral protein sequences,” *Proc. Natl. Acad. Sci. U. S. A.*, vol. 103, no. 14, pp. 5431–5436, 2006.
- [81] R. Merkl and R. Sterner, “Ancestral protein reconstruction: Techniques and applications,” *Biol. Chem.*, vol. 397, no. 1, pp. 1–21, 2016.
- [82] J. W. Thornton, “Resurrecting ancient genes: Experimental analysis of extinct molecules,” *Nat. Rev. Genet.*, vol. 5, no. 5, pp. 366–375, 2004.
- [83] I. N. Shindyalov, N. A. Kolchanov, and C. Sander, “Can three-dimensional contacts in protein structures be predicted by analysis of correlated mutations?,” *Protein Eng. Des. Sel.*, vol. 7, no. 3, pp. 349–358, 1994.
- [84] P. M. Zakas *et al.*, “Enhancing the pharmaceutical properties of protein drugs by ancestral sequence reconstruction,” *Nat. Biotechnol.*, vol. 35, no. 1, pp. 35–37, 2017.
- [85] N. Barruetabeña *et al.*, “Resurrection of efficient Precambrian endoglucanases for lignocellulosic biomass hydrolysis,” *Commun. Chem.*, vol. 2, no. 1, p. 76, 2019.
- [86] F. Robert and M. Chaussidon, “A palaeotemperature curve for the Precambrian oceans based on silicon isotopes in cherts,” *Nature*, vol. 443, no. 7114, pp. 969–972, 2006.
- [87] M. Richter, C. Schulenburg, D. Jankowska, T. Heck, and G. Faccio, “Novel materials through Nature’s catalysts,” *Mater. Today*, vol. 18, no. 8, pp. 459–467, 2015.
- [88] O. Kirk, T. V. Borchert, and C. C. Fuglsang, “Industrial enzyme applications,” *Curr. Opin. Biotechnol.*, vol. 13, no. 4, pp. 345–351, 2002.

- [89] B. A. Lerma, "Isolation , characterization and applications of nanocellulose produced by ancestral enzymes," 2019.
- [90] X. J. Shen, P. L. Huang, J. H. Chen, Y. Y. Wu, Q. Y. Liu, and R. C. Sun, "Comparison of acid-hydrolyzed and TEMPO-oxidized nanocellulose for reinforcing alginate fibers," *BioResources*, vol. 12, no. 4, pp. 8180–8198, 2017.
- [91] T. Saito and A. Isogai, "TEMPO-mediated oxidation of native cellulose. The effect of oxidation conditions on chemical and crystal structures of the water-insoluble fractions," *Biomacromolecules*, vol. 5, no. 5, pp. 1983–1989, 2004.
- [92] A. Rees *et al.*, "3D bioprinting of carboxymethylated-periodate oxidized nanocellulose constructs for wound dressing applications," *Biomed Res. Int.*, vol. 2015, 2015.
- [93] H. J. BLUMENTHAL and S. ROSEMAN, "Quantitative estimation of chitin in fungi.," *J. Bacteriol.*, vol. 74, no. 2, pp. 222–224, 1957.
- [94] M. Rinaudo, "Chitin and chitosan: Properties and applications," *Prog. Polym. Sci.*, vol. 31, no. 7, pp. 603–632, 2006.
- [95] F. Khoushab and M. Yamabhai, "Chitin research revisited," *Mar. Drugs*, vol. 8, no. 7, pp. 1988–2012, 2010.
- [96] F. Shahidi, J. K. V. Arachchi, and Y. J. Jeon, "Food applications of chitin and chitosans," *Trends Food Sci. Technol.*, vol. 10, no. 2, pp. 37–51, 1999.
- [97] K. V. Harish Prashanth and R. N. Tharanathan, "Chitin/chitosan: modifications and their unlimited application potential-an overview," *Trends Food Sci. Technol.*, vol. 18, no. 3, pp. 117–131, 2007.
- [98] R. Sharp, "A Review of the Applications of Chitin and Its Derivatives in Agriculture to Modify Plant-Microbial Interactions and Improve Crop Yields," *Agronomy*, vol. 3, no. 4, pp. 757–793,

2013.

- [99] A. Bhatnagar and M. Sillanpää, “Applications of chitin- and chitosan-derivatives for the detoxification of water and wastewater - A short review,” *Adv. Colloid Interface Sci.*, vol. 152, no. 1–2, pp. 26–38, 2009.
- [100] T. Hebrew, “The molecular biology of chitin digestion Rachel Cohen-Kupiec and Ilan Chet,” *Curr. Opin. Biotechnol.*, pp. 270–277, 1998.
- [101] C. R. Berger, M. E. Roloff, and D. R. Roskos-ewoldsen, “Communication Science Edited by,” vol. II.
- [102] S. Nikolov *et al.*, “Robustness and optimal use of design principles of arthropod exoskeletons studied by ab initio-based multiscale simulations,” *J. Mech. Behav. Biomed. Mater.*, vol. 4, no. 2, pp. 129–145, 2011.
- [103] A. Ilnicka and J. P. Lukaszewicz, “Discussion remarks on the role of wood and chitin constituents during carbonization,” *Front. Mater.*, vol. 2, no. March, pp. 1–6, 2015.
- [104] D. Raabe *et al.*, “Microstructure and crystallographic texture of the chitin-protein network in the biological composite material of the exoskeleton of the lobster *Homarus americanus*,” *Mater. Sci. Eng. A*, vol. 421, no. 1–2, pp. 143–153, 2006.
- [105] J. Blackwell, “Physical methods for the determination of chitin structure and conformation,” *Methods Enzymol.*, vol. 161, no. C, pp. 435–442, 1988.
- [106] Y. Fan, T. Saito, and A. Isogai, “Chitin nanocrystals prepared by TEMPO-mediated oxidation of  $\alpha$ -chitin,” *Biomacromolecules*, vol. 9, no. 1, pp. 192–198, 2008.
- [107] G. N. Ramachandran and C. Ramakrishnan, “The structure of chitin,” *BBA - Biochim. Biophys. Acta*, vol. 63, no. 2, pp. 307–309, 1962.



- [108] Y. Lu, L. Weng, and L. Zhang, "Morphology and properties of soy protein isolate thermoplastics reinforced with chitin whiskers," *Biomacromolecules*, vol. 5, no. 3, pp. 1046–1051, 2004.
- [109] M. V. Tzoumaki, T. Moschakis, V. Kiosseoglou, and C. G. Biliaderis, "Oil-in-water emulsions stabilized by chitin nanocrystal particles," *Food Hydrocoll.*, vol. 25, no. 6, pp. 1521–1529, 2011.
- [110] J. F. Revol and R. H. Marchessault, "In vitro chiral nematic ordering of chitin crystallites," *Int. J. Biol. Macromol.*, vol. 15, no. 6, pp. 329–335, 1993.
- [111] M. V. Tzoumaki, T. Moschakis, and C. G. Biliaderis, "Metastability of nematic gels made of aqueous chitin nanocrystal dispersions," *Biomacromolecules*, vol. 11, no. 1, pp. 175–181, 2010.
- [112] H. P. Zhao, X. Q. Feng, and H. Gao, "Ultrasonic technique for extracting nanofibers from nature materials," *Appl. Phys. Lett.*, vol. 90, no. 7, pp. 97–99, 2007.
- [113] B. M. Min *et al.*, "Chitin and chitosan nanofibers: Electrospinning of chitin and deacetylation of chitin nanofibers," *Polymer (Guildf.)*, vol. 45, no. 21, pp. 7137–7142, 2004.
- [114] S. Ifuku *et al.*, "Preparation of chitin nanofibers with a uniform width as  $\alpha$ -chitin from crab shells," *Biomacromolecules*, vol. 10, no. 6, pp. 1584–1588, 2009.
- [115] M. Mincea, A. Negrulescu, and V. Ostafe, "Preparation, modification, and applications of chitin nanowhiskers: A review," *Rev. Adv. Mater. Sci.*, vol. 30, no. 3, pp. 225–242, 2012.
- [116] J. B. Zeng, Y. S. He, S. L. Li, and Y. Z. Wang, "Chitin whiskers: An overview," *Biomacromolecules*, vol. 13, no. 1, pp. 1–11, 2012.
- [117] A. S. Sahai and M. S. Manocha, "Chitinases of fungi and plants:

- their involvement in morphogenesis and host-parasite interaction,” *FEMS Microbiol. Rev.*, vol. 11, no. 4, pp. 317–338, 1993.
- [118] T. Oku and K. Ishikawa, “Analysis of the hyperthermophilic chitinase from *Pyrococcus furiosus*: Activity toward crystalline chitin,” *Biosci. Biotechnol. Biochem.*, vol. 70, no. 7, pp. 1696–1701, 2006.
- [119] T. Tanaka, T. Fukui, and T. Imanaka, “Different Cleavage Specificities of the Dual Catalytic Domains in Chitinase from the Hyperthermophilic Archaeon *Thermococcus kodakaraensis* KOD1,” *J. Biol. Chem.*, vol. 276, no. 38, pp. 35629–35635, 2001.
- [120] K. G. Nair, A. Dufresne, A. Gandini, and M. N. Belgacem, “Crab shell chitin whiskers reinforced natural rubber nanocomposites. 3. Effect of Chemical Modification of chitin whiskers,” *Biomacromolecules*, vol. 4, no. 6, pp. 1835–1842, 2003.
- [121] Z. Li, R. Yang, F. Yang, M. Zhang, and B. Wang, “Structure and properties of chitin whisker reinforced papers for food packaging application,” *BioResources*, vol. 10, no. 2, pp. 2995–3004, 2015.
- [122] Y. Feng *et al.*, “Novel nanofibrillated cellulose/chitin whisker hybrid nanocomposites and their use for mechanical performance enhancements,” *BioResources*, vol. 13, no. 2, pp. 3030–3044, 2018.
- [123] N. I. Platnick and H. D. Cameron, “Cladistic Methods in Textual, Linguistic, and Phylogenetic Analysis,” *Syst. Zool.*, vol. 26, no. 4, p. 380, 2006.
- [124] J. J. Tehrani, “The phylogeny of little red riding hood,” *PLoS One*, vol. 8, no. 11, 2013.
- [125] R. S. Walker, K. R. Hill, M. V. Flinn, and R. M. Ellsworth, “Evolutionary history of hunter-gatherer marriage practices,” *PLoS One*, vol. 6, no. 4, pp. 2–7, 2011.
- [126] V. Hanson-Smith, B. Kolaczowski, and J. W. Thornton,

- “Robustness of ancestral sequence reconstruction to phylogenetic uncertainty,” *Mol. Biol. Evol.*, vol. 27, no. 9, pp. 1988–1999, 2010.
- [127] J. A. Eisen, “Phylogenomics: Improving functional predictions for uncharacterized genes by evolutionary analysis,” *Genome Res.*, vol. 8, no. 3, pp. 163–167, 1998.
- [128] L. Pauling and L.a.E.Z, “Chemical Paleogenetics.” .
- [129] G. J. Morgan, E. Zuckerkandl, and L. Pauling, “and the molecular evolutionary clock,” *J Hist Biol*, vol. 31, no. 2, pp. 155–178, 1998.
- [130] W. M. Fitch and W. M. Fitch, “Society of Systematic Biologists Toward Defining the Course of Evolution : Minimum Change for a Specific Tree Topology TOWARD DEFINING THE COURSE OF EVOLUTION : MINIMUM CHANGE FOR A SPECIFIC TREE T ’ OPOLOGY,” vol. 20, no. 4, pp. 406–416, 2013.
- [131] A. goleman, daniel; boyatzis, Richard; Mckee, “濟無No Title No Title,” *J. Chem. Inf. Model.*, vol. 53, no. 9, pp. 1689–1699, 2019.
- [132] Z. Yang, S. Kumar, and M. Nei, “A new method of inference of ancestral nucleotide and amino acid sequences,” *Genetics*, vol. 141, no. 4, pp. 1641–1650, 1995.
- [133] J. M. Koshi and R. A. Goldstein, “Probabilistic reconstruction of ancestral protein sequences,” *J. Mol. Evol.*, vol. 42, no. 2, pp. 313–320, 1996.
- [134] T. R. Schultz, R. B. Cocroft, and G. A. Churchill, “The Reconstruction of Ancestral Character States,” *Evolution (N. Y.)*, vol. 50, no. 2, p. 504, 1996.
- [135] J. P. Huelsenbeck, B. Larget, and D. Swofford, “A compound Poisson process for relaxing the molecular clock,” *Genetics*, vol. 154, no. 4, pp. 1879–1892, 2000.
- [136] A. Eyre-Walker, “Problems with parsimony in sequences of biased base composition,” *J. Mol. Evol.*, vol. 47, no. 6, pp. 686–

690, 1998.

- [137] P. D. Williams, D. D. Pollock, B. P. Blackburne, and R. A. Goldstein, “Assessing the accuracy of ancestral protein reconstruction methods,” *PLoS Comput. Biol.*, vol. 2, no. 6, pp. 0598–0605, 2006.
- [138] J. Felsenstein, “Evolutionary trees from DNA sequences: A maximum likelihood approach,” *J. Mol. Evol.*, vol. 17, no. 6, pp. 368–376, 1981.
- [139] S. Biologists, “Society of Systematic Biologists Empirical and Hierarchical Bayesian Estimation of Ancestral States Author ( s ): John P . Huelsenbeck and Jonathan P . Bollback Published by : Oxford University Press for the Society of Systematic Biologists Stable URL : h,” vol. 50, no. 3, pp. 351–366, 2018.
- [140] K. Lai, *Chapter 10 WheatGenome . info : A Resource for Wheat Genomics*, vol. 1374. 2016.
- [141] S. Henikoff and J. G. Henikoff, “Amino acid substitution matrices from protein blocks,” *Proc. Natl. Acad. Sci. U. S. A.*, vol. 89, no. 22, pp. 10915–10919, 1992.
- [142] M. Manuel, “A new semi-subterranean diving beetle of the *Hydroporus normandi*-complex from south-eastern France, with notes on other taxa of the complex (Coleoptera: Dytiscidae),” *Zootaxa*, vol. 3652, no. 4, pp. 453–474, 2013.
- [143] R. V. Engeset *et al.*, “Improving runoff simulations using satellite-observed time-series of snow covered area,” *Nord. Hydrol.*, vol. 34, no. 4, pp. 281–294, 2003.
- [144] K. Tamura, G. Stecher, D. Peterson, A. Filipski, and S. Kumar, “MEGA6: Molecular evolutionary genetics analysis version 6.0,” *Mol. Biol. Evol.*, vol. 30, no. 12, pp. 2725–2729, 2013.
- [145] J. Castresana, “Selection of conserved blocks from multiple alignments for their use in phylogenetic analysis,” *Mol. Biol.*

- Evol.*, vol. 17, no. 4, pp. 540–552, 2000.
- [146] Y. K. Edward, M. J. Christopher, and T. E. Danielle, “Engineering transcriptional regulation to control Pdu microcompartment formation,” *PLoS One*, vol. 9, no. 11, pp. 1–14, 2014.
- [147] B. Wang, P. H. Walton, and C. Rovira, “Molecular Mechanisms of Oxygen Activation and Hydrogen Peroxide Formation in Lytic Polysaccharide Monooxygenases,” *ACS Catal.*, vol. 9, pp. 4958–4969, 2019.
- [148] C. Ouephanit, N. Boonvitthya, M. Theerachat, S. Bozonnet, and W. Chulalaksananukul, “Efficient expression and secretion of endo-1,4- $\beta$ -xylanase from *Penicillium citrinum* in non-conventional yeast *Yarrowia lipolytica* directed by the native and the preproLIP2 signal peptides,” *Protein Expr. Purif.*, vol. 160, no. March, pp. 1–6, 2019.
- [149] A. Törrönen, A. Harkki, and J. Rouvinen, “Three-dimensional structure of endo-1,4-beta-xylanase II from *Trichoderma reesei*: two conformational states in the active site.,” *EMBO J.*, vol. 13, no. 11, pp. 2493–2501, 1994.
- [150] M. G. Godoy, G. M. Amorim, M. S. Barreto, and D. M. G. Freire, *Agricultural Residues as Animal Feed*. Elsevier B.V., 2018.
- [151] B. V. McCleary and P. McGeough, “A Comparison of Polysaccharide Substrates and Reducing Sugar Methods for the Measurement of endo-1,4- $\beta$ -Xylanase,” *Appl. Biochem. Biotechnol.*, vol. 177, no. 5, pp. 1152–1163, 2015.
- [152] Y. H. P. Zhang and L. R. Lynd, “Toward an aggregated understanding of enzymatic hydrolysis of cellulose: Noncomplexed cellulase systems,” *Biotechnol. Bioeng.*, vol. 88, no. 7, pp. 797–824, 2004.
- [153] J. Hong, X. Ye, and Y. H. P. Zhang, “Quantitative determination of cellulose accessibility to cellulase based on adsorption of a nonhydrolytic fusion protein containing CBM and GFP with its

- applications,” *Langmuir*, vol. 23, no. 25, pp. 12535–12540, 2007.
- [154] T. K. Ghose, “Measurement of cellulase activities,” *Pure Appl. Chem.*, vol. 59, no. 2, pp. 257–268, 1987.
- [155] E. Breslmayr *et al.*, “A fast and sensitive activity assay for lytic polysaccharide monooxygenase,” *Biotechnol. Biofuels*, vol. 11, no. 1, pp. 1–13, 2018.
- [156] G. Janusz, A. Pawlik, J. Sulej, U. Świdarska-Burek, A. Jarosz-Wilkolazka, and A. Paszczyński, “Lignin degradation: Microorganisms, enzymes involved, genomes analysis and evolution,” *FEMS Microbiol. Rev.*, vol. 41, no. 6, pp. 941–962, 2017.
- [157] A. J. Drummond and A. Rambaut, “BMC Evolutionary Biology BEAST: Bayesian evolutionary analysis by sampling trees,” *BioMed Cent.*, vol. 7, no. 214, pp. 1–8, 2007.
- [158] D. L. Ayres *et al.*, “BEAGLE: An application programming interface and high-performance computing library for statistical phylogenetics,” *Syst. Biol.*, vol. 61, no. 1, pp. 170–173, 2012.
- [159] A. Rambaut, A. J. Drummond, D. Xie, G. Baele, and M. A. Suchard, “Posterior summarization in Bayesian phylogenetics using Tracer 1.7,” *Syst. Biol.*, vol. 67, no. 5, pp. 901–904, 2018.
- [160] Z. Yang, “PAML 4: Phylogenetic analysis by maximum likelihood,” *Mol. Biol. Evol.*, vol. 24, no. 8, pp. 1586–1591, 2007.
- [161] J. Adachi and M. Hasegawa, “Model of amino acid substitution in proteins encoded by mitochondrial DNA,” *J. Mol. Evol.*, vol. 42, no. 4, pp. 459–468, 1996.
- [162] A. Filipowski, O. Murillo, A. Freydenzon, K. Tamura, and S. Kumar, “Prospects for building large timetrees using molecular data with incomplete gene coverage among species,” *Mol. Biol. Evol.*, vol. 31, no. 9, pp. 2542–2550, 2014.
- [163] Y. Kato and D. J. Nevins, “Enzymic Dissociation of Zea Shoot

- Cell Wall Polysaccharides ,” *Plant Physiol.*, vol. 75, no. 3, pp. 759–765, 1984.
- [164] P. Sá-Pereira, M. Costa-Ferreira, and M. R. Aires-Barros, “Enzymatic properties of a neutral endo-1,3(4)- $\beta$ -xylanase Xyl II from *Bacillus subtilis*,” *J. Biotechnol.*, vol. 94, no. 3, pp. 265–275, 2002.
- [165] R. Bourbonnais and P. Claire, “Hicrobielngy,” pp. 201–206, 1986.
- [166] T. Pupko, I. Pe’er, R. Shamir, and D. Graur, “A fast algorithm for joint reconstruction of ancestral amino acid sequences,” *Mol. Biol. Evol.*, vol. 17, no. 6, pp. 890–896, 2000.
- [167] M. Galla, K. Wicke, and M. Fischer, “On the statistical inconsistency of Maximum Parsimony for k -tuple-site data,” vol. 0, no. 0, pp. 1–23, 2013.
- [168] M. J. Bailey, P. Biely, and K. Poutanen, “Interlaboratory testing of methods for assay of xylanase activity,” *J. Biotechnol.*, vol. 23, no. 3, pp. 257–270, 1992.
- [169] M. Devarapalli and H. K. Atiyeh, “A review of conversion processes for bioethanol production with a focus on syngas fermentation,” *Biofuel Res. J.*, vol. 2, no. 3, pp. 268–280, 2015.
- [170] J. Hu, V. Arantes, and J. N. Saddler, “The enhancement of enzymatic hydrolysis of lignocellulosic substrates by the addition of accessory enzymes such as xylanase: Is it an additive or synergistic effect?,” *Biotechnol. Biofuels*, vol. 4, no. 1, p. 36, 2011.
- [171] R. Kumar and C. E. Wyman, “Effect of xylanase supplementation of cellulase on digestion of corn stover solids prepared by leading pretreatment technologies,” *Bioresour. Technol.*, vol. 100, no. 18, pp. 4203–4213, 2009.
- [172] A. Requejo, A. Rodríguez, J. L. Colodette, J. L. Gomide, and L. Jiménez, “TCF bleaching sequence in kraft pulping of olive tree

- pruning residues,” *Bioresour. Technol.*, vol. 117, pp. 117–123, 2012.
- [173] C. Characterization, O. F. Pulp, C. In, U. Softwood, K. Fibers, and R. With, “CHEMICAL CHARACTERIZATION OF PULP COMPONENTS IN,” vol. 2010, no. 2006, pp. 616–629, 2010.
- [174] E. Lindfors and S. Forest, “Structural Changes in Lignin During Kraft Pulping,” vol. 38, pp. 151–158, 1984.
- [175] J. Hu, D. Tian, S. Renneckar, and J. N. Saddler, “Enzyme mediated nanofibrillation of cellulose by the synergistic actions of an endoglucanase , lytic polysaccharide monooxygenase ( LPMO ) and xylanase,” *Sci. Rep.*, no. October 2017, pp. 4–11, 2018.
- [176] A. Peciulyte *et al.*, “Redox processes acidify and decarboxylate steam-pretreated lignocellulosic biomass and are modulated by LPMO and catalase,” *Biotechnol. Biofuels*, vol. 11, no. 1, pp. 1–16, 2018.
- [177] F. Sabbadin *et al.*, “An ancient family of lytic polysaccharide monooxygenases with roles in arthropod development and biomass digestion,” *Nat. Commun.*, vol. 9, no. 1, 2018.
- [178] U. F. Rodríguez-Zúñiga, D. Cannella, R. D. C. Giordano, R. D. L. C. Giordano, H. Jørgensen, and C. Felby, “Lignocellulose pretreatment technologies affect the level of enzymatic cellulose oxidation by LPMO,” *Green Chem.*, vol. 17, no. 5, pp. 2896–2903, 2015.
- [179] Y. Gumulya *et al.*, “Engineering highly functional thermostable proteins using ancestral sequence reconstruction,” *Nat. Catal.*, vol. 1, no. 11, pp. 878–888, 2018.
- [180] E. A. Gaucher, J. M. Thomson, M. F. Burgan, and S. A. Benner, “Inferring the palaeoenvironment of ancient bacteria on the basis of resurrected proteins,” *Nature*, vol. 425, no. 6955, pp. 285–288, 2003.



- [181] J. Bouchard, N. Abatzoglou, E. Chornet, and R. P. Overend, "Characterization of depolymerized cellulosic residues - Part 1: Residues obtained by acid hydrolysis processes," *Wood Sci. Technol.*, vol. 23, no. 4, pp. 343–355, 1989.
- [182] M. Åkerholm, B. Hinterstoisser, and L. Salmén, "Characterization of the crystalline structure of cellulose using static and dynamic FT-IR spectroscopy," *Carbohydr. Res.*, vol. 339, no. 3, pp. 569–578, 2004.
- [183] Y. Cao and H. Tan, "Study on crystal structures of enzyme-hydrolyzed cellulosic materials by X-ray diffraction," *Enzyme Microb. Technol.*, vol. 36, no. 2–3, pp. 314–317, 2005.
- [184] S. Fujisawa, Y. Okita, H. Fukuzumi, T. Saito, and A. Isogai, "Preparation and characterization of TEMPO-oxidized cellulose nanofibril films with free carboxyl groups," *Carbohydr. Polym.*, vol. 84, no. 1, pp. 579–583, 2011.
- [185] W. L. Teng, E. Khor, T. K. Tan, L. Y. Lim, and S. C. Tan, "Concurrent production of chitin from shrimp shells and fungi," *Carbohydr. Res.*, vol. 332, no. 3, pp. 305–316, 2001.
- [186] F. Boßelmann, P. Romano, H. Fabritius, D. Raabe, and M. Epple, "The composition of the exoskeleton of two crustacea: The American lobster *Homarus americanus* and the edible crab *Cancer pagurus*," *Thermochim. Acta*, vol. 463, no. 1–2, pp. 65–68, 2007.
- [187] D. Raabe, C. Sachs, and P. Romano, "The crustacean exoskeleton as an example of a structurally and mechanically graded biological nanocomposite material," *Acta Mater.*, vol. 53, no. 15, pp. 4281–4292, 2005.
- [188] B. Bissaro, I. Isaksen, G. Vaaje-Kolstad, V. G. H. Eijsink, and Å. K. Røhr, "How a Lytic Polysaccharide Monooxygenase Binds Crystalline Chitin," *Biochemistry*, vol. 57, no. 12, pp. 1893–1906, 2018.
- [189] T. Fukazimo and K. J. Kramer, "Mechanism of Chitin Hydrolysis

- By the Binary Chitinase Retention Time ( Min ),” *Insect Biochem.*, vol. 15, no. 2, pp. 141–145, 1985.
- [190] M. S. Reid, S. A. Kedzior, M. Villalobos, and E. D. Cranston, “Effect of Ionic Strength and Surface Charge Density on the Kinetics of Cellulose Nanocrystal Thin Film Swelling,” *Langmuir*, vol. 33, no. 30, pp. 7403–7411, 2017.
- [191] Y. Tang, S. Yang, N. Zhang, and J. Zhang, “Preparation and characterization of nanocrystalline cellulose via low-intensity ultrasonic-assisted sulfuric acid hydrolysis,” *Cellulose*, vol. 21, no. 1, pp. 335–346, 2014.
- [192] L. Liu *et al.*, “High Axial Ratio Nanochitins for Ultrastrong and Shape-Recoverable Hydrogels and Cryogels via Ice Templating,” *ACS Nano*, vol. 13, no. 3, pp. 2927–2935, 2019.
- [193] M. Lewin, “Oxidation and aging of cellulose,” *Macromol. Symp.*, vol. 118, pp. 715–724, 1997.
- [194] K. Ahn *et al.*, “Yellowing and brightness reversion of celluloses: CO or COOH, who is the culprit?,” *Cellulose*, vol. 26, no. 1, pp. 429–444, 2019.
- [195] W. T. Goodrich, J. D.; Winter, “Alpha-chitin nanocrystals prepared from shrimp shells and their specific properties,” *Biomacromolecules*, no. 8, p. 252– 257., 2007.
- [196] M. M. De Souza Lima and R. Borsali, “Rodlike cellulose microcrystals: Structure, properties, and applications,” *Macromol. Rapid Commun.*, vol. 25, no. 7, pp. 771–787, 2004.
- [197] Y. Fan, H. Fukuzumi, T. Saito, and A. Isogai, “Comparative characterization of aqueous dispersions and cast films of different chitin nanowhiskers/nanofibers,” *Int. J. Biol. Macromol.*, vol. 50, no. 1, pp. 69–76, 2012.
- [198] J. D. Goodrich and W. T. Winter, “ $\alpha$ -Chitin nanocrystals prepared from shrimp shells and their specific surface area measurement,”

- Biomacromolecules*, vol. 8, no. 1, pp. 252–257, 2007.
- [199] B. Focher, A. Naggi, G. Torri, A. Cosani, and M. Terbojevich, “Chitosans from *Euphausia superba*. 2: Characterization of solid state structure,” *Carbohydr. Polym.*, vol. 18, no. 1, pp. 43–49, 1992.
- [200] “27- 270,” vol. 31, no. 2006, p. 38041, 2007.
- [201] M. Kaya *et al.*, “Differentiations of Chitin content and surface morphologies of chitins extracted from male and female grasshopper species,” *PLoS One*, vol. 10, no. 1, 2015.
- [202] M. Poletto, H. L. Ornaghi Júnior, and A. J. Zattera, “Native cellulose: Structure, characterization and thermal properties,” *Materials (Basel)*, vol. 7, no. 9, pp. 6105–6119, 2014.
- [203] Q. Wang, X. Yan, Y. Chang, L. Ren, and J. Zhou, “Fabrication and characterization of chitin nanofibers through esterification and ultrasound treatment,” *Carbohydr. Polym.*, vol. 180, pp. 81–87, 2018.
- [204] W. C. Tsai, S. T. Wang, K. L. B. Chang, and M. L. Tsai, “Enhancing saltiness perception using chitin nanomaterials,” *Polymers (Basel)*, vol. 11, no. 4, 2019.
- [205] J. Majtán, K. Bíliková, O. Markovič, J. Gróf, G. Kogan, and J. Šimúth, “Isolation and characterization of chitin from bumblebee (*Bombus terrestris*),” *Int. J. Biol. Macromol.*, vol. 40, no. 3, pp. 237–241, 2007.
- [206] Y. Kato, J. Kaminaga, R. Matsuo, and A. Isogai, “TEMPO-mediated oxidation of chitin, regenerated chitin and N-acetylated chitosan,” *Carbohydr. Polym.*, vol. 58, no. 4, pp. 421–426, 2004.
- [207] E. Szymańska and K. Winnicka, “Stability of chitosan - A challenge for pharmaceutical and biomedical applications,” *Mar. Drugs*, vol. 13, no. 4, pp. 1819–1846, 2015.
- [208] H. Moussout, H. Ahlafi, M. Aazza, and M. Bourakhouadar,

- “Kinetics and mechanism of the thermal degradation of biopolymers chitin and chitosan using thermogravimetric analysis,” *Polym. Degrad. Stab.*, vol. 130, pp. 1–9, 2016.
- [209] M. Ziegler-Borowska, D. Chełminiak, and H. Kaczmarek, “Thermal stability of magnetic nanoparticles coated by blends of modified chitosan and poly(quaternary ammonium) salt,” *J. Therm. Anal. Calorim.*, vol. 119, no. 1, pp. 499–506, 2015.
- [210] A. A. Oun and J. W. Rhim, “Effect of oxidized chitin nanocrystals isolated by ammonium persulfate method on the properties of carboxymethyl cellulose-based films,” *Carbohydr. Polym.*, vol. 175, pp. 712–720, 2017.
- [211] Y. Zhang, C. Xue, Y. Xue, R. Gao, and X. Zhang, “Determination of the degree of deacetylation of chitin and chitosan by X-ray powder diffraction,” *Carbohydr. Res.*, vol. 340, no. 11, pp. 1914–1917, 2005.
- [212] V. Moses, R. Hatherley, and Ö. Tastan Bishop, “Bioinformatic characterization of type-specific sequence and structural features in auxiliary activity family 9 proteins,” *Biotechnol. Biofuels*, vol. 9, no. 1, pp. 1–17, 2016.
- [213] H. Ehrlich *et al.*, “Discovery of 505-million-year old chitin in the basal demosponge *Vauxia gracilentia*,” *Sci. Rep.*, vol. 3, pp. 17–20, 2013.
- [214] C. C. Loron, C. François, R. H. Rainbird, E. C. Turner, S. Borensztajn, and E. J. Javaux, “Early fungi from the Proterozoic era in Arctic Canada,” *Nature*, vol. 570, no. 7760, pp. 232–235, 2019.
- [215] M. L. Romero-Romero, V. A. Risso, S. Martinez-Rodriguez, E. A. Gaucher, B. Ibarra-Molero, and J. M. Sanchez-Ruiz, “Selection for protein kinetic stability connects denaturation temperatures to organismal temperatures and provides clues to archaean life,” *PLoS One*, vol. 11, no. 6, pp. 1–38, 2016.

- [216] A. K. Garcia, J. W. Schopf, S. I. Yokobori, S. Akanuma, and A. Yamagishi, “Reconstructed ancestral enzymes suggest long-Term cooling of Earth’s photic zone since the Archean,” *Proc. Natl. Acad. Sci. U. S. A.*, vol. 114, no. 18, pp. 4619–4624, 2017.
- [217] M. Richter, C. Schulenburg, D. Jankowska, T. Heck, and G. Faccio, “Novel materials through Nature’s catalysts,” *Mater. Today*, vol. 18, no. 8, pp. 459–467, 2015.



# Appendix

---

In appendix I I show all the sequences that were used in the alienation to construct the phylogenetic trees. Underline I show the NCBI code to find the sequences on their internet database, on its right the organisms name of the corresponding protein. Below the amino acid sequence. In appendix II I show the ancestral sequences of each node and their corresponding query sequences.

## APPENDIX I

### List of Endo-1,4-beta-Xln A

#### proteins from the species used in the construction of the phylogenetic tree

P18429 *Bacillus subtilis* (Query)

KNFLVGLSAALMSISLFSATASAASTDYWQNWTDGGGIVNAVNGSGG  
 NYSVNWSNTGNFVVGKGWTTGSPFRTINYNAGVWAPNGNGYLTLYG  
 WTRSPLIEYYVVDSWGTYRPTGTYKGTVKSDGGTYDIYTTTRYNAPSI  
 DGDRTTFTQYWSVRQSKRPTGSNATITFSNHVNAWKSHGMNLGSNWA  
 YQVMATEGYQSSGSSNVTW

ACT21830.1 *Bacillus megaterium*

KNFLVGLTAAFMSISMFSATASAAGTDYWQNWTDGGGTVNAVNGSG  
 GNYSVNWSNTGNFVVGKGWTTGSPFRTINYNAGVWAPNGNGYLTLY  
 GWTRSPLIEYYVVDSWGTYRPTGTYKGTVKSDGGTYDIYTTTRYNAPS  
 IDGDRTTFTQYWSVRQTKRPTGSNATITFSNHVNAWKSHGMNLGSNW  
 AYQVMATEGYQSSGSSNVTW

AAM08360.1 *Bacillus circulans*

KNFLVGLSAALMRIILFSATASAASTDYWQNWTDGGGIVNAVNGSGG  
 NYSVNWSNTGNFVVGKGWTTGSPFRTINYNAGVWAPNGNGYLTLYG  
 WPRSPLIEYYVVDSWGTYRPTGTYKGTVKSDGGTYDIYTTTRYNAPSID  
 GDRTTFTQYWSVRQTKRPTGSNATITFSNHVNAWKSHGMNLGSNWAY  
 QVMATGGYQSSGSSNVTW

WP\_075747623.1 *Bacillus licheniformis*

KKFLVGLTAALMSISLFSATASAAGTDYWQNWTDGGGVVNAVNGAG  
 GNYSVNWSNTGNFVVGKGWTTGSPFRTINYNAGVWAPNGNGYLTLY  
 GWTRSPLIEYYVVDSWGTYRPTGTYKGTVKSDGGTYDIYTTTRYNAPS  
 IDGDNTTFTQYWSVRQTKRPTGSNATITFSNHVNAWKSHGMNLGSNW  
 SYQVLATEGYQSSGSSNVTW

WP\_046226114.1 *Paenibacillus dauci*

KKFLTILAVSMSSSVFAATSSAATDYWQNWTDGGGTVNSVNGTGGN  
 YSVNWQNTGNFVVGKGWTTGSPNRVINYNAGLWAPSGNGYLTLYGW  
 TRNSLIEYYVVDSWGTYRPTGTYKGTVTSDDGGVYDIYTTTRYDAPSIEG  
 DHKTFTQYWSVRQTKRPTGSNATITFSNHVKAWASHGMKLGSTWSYQ  
 VMATEGYQSSGSSNVTW

WP\_060532780.1 *Paenibacillus bovis*

KKFLTILAIMSSSVFAATSSAATDYWQNWTDGGGTVNSVNGNGGN  
 YSVNWQNTGNFVVGKGWTTGSPNRVINYNAGLWAPSGNGYLTLYGW



TRNSLIEYYVVDSWGTYRPTGTYKGTVTSDGGVYDIYTTTRYDAPSIEG  
DHKTFTQYWSVRQTKRPTGSNATITFSNHVKAWASHGMNLGSTWSYQ  
VLATEGYQSSGSSNVTW

WP\_046216042.1 *Paenibacillus wulumuqiensis*

KKFLTILAIMSSSVFAATSSAATDYWQNWDGGGTVNAVNGAGGN  
YSVNWQNTGNFVVGKGWTTGSPNRVVNYNAGQWAPSGNGYLTLYG  
WTRNSLIEYYVVDSWGTYRPTGTYKGTVTSDGGVYDIYTTTRYDAPSI  
EGDHKTFTQYWSVRQTKRPTGSNATITFSNHVKAWASHGMNLGSTWS  
YQVMATEGYKSSGSSNVTW

CAJ87325.1 *Thermobacillus xylanilyticus*

YWQYWTDGIGYVNATNGQGGNYSVSWNSNGNFVIGKGWQYGAHNR  
VVNYNAGAWQPNGNAYLTLYGWTNRNPLIEYYVVDSWGYSYRPTGDYR  
GSVYSDGAWYDLYHSWRYNAPSIDGTQTFQQYWSVRQQRPTGSNVS  
ITFENHVNAWGAAGMPMGSSWSYQVLATEGYSSGYSNVTW

WP\_015253740.1 *Thermobacillus composti*

KLMAVLVAVAMVSALFAVNGASYWQYWTDGIGYVNATNGQGGNYS  
VSWNSNGNFVIGKGWQYGAHNRVVNYNAGAWQPNGNAYLTLYGWT  
RNPLIEYYVVDSWGYSYRPTGDYRGSVYSDGAWYDLYHSWRYNAPSID  
GTQTFQQYWSVRQQRPTGSNVSITFENHVNAWGAAGMPMGSSWSY  
QVLATEGYSSGYSNVTW

WP\_089855761.1 *Halolactibacillus miurensis*

MFFLAIVFCFALILPTVIVTSNETGTHDYEYWKDSGGSGIMTLNNGGTF  
AEWSNVNINILFRKGKKFDETTQTSINY-  
GANYQPNGNSYLTVYGWAVDPLVEFYIVDSWGSYRPTGTHKGTINVD  
GGTYDIYETTRTNQPSIKG-TATFKQYWSVRTSKRTSGTISV---  
SEHFKAWENLGMQMGMY-EVALTVEGYQSSGSADVYSN

WP\_090795741.1 *Pelagirhabdus alkalitolerans*

KTKYALMAICFISLLATVTSNELGTHDYEYWKDSGGSGSMTLNGGGTF  
SAEWSNVNINILFRKGQRFDETRTRSIDYGVNYQPNGNSYLTVYGWVDP  
LVEYYIVDSWGTWRPPGANSQTVQVDGGTYDIYETTRVNQPSIRGTQT  
FQQYWSVRRDKRTSGTISVSEHFRAWEQHGMPLGNLY-  
EAALTIEGYQSSGQANVYRN

WP\_080062516.1 *Clostridium hungatei*

KKLFLGLFLAVMSLTSALPSYAATDYWQNWDGGGTVRATNGSGG  
NFSVTWQNCGNFVVGKGWGSGNASRVCNYNAGQFAPSGNGYLTFYG  
WTRNALIEYYIVDSWGTYRPTGTYKGSVSSDGGTYDIYTTQRVNAPSID  
G-  
TKTFTQYWSVRQSKRATGSNVAITFSNHVNAWKSKGMNLGSSWSYQA  
LCVEGYQSSGSANVTW

WP\_020814600.1 *Clostridium papyrosolvans*

KKVLGLIFAISMSSMFAGTTYAYWQNWDGGGTVNVTNGSGGNFSVN  
WYNCGNFVVGKGWNYGTANRVCNYNAGVFSPSGNGYLSFYGWTRNS  
LIEYYIVDTWGTYRPTGTYKGSVTSDDGGTYDIYTTQRYNAPSIDGTQSF  
TQFWSVRQSKRPTGQNVQINFANHVNAWKSKGMNLGSSWSYQALCV  
EGYQSSGSANVTW

WP\_054739261.1 *Cellulosilyticum ruminicola*

KKLLTVFCIATMALATNVQATDYWQNWTDGGGYVNAVNGQGGNYS  
VSWSNCGNFVVGKGWNYGTPNRVVGYNAGAFQPSGNGYLSFYGWTR  
NSLIEYYIVDTWGTYPRTGTYKGSVYSDGGNYDIYTTMRYNQPSIDG-  
TQTFQYWSVRQSKRPTGTNSQITFQNHVNAWQRCGMYLGSNWSYQ  
ALCVEGYQSSGYANVTWV

WP\_103201672.1 *Herbinix hemicellulosilytica*

RKAIALIFAASLCSTMLAGNAYYWQYWTDGGGYVNAVNGSGGNFSV  
NWYNCGNFVVGKGWATGSPNRVINYNAGVWAPSGNGYLTLYGWTR  
NALIEYYVVDWSGNWRPPGSNSGTVYSDGGTYDIYRTMRYNAPSIDG-  
TQTFQYWSVRTSKRPTGSNVSITFANHVNAWASRGLYLGSWSYQV  
MAVEGYQSSGSANVTWV

WP\_078766814.1 *Eubacterium uniforme*

AGVLCVAVVALPPLTATKVYDSKTGKIDFSLWKDYGNTSMKLNNGGA  
FECQWSNIGNALFRTGKTLDSKRSVNYSANYQPNGNSYLCVYGWSR  
NPLVEYYIVDSWGSWRPTGQYKQISVDGGTYDLYQDTRYNAPSIDGN  
TTFTQFWSVRTSKRTSGTISVSKHFDAAWQHGMNLTGNLT-  
EVALTVEGYKSSGYANVTNA

WP\_015906728.1 *Caldicellulosiruptor bescii*

KVLIAVLMCFMLGNPFYALTSNASGTYYYELWKDSGNTTMTVDTGGR  
FSCQWSNINLFRGTGKKFSTAWGTVKITYSATYNPNGNSYLCIYGWSRNP  
LVEFYIVESWGTWRPPGATSGTVTIDGGTYDIYKTTRVNQPSIEGTTTFD  
QYWSVRTSKRTSGTVTVDHFKAWAAKGLNLGTID-  
QITLCVEGYQSSGSANITQN

WP\_013411078.1 *Caldicellulosiruptor owensensis*

KLLLAVLMCVVLGNPFYALTSNASGTYYYELWKDSGNTTMTVDTGGR  
FSCQWSNINLFRGTGKKFSTAWGTVKITYSATYNPNGNSYLCIYGWSRNP  
LVEFYIVESWGSWRPPGATSGTVTIDGGTYDIYKTTRVNQPSIEGTTTFD  
QYWSVRTSKRTSGTVTVDHFKAWAAKGLNLGTID-  
QITLCVEGYQSSGSANITQN

SLC61209.1 *Mycobacterium abscessus*

KKFLVGLTAAAFMSISMFSATASAAGTDYWQNWTDGGGTVNAVNGSG  
GNYSVNWSNTGNFVVGKGWTTGSPFRTINYNAGVWAPNGNGYLTLY  
GWTRAPLIEYYVVDWSGTYPRTGTYKGTVKSDGGTYDIYTTTRYNAPS  
IDGDNFTFTQYWSVRQSKRPTGSNAAITFSNHVNAWKSHGMNLSNW  
AYQVLATEGYKSSGSSNVTWV

WP\_033332249.1 *Actinomadura madurae*

IGAIGAILTAAMALMPAITSNQTGFHYSFWTDSSGTVSMELGSSGGNY  
STSWRNTGNFVAGKGWSTGGRRSVNYSGSFNPSGNAYLTLYGWTRNP  
LIEYYIVDNWGTYPRTGTYKGTVTSDDGGTYDIYETTRYNAPSIEGTRTF  
QQYWSVRQSKRTGGTISAGNHFDAAWAGHGMNLSHSD-  
YQILATEGYQSSGNSNITIG

WP\_015772628.1 *Jonesia denitrificans*

ATLASVVALVAGTLAMATINDNTQGFYTHWTDAPGTASITLGSGGN  
YSTRWSNTGNFVSGKGWATGSRRTVNYSAQFNPSGNGYLTLYGWTRG  
PLVEYYIIIESWGTYPRTGEFKGTVTTDGGTYDIYKTRVNKPSIESDYST  
FDQYWSVRQQKRTSGSITVANHFDAWARHGMLGTHD-  
YQVMATEGYQSSGSSNVTIS

WP\_095567270.1 *Plantactinospora*

RLLTGGACAVALVAAILPITSNQTGTNFFSFWTDGGGSVSMDLGSGGN  
YSTTWSNVGNFVAGKGWKPGTRQTVTYSGSFNPSGNAYLALYGWTR  
NPLVEYYIVDNWGTYPRTGTYKGTVTSDDGGTYDIYETTRYNAPSIEGN  
QTFNQYWSVRQSKKTGGTITGNHFDAWASHGMNLGSHD-  
YQILATEGYQSSGSSNITVG

WP\_012877523.1 *Xylanimonas cellulositytica*

TIAAAGASLAMLVAGVAAISTNGTGNSFYFWTDSFGTVSMELGSGGN  
YSTSWSNTGNFVAGKGWSTGSARTITYSGSFNPSGNAYLTVYGWSRNP  
LVEYYIVDSWGTYPRTGTHMGTVTSDGGTYDIYKTRTNPSIEGDSST  
FDQFWSVRQSKRVGGTITTANHFNAWASKGMNLGSHD-  
YQIVATEGYQSSGSSNITVG

SFD76457.1 *Streptomyces aidingensis*

ACAALVGAALLPITQNSTGDFYSFWTDAPGTVTMNTGSGGNYSTQW  
SNTGNFVAGKGWSTGSSRTVTYSGTFNPSGNAYLTLYGWSRNPLVEYY  
IVDNWGTYPRTGTYKGTVNSDGGTYDIYETTRNNAPSIEGTQTFKQFW  
SVRQQKRTGGTITGNHFNAWAGHGMLGSHD-  
YQIMATEGYQSSGSSNITVG

WP\_100203418.1 *Streptomyces*

MVGAALLPITQNSTGDFYSFWTDAPGTVTMNTGSGGNYSTQWSNTG  
NFVAGKGWSTGSSRTVTYSGTFNPSGNAYLTLYGWSRNPLVEYYIVDN  
WGTYPRTGTYKGTVNSDGGTYDIYETTRNNAPSIEGTQTFKQFWSVRQ  
QKRTGGTITGNHFNAWAGHGMLGSHD-  
YQIMATEGYQSSGSSNITVG

CAJ57849.1 *Cellulomonas flavigena*

KQLVAGVAVAGLVGLAIAVTSNQTGNSYYSFWTDSQGTVSMELGSGG  
NYSTSWRTTGNFVAGKGWQTGSGRACYSYSGQFTPSGNAYLTLYGWTT  
GPLIEYYIVDNWGTYPRTGTYMGTVNSDGGTYDIYRTQRVNQPSIQGT  
ATFYQYWSVRQQKRTGGTITAAANHFNAWASKGMNLGSHN-  
YQILATEGYQSSGSSNITVS

WP\_061296570.1 *Herbidospira cretacea*

GLAAAGIWATVIAMVLSVTTNQTGTNWFNFWTDSQGTVSMELGSGG  
NYSTSWRNTGNFVAGKGWQTGGRRSVSYSGSFNPSGNAYLTLYGWTR  
NPLIEYYIVDNWGTYPRTGSYKGTVTSDDGGTYDIYETTRTNAPSIEGTRT  
FKQFWSVRQQKKTGGTITSGNHFDASRAGMQLGNHD-  
YMILATEGYQSSGSSNITIG

WP\_033216338.1 *Kitasatospora phosalacinea*

ARVPLALAAVLLPGTAVTTNQTGNDFYSFWSDGNGSSMSLNNGG  
NYGTSWSNVGNFVAGKGWSTGSRNPVTYSGTWSTNGNAYLSLYGWT  
TNPLVEYYVVENYGSYKPTGSYKGTVTTDGGTYDIYETTRYNAPSIEG-

NKTFNQYWSVRQSKRTGGTITVGNHFD AWARYGMNLGTMN-  
YEILATEGYQSSGNSNITLG

WP\_077689185.1 *Nocardiosis alkaliphila*

LTGAGALAVAAPSLLLPGLTENQTGTHFY SFWTDGGGSVSM TLGSGGS  
YSTQWRDTGNFVCGKGWHNGGYRNVNYSGSFHPSPGNGYLCLYGWTS  
NPLVEYYIVEAFGTYPGEGDYRGTVYSDGGTYDMYHTMRYNAPSVEG  
DSRTFPQFWSVRQSQRTGGTINTGNHFNAWGGAGMQLGSFDHYMILA  
TEGYQSSGSSNLSVS

WP\_051235018.1 *Marinimicrobium agarilyticum*

KSLSFALLTGATALGVSTICDNQTGN NYYYTHWTDGGGSACMTLGSEG  
NYSYEW SNTGNFVGGKGWSTGASNRIIGYNAGNYSPPSGNSYLTLYGW  
TTGPLVEYYVVD SWGSYRPGGTPAGTVTTDGGTYDLYRTQRVNKPSIE  
G-NTTFYQYWSVR TSKRPQGNNTITFQNHVDAWARQGWN LGSHN-  
YQVLATEGWQSSGSSNVSVW

WP\_052481306.1 *Gilvimarinus agarilyticus*

KKSLTAFIGAAAALCITALTSNQTGTHYYSFWTDAPGTVSMTLGSGGN  
YTSQWSNTGNWVGGKGWNP GGRRTVSYSGTFNPSGNGYLTLYGWTT  
SPLIEYYIVDNWGSYRPSGTYYGT VNTDGGTYDIYRTQRVNQPSIQGTA  
TFYQYWSVRQQKRTGGTIT TGNHFD AWASHGLNLGNHD-  
YVM MATEGYQSSGNSNITLG

WP\_020210149.1 *Gilvimarinus chinensis*

VKKIASLVAATTALCFTSLTSNQTGTHYYSFWTDAPGTVSMTLGSGGN  
YSSQWSNTGNWVGGKGWNP GGRRTVNYSGTFNPSGNGYLTLYGWTR  
SPLIEYYIVDNWGT YRPSGTYYGT VYSDGGTYDIYRTQRVNQPSIEGTA  
TFYQYWSVRQQKRTGGTIT TGNHFD AWASHGLNLGNHD-  
YVM MATEGYQSSGNSNITLG

AAT81215.1 *Microbulbifer hydrolyticus*

RSTLSVFALGVIASLGFSLTSNQTGNHFY SFWTDAPGTVSMTLGAGGN  
YSSWSNTGNWVGGKGWNP GGRRTVNYSGTFNPSGNGYLTLYGWTR  
NPLVEYYIVDNWGSYRPSGTYYGT VNTDGGTYDIYRTQRVNKPSIEGD  
SSTFYQYWSVRQQKRTGGTITAGNHGNHFD AWASHGMNLGTHD-  
YVM MATEGYQSSGNSNITLG

BAB79287.1 *Pseudomonas*

KKSLAILTTAAAVLSVAALTSNQTGTHYYSFWTDAPGTVSMTLGSGGN  
YSSQWSNTGNWVGGKGWNP GGRRTVSYSGTFNPSGNGYLTLYGWTT  
SPLIEYYIVDNWGSYRPSGTYYGT VNTDGGTYDIYRTQRVNQPSIQGTA  
TFYQYWSVRQQKRTGGTIT TGNHFD AWASHGLNLGNHD-  
YVM MATEGYQSSGNSNITLG

WP\_077337594.1 *Vibrio ruber*

KKFLTILTVTAAALSATVLT SNETGIHYYSFWTDAPGTVSMTLGDGGN  
YSSQWHNTGNWVGGKGWNP GGRRTVNYSGTFNPSGNGYLALYGWTT  
NPLVEYYIIDNWGSYRPN GTYYGT VNTDGGTYDIYRTL RVDKPSIEGNK  
STFYQYWSVRQQKRTGGTIT TGNHFD AWASKGLNLGTFN-  
YVM MATEGYQSSGSSNITLG

WP\_077316466.1 *Vibrio gazogenes*

KKFLTILTVTAGVLSATALTSNETGTHYYSFWTDAPGTVSMTLGNGGS  
YSSQWRNTGNWVGGKGWNPGGRRSVQYSGTFSPSGNGYLALYGWTT  
NPLVEYYIIENWGSYRPNGTYYGTVNTDGGTYDIYRTLRLVDKPSIEGDR  
STFYQYWSVRQQKRTGGTITTTGNHFDAWASKGLNLGKFN-  
YMMATEGYQSSGSSNITLG

WP\_084717381.1 *Vibrio rhizosphaerae*

KKLLTILTVTAAALSATVLTSTNETGTHYYSFWTDAPGTVSMTLGNGGN  
YSSQWRNTGNWVGGKGWNPGGRRSVNYSGTFNPSGNGYLALYGWTT  
NPLIEYYIVDNWGSYRPGGTYYGTVNTDGGTYDIYRTLRLVDKPSIEGNK  
STFYQYWSVRQQKRTGGTITTTGNHFDAWASKGLNLGKFN-  
YMIMATEGYQSSGSSNIVLG

WP\_078045385.1 *Cellvibrio*

KNIFTAFIGAAALCATLSSNSTGTHYYSFWKDSGNATMTLQAGGRYTS  
QWNSGNWVGGKGWNPNGSTRVINYSYSNSQNSYLALYGWTRSPLI  
EYYVIESYGSYNPGGTDYGSFQSDGATYNVRRRCQRVNQPSIDGNQTFY  
QYFSVRNPKKISGTITFANHVNFWASKGLNLGNHN-  
YQVLATEGYQSTGSSDITVS

WP\_073319678.1 *Aestuariibacter aggregatus*

KRLAMGLSLLTCSLGVITALYENETGTHYYSFWKDSGNANFTLQPGGR  
YQSQWNSGNWVGGKGWNPGGKRTVNYSGYDSSQNSYLALYGWSQ  
NPLVEYYIIIESYGSYDPGGVDYGTTFQSDGATYKIRRCQRVQQPSIEGTQ  
TFYQYFSVRQPIKISGTITTTGNHFDAWASVGLNLGTFN-  
YMMATEGYQSSGSSDITVS

WP\_015817458.1 *Teredinibacter turnerae*

NSALAAAVLAATATVFTALTSNSTGTHYYSFWKDSGDASFTLHNGGR  
YASEWNSTNNWVGGKGWNPGGAKVVNYEGYYSNSQNSYLALYGWT  
KNPLIEYYIIIESYGSYNPGGTNYGSFQSDGATYNVRRRCQRVQQPSIEGTA  
TFYQYFSVRSPKKISGTINVGNHFNWASQGLNLGSHD-  
YMLATEGYRSTGSSDISV

## C-LPMO

### proteins from the species used in the construction of the phylogenetic tree

AAD27623.1 *Streptomyces viridosporus* (query)

HGVAMVPGSRTYLCQLDAITGTGALNPTNPACRDALNKSGSSALYNW  
FAVLDSRAAGRPGYVPDGTLCASGDRSPYDFSAYNAARADWPRTHL  
TSGATVKVQYSNWAHPGDFRVYLTKPGWSPTSPLGWNDLELIQTVT

NPPQQGSPGTNGGHYYWDLKLPSGRSGDRLIFMQWVRSQENFFSC  
DI

WP\_037928552.1 *Streptomyces toyocaensis*

HGVAMMPGSRTYLCQLDAVTGTGALDPSNPACRDALNESGATALYN  
WFAVLDSNAGGRGAGYVPDGTLCASGDRSPYDFSAYNAARADWPRT  
HLTSGATIKVQYSNWAHPGDFRVYLTCPGWSPTSQLGWDDLELIQTV  
TNPPQQGSPGTNGGHYYWNLNLPGRSGDALIFMQWVRSQENFFSC  
SDV

WP\_055629450.1 *Streptomyces hirsutus*

HGVAMMPGSRTYLCQLDATTGTGALDPTNPACRAALNQGASALYN  
WFAVLDSQAAGRPGYVPDGKLCASGDRSPYNFSAYNAARSDWPRT  
LTSGATIKAQYSNWAHPGDFRVYITKPGWSPTSQLGWNDLELIQTVT  
NPPQQGSPGTNGGHYYWNLKLPGRSGDALIFMQWVRSQENFFSC  
DV

WP\_044379538.1 *Streptomyces cyaneogriseus*

HGVAMMPGSRTYLCQLDAVSGTGALNPTNPACRDALS KSGATALYN  
WFAVLDSNAGGRGAGYVPDGKLCASGDRSPYDFSAYNAARADWPRT  
HLTSGATIKVQYSNWAHPGDFRVYVTKPGWSPTSPLGWS DLELIQTV  
TNPPQQGGAGSNGGHYYWDLKLPSGRSGDALIFMQWVRSQENFFS  
CSDI

WP\_055607049.1 *Streptomyces prasinus*

HGVAMMPGSRTYLCQLDAITGTGSLDPTNPACRAALNQGASALYNW  
FAVLDSRAAGRGQGYVPDGTLCASGDRSPYDFSAYNAARSDWPRT  
TSGATIKAQYSNWAHPGDFRVYITKPGWSPTSQLGWNDLELIQTVTD  
PPQQGSPGANGGHYYWNLKLPGRSGDAVIFMQWVRSQENFFSCSD  
V

KMS77933.1 *Streptomyces leeuwenhoekii*

HGVAMMPGSRTYLCQLDAISGTGALNPTNPACRDALS KSGSTALYNW  
FAVLDSNAGGRGAGYVPDGKLCASGDRSPYDFSAYNAARADWPRT  
TSGATIKVQYSNWAHPGDFRVYVTKPGWSPTSQLGWS DLELIQTVTN  
PPQQGGAGSNGGHYYWDLKLPSGRSGDALIFMQWVRSQENFFSC  
DI

WP\_067284436.1 *Streptomyces jeddahensis*

HGVAMMPGSRTYLCQLDAITETGALDPTNPACQDALNESGANALYNW  
YAVLDAKAGGRPGYVPDGTLCASGDRSPYDFSAYNAARADWPRT  
TSGATMRVQYSNWAHPGDFRVYLSKPGWSPTSTL GWDDLELIQTVT  
DPPQQGSPGNDGGHYYWDLTLPSGRSGDALIFIQWVRSQENFFSCSD  
V

WP\_102928211.1 *Streptomyces diastaticus*

HGVAMMPGSRTYLCQLDAKTGTGALDPTNPACQAALDQSGATALYN  
WFAVLDSNAGGRGAGYVPDGTLCASGDRSPYDFSAYNAARGDWPRT  
HLTSGATIPVQYSNWAHPGDFRVYLTCPGWSPTSELGWDDLELIQTV  
TNPPQQGSPGTDGGHYYWDLALPSGRSGDALIFMQWVRSQENFFSC  
SDV

WP\_030181860.1 *Streptomyces violaceorubidus*

HGVAMMPGSRTYLCQLDAKTGTGALDPTNPACRSALDRSGATALYN  
WFAVLDSNAGGRGAGYVPDGTLCAGDRSPYDFSAYNAARSDWPRTH  
LTSGATIPVQYSNWAHPGDFRVYLTKPGWSPTSELGWDDLELIQTVT  
NPPQQGSPGTDGGHYYWNLALPSGRSGDALIFMQWVRSDSQENFFSCS  
DV

WP\_012879227.1 *Xylanimonas cellulositytica*

HGAEVFPGSRQYLCWVDGQSASGALDPSNPACASALAVSGSGAYYNW  
FGNLDSNGAGRTEGYIPDGTICSGGDRGPYDFSANAPRTDWPTTHLTA  
GATYEFQHNNWAQHPGRFDVYVTRAGFDPTKPLGWSLELIDSVTNPP  
DTGGPGSD-NYYYWDVTLPADRTGRHIVFTHWVRSDSTENFYSCSDV

WP\_043615549.1 *Nonomuraea candida*

HGVSMFPGSRTFLCWQDGLRDNGQILPYNPACAAAVNQSGTTPLYNW  
FAVLRSDGAGRTTGFIPDGQICSGGTGGPYDFSAYNAVRNDWPLTHLTS  
GATIQRHSNWAHPGFSFKYYVTKNGWNPNGPLKWSLEQFGSVTNP  
PKSGGAGGL-NYYYWNAQLPSGKSGRHIIFTHWIRSDSNENFYSCSDV

WP\_084959626.1 *Thermoactinospora rubra*

HGVTMFPGSRTFLCWQDGLRENGQIIPYNPACAAVAQSGTTPLYNWF  
AVLRSDGGRTTGFIPDGQICSGGTGGPYDFTPYNAVRNDWPLTHLTA  
GRTIQVRHSNWAHPGSFVYITKNGWNPNAPLRWADLESIGSVANPP  
QSGGPGEL-NYYYWNLQLPSGKTGRHIIFHWRSDSQENFYSCSDV

WP\_103960203.1 *Nonomuraea solani*

HGVSMFPGSRTFLCWQDGLRDNGQIIPYNPACGAAVNQSGATPLYNWF  
AVLRSDGAGRTTGFIPDGQICSGGTGGPYDFSAYNAVRSDWPLTHLTS  
ATIQRHSNWAHPGSFNYYVTKNGWNPNGPLKWSLEPFSGSVTNPP  
KTGGAGAL-NYYYWNAATLPSGKSGRHIIFTHWIRSDSNENFYSCSDV

WP\_083929395.1 *Catelliglobosipora koreensis*

HGATMFPGSRTWLWCYQDGLRPNGAIEAYNPACAAIAQNGTTPLYNW  
FAVLRSDAAGRTVGFIPDGQLCSAGTGGPYNFSAAYNAARTDWPLTHLT  
TGANIQFRHSNWAHPGTFYLAITRQGSPTSPLAWSDLQEFASVTNPP  
ANGGPGAL-NYYYWNAQLPTGRSGRAIIRWVRSDSNENFFSCSDV

WP\_088645651.1 *Micromonospora wenchangensis*

HGTPIVPGSRTYLCWQDGLTTTGEIRPNNPACSAAVAQSGTNSLYNWF  
VLRSDAGGRTVGFIPDGKLCSGGNTGFAGYDLARTDWPLTHLTSGARL  
DFKYSNWAHPGTFYFYVTKDSWSPTRPLAWSLEPFLTVTNPPQGA  
SGTNDGHYYFSGNLPSGKSGRHIISRWVRSDSQENFFGCSDV

WP\_018216208.1 *Salinispora pacifica*

HGAAMVPGSRTFLCWRDGLSPTGEIQPYNPACSAAVDQSGANSLYNW  
FSVLRSDAAGRTVGFIPDGQLCSGGNSGFLGYDLARTDWPLTHLTAGQ  
SIEFRYSNWAHPGTFYFYITKDSWSPTRPLAWNDLEPFLTVTNPPQRG  
GPGTNDGHYYFTGTLPADKSGRHIIYSRWVRSDSPENFFGCSDV

WP\_098463482.1 *Isopterocola jiangsuensis*

HGAQMFPGRSRYFCWVDGTSAGGDISPTNPACADAVAASGKTPLYNW  
FGNLDSNGAGRTVGYVPDGRICDGGGRGPYDFEPYNAPRTDWPTTHLT

AGDTYEFRHNNWAAHPGRFDVYLTTEGFDPTAPLAWDDLELVDSVTD  
PPASGGPGDL-

NHYSWDVTLPADRTGRHVVFTHWVRSDSAENFYSCSDV

WP\_067315554.1 *Micromonospora rifamycinica*

HGTPIVPGSRTYLCWQDGLSPTGEIRPNNPACSAAVAQSGTNSLYNWFS  
VLRSDAGGRTVGFIPDGKLCSGGNTGFAGYDLARTDWPLTHLTSGARL  
DFKYSNWAHHPGTFYFYVTKDSWSPTRPLAWSLEPFLTVTNPPQRGA  
SGTNEGHIYFSGNLPSGKSGRHIIYSRWVRSQENFFGCSDV

WP\_023362433.1 *Actinoplanes friuliensis*

HGAMMAPGSRTYFCWKDGLSGNGSIVPKNPACAAAVSQSGTTPLYNW  
FAVLRSDGGGRTSGFIPDGQLCSGGTGGPYDFTGYNLARNNDWPQTHLT  
AGASMRFDYNNWAKHPGTFSLYITKDSWSPTRPLAWSLEPFSQVVP  
TSVGGPGTNDGRYSWTANLPSGKSGKHLIYSVWSRSDSQETFYGCSDV

WP\_043522496.1 *Actinoplanes utahensis*

HGAIQVPGSRTWFCYQDGRNPTGAIEPKNPACAAVAQSGVTSLYNWF  
AVLRSDGAGRVDGFIPDGQLCSGGTGGPYNFSGFNLARNNDWPTHTLTA  
GANVQFKYNNWAKHPGTFSLYITKDGYPDKPLAWSLEPFDQVTNPP  
ANGGPGTDDGHYYWNGKLPAGKTGKHLIYSVWSRSDSQETFYGCSDV

WP\_051759284.1 *Herbidospira cretacea*

HGAMMMPGSRTYLCWKDGLNSSGAIQPNNPACAAVAQSGTNSLYN  
WFATLRSDGAGRMSGFIPDGSLCSGGAVVYNFSGFDLARNDWPVTHLT  
SGANIQIRYNKWAHHPGTFRLYITKNTWSPTRPLAWSLEPFDSSSTNPP  
SVGNPGENAYYYWNANLPSGKSGRHIIYSVWQRSDSNETFYGCSDV

WP\_013131295.1 *Thermobispora bispora*

HGAMMMPGSRTYLCWKDGLTPQGNIVPNNPACAAVAQSGTNALYN  
WFAVLRSDGAGRTRGYIPDGKLCADAKVYDFSGFDLARDDWPVTHL  
TAGATIQIRYNMWAHHPGTFRLYVTKDSWDPNRPLSWDDLEPFSEVTD  
PPSVGSPGNEDAYYYWNAKLLENKSGRHIIYSIWQRSDSQETFYNCSDV

WP\_081476174.1 *Verrucosispora maris*

HGAAMTPGARTYLCWRDGLSPTGEIRPQNPACSAAVAQSGANSLYNW  
FSVLRSDAGGRTTGFIPDGQLCSGGATGFRGFDLARDDWPLTHLTAGR  
TMEFRYSNWAHHPGTFYFYVTKNSWSPNRLAWSLEPFLTVTNPPQR  
GAVGTNDGHYYFTGTLANKSGRHIIYSRWVRSQENFFGCSDV

PRY54227.1 *Glycomyces artemisiae*

HGATVFPGRQYLCYFDALGGNGALDPYNEACQSALDQVGPTPFYNW  
FGNLDSNGAGKTVGYIPDGQICDGGGRGPYDFSAFNDPGNWPKTHVTA  
GDTVQWRYNNWAHHPGRFDLYITKDGWDPSQPLAWDDLEKFQFTFN  
PASNGGPGSDDHYYYANLTLPQ-

KSGYHMFVTHWVRSNENFYACSDV

SDZ55585.1 *Asanoa ishikariensis*

HGTPMSPGSRFTLCWKDGLSQQGDIQPHNPACTAAVQQGGTNPLYNW  
FSVLRSDAAGRTVGFIQDQQLCSGGNSTFAAYNQARNNDWPLTHLTAGS  
RFDFKYSNWAHHPGTFYFYVTRDSWSPTRALAWNDLEPFLTVTNPPQN  
GGPGTNEGHIYFSGNLPSNKSGRHIIYSRWVRADSNENFFGCSDV

WP\_068755309.1 *Thermobifida cellulositytica*



HGAMTYPATRSYQCYRDGDNGGGGLAPTNPVCQNLLAENGNYPFY  
WFGNLSNAGGRHREIIPDGKLCGPHQPFSGLNAVSEHWPTTTLQAGSTI  
TFQYNAWAPHPGTWYLYVTKDGDWPNPLGWDDLEPFQVTPPIRQ  
G-GPEGPEYYWESTLPN-KSGRHIIYSIWQRSDSPEAFYDCTDV

WP\_061783670.1 *Thermobifida fusca*

HGAMTYPPTRSICYVNGEGGGGNIAPTNPACQNLLAENGNYPFY  
GNLISDAGGRHREIIPDGQLCGPHQPFSGLNLVSEHWPTTTLVAGSTITF  
QYNAWAPHPGTWYLYVTKDGDWPNPLGWDDLEPFHTVTDPPIRPG-  
GPEGPEYYWDATLPN-KSGRHIIYSIWQRSDSPEAFYDCTDV

WP\_036015456.1 *Lentzea albidocapillata*

HGSMVWPGSRTYLCYEDGAGGGGDLQPTNPACAAVAQGGKQPLWD  
WFGNLSNAAGRHRHREIIPDGNLCGPTTKYSAYNLTRADWPVTQVQANS  
TVTLRYNAWAPHPGTWEQYVTKDGFDPMTPLKWSLEPFQVTPNPL  
ANGEYAWQARLPN-KSGRHIIYSLWQRSDSPEAFYSCSDV

WP\_090096265.1 *Lentzea jiangxiensis*

HGSMVWPGSRTYLCYEDGVGGGGDLQPTNPACAAVAQGGKQPLWD  
WFGNLSNAAGRHRHREIVPDGSLCGPTTKFAAYNLPRADWPVTQVTANS  
TVTFRYNAWAPHPGTWEQYVTKDGFDPKPLKWSLEPFQVTPNPL  
ANGEYAWQARLPN-KTGRHIIYSLWQRSDSPEAFYSCSDV

AEN11025.1 *Streptomyces*

HGVAMTPGSRTYLCQLDALSGTGALNPTNPACRDALSQSGANALYNW  
FAVLDSNAGGRGAGYVPDGLCSAGDRSPYDFSAYNAARADWPRTHL  
TSGATLKVQYSNWAHPGDFRVYLTCPGWAPTSELAWDDLQLVQTVS  
NPPQGGAGTNGGHYYWDLALPSGRSGDALMFIQWVRSQSQENFFSC  
SDI

WP\_048404375.1 *Chromobacterium violaceum*

HGTMEIPINRTYSCFLEGPEAPKTPACQAAKQAGGTQAMYDWNGINQN  
PSGDNHQAVVPDGTLCGGKAEFKGFNLAREDWRRTNIVPDANGNYE  
FIYKATAPHAFKfyVTKNGWNPTQALKWSDLELFGTVGNPQQDAGKR  
YHMTLKLPPQGGKTKGHIIFNVWKRSDSEAFYSCSDV

WP\_076226074.1 *Chromobacterium pseudoviolaceum*

HGTMEIPINRTYSCFLEGPEAPKTPACQAAKQAGGTQAMYDWNGINQN  
PSGDNHQAVVPDGTLCGGKAEFKGFNLAREDWRRTNIVPDANGNYE  
FIYKATAPHAFKfyVTKNGWNPTQALKWSDLELFGTVGNPQQDAGKR  
YHMTLKLPPQGGKTKGHIIFNVWKRSDSEAFYSCSDV

WP\_071113852.1 *Chromobacterium sphagni*

HGTMEVPINRTYSCYKEGAESPKSAACQAAKQAGGVQAMYDWNGIN  
QNPPGDNHQAVVPDGTLCAGQSKFKGFNLARTDWPATNIVPNASGN  
FEFIYKAPAPHAFRFYVTKNGWNPSQPLKWSLELFGTYGNPPLDANQ  
RYHMTMKLPTGKTGRHIIYNVWKRSDSEAFYSCSDV

WP\_047244066.1 *Chromobacterium subsugae*

HGTMEVPINRTYSCFLEGPEAPKTAACQAAQVGGTQAMYDWNGINQ  
NPQGDNHQAAVVPDGTLCGGKAEFKGFNLARRDWRATSIVPDANGNY  
EFIYKATAPHAFKfyITKNGWNPDPLKWSLELFGTAGNPQQDAKR  
YHMTLKLPPQGGKTKGHIIFNVWKRSDSEAFYSCSDV

WP\_107801020.1 *Chromobacterium panama*

HGTMEVPINRTYNCFKEGAESPksAACQEARRVGGTQAMYDWNGINQ  
NPQGDNHAAVVPDGKLCAGGQDKFKGFNLGRDWPCKLVPDANGN  
YEFVYHATAPHSFKFYVTKNGWDQTKPLKWSLDLPFHTVGNPPLDAN  
KRYHMVAKLPAGKSGPHIIFNVWKRADSEEFYSCSDV

WP\_081689029.1 *Inquilinus limosus*

MPISRVIYACYQEGPETPKSEACKAAKAVGGAQAFYDWNQVRQGDAG  
GNHQAVVPDGQLCSGGGAEFRGLDLARPDWTKSSIAPTAAGDYTFVW  
KATAPHAFQYYITKNGWSPNAPLKWSLDLEAFATVGSAAQKVGdqYR  
MTVKLPQGRKGDHVIYGIWQRADSREAFYACSDV

WP\_057949360.1 *Lysobacter enzymogenes*

HGSMVHPKSRIYACKQGDAENPSDPACRAAWQVSGSAMFYDWMSINR  
ADADGRHRAVVPDGQLCSGGNPTFAGLDLARADWQAQPIAADANGRF  
AFLFKGTAPHAWTFYITRDGWNPERPLHWSLDLEPFCTLGNVPLGSDGN  
YRLDCPLPK-RSGRHVIYNTWQRSDESTAFYTCMDV

WP\_010482246.1 *Pseudomonas geniculata*

HGTMTTPISRVIYACFQGNPENPTNPACAAAKAVGGSSQAFYDWNQINQ  
ANANGNHQAVVPDGKLCSGNNPTFRGLDVNRSDWQTTPIHADANGKF  
TFVFKATAPHAWRFYVTREGWQPGSPLGWADLQEFCTLGNTPLSADG  
TYKLQCTLPQ-RTGQHVIYNTWQRSDESTAFYTCMDV

WP\_049412354.1 *Stenotrophomonas maltophilia*

HGTMTTPISRVIYACFQGNPENPTNPACAAAKAIGGSQAFYDWNQINQA  
NANGNHQAVVPDGKLCSGNNPTFRGLDVNRSDWQTTPIHADANGKFT  
FVFKATAPHAWRFYVTREGWQPGSPLGWADLQEFCTLGNTPLSADGT  
YKLQCTLPQRTGQHVIYNTWQRSDESTAFYTCMDV

WP\_053443696.1 *Stenotrophomonas maltophilia*

HGTMTTPISRVIYACFQGNPENPTNPACAAAKAIGGSQAFYDWNQINQA  
NANGNHQAVVPDGKLCSGNNPTFRGLDVNRSDWQTTPIHADANGKFT  
FVFKATAPHAWRFYVTREGWQPGSPLGWADLQEFCTLGNTPLSADGT  
YKLQCTLPQ-RTGQHVIYNTWQRSDESTAFYTCMDV

WP\_074725696.1 *Stenotrophomonas pavanii*

HGTMTTPVSRVIYACFQGNPENPTNPACAAAKAVGGSSQAFYDWNQINQ  
ANANGNHQAVVPDGKLCSGNNPTFRGLDVNRSDWPTTPIQPDANGKF  
TFVFKATAPHAWRFVVTREGWQPGSPLRWADLQEFCTLGNTPLSADGT  
YKLQCTLPQ-RSGQHVIYNTWQRSDESTAFYTCMDV

WP\_100553964.1 *Stenotrophomonas lactitubi*

HGTMSKPSSRVIYACYQGNPENPTNPACAAAKAIGGAQPFYDWSGINQ  
ANANGNHQAVVPDGQLCSGGNSKYRGLDLDRSDWSTTPIRADGNRY  
TFEFLAPAPHAWKFYVTREGWQPGSPVGWSDLQEFCTLGNVPLSEGGV  
YKLDCLPQ-RTGQHVIYNTWQRSDESTAFYTCMDV

WP\_061513394.1 *Legionella pneumophila*

HGSMEVPISRTYQCYKEGPESPKSAACKAAVQIGGTQPLYNWHVEVNQA  
AANDRHRELIADGQLCAGGRDFFKGFNLARNDWTTTVVHPDSNGRFQ  
FVYVATAPHKFKFYVTKDGYDFNTPLKWSLDLEPFCTITSVLANGRYQ  
MDCPLPANKTGKRIFYVIWQREDSPEAFYSCSDV

WP\_095984428.1 *Cystobacter fuscus*

HGSIEIPISR VYNCYKEGPETPQSAACKAAIAYGGTQAFYDWNGVRQG  
NANGQHRALIPDGKLCSAANESHKGLDLARSDWPAKRIAPNAQGRFDF  
VYHATAPHAHQFFVTRQGYNPTQPLKWSGLEPFCTVGTTPNQNNRYTL  
NCPFPTGRTGRHVIYNIWQRSDSPEAFYACVDV

WP\_071901846.1 *Cystobacter ferrugineus*

HGSIEIPISR VYNCYKEGPETPQSAACKAAIAYGGTQAFYDWNGVRQG  
NANGQHRALIPDGKLCSAANESHKGLDLARSDWPAKRIAPNAQGRFDF  
VYHATAPHAHQFFITRQGYNPSQPLKWSGLEPFCTVGTSTPLQNNRYTLN  
CPFPTGKTGRHVIYNIWQRSDSPEAFYACVDV

WP\_046713188.1 *Myxococcus fulvus*

HGSMEVPLSRVYSCFKEGPETPKSAACKAAIQSGGTQALYDWNGVRQ  
GNANGRHRELADGKLCSAANESHKGLDLARTDWPATLISPSSNRFDV  
VFHATAVHAFHLYVTKEGYNPALPLKWSGLEPFCTLTAPAPQNNRYRF  
TCPFPQGRGTGQHVIYAIWQRSDSPEAFYACTDV

WP\_074725695.1 *Stenotrophomonas pavanii*

HGTLSKPF SRVYACYQGNPENPSHPACAAAKAIGGAQPFYDWAGINQA  
EADGNHQAVVPDGLCSGGNSKYRGLDLNRSDWQTSPIRADARGRYT  
FEFKAPAHAWRFYVTREGWQPGSPLRWADLEAFCTLGNVPLSGDVY  
KLDCLPK-RSQHVIYNTWQRSDSKEAFYTCADV

WP\_088497014.1 *Stenotrophomonas maltophilia*

HGTMTTPVSRVYACFQGNPENPTNPACAAAKAIGGSQAFYDWNGINQ  
ANANGNHQAVVPDGLCSGNNPTFRGLDVNRSDWQTTPIQPDANGRF  
TFVFKATAPHAWRFFVTREGWQPGGPLRWADLQEFCTLGNTPLSADG  
TYKLQCTLPQ-RSQHVIYNTWQRSDSSTEAFYTCMDV

## Ch-LPMO

### **Monoxygenases proteins from the species used in the construction of the phylogenetic tree**

WP\_098855344.1 *Bacillus thuringiensis* (Query)

MKKNLSLQKMKKVILSGGVLLTGLLTFGFSEKASAHGYVESPASRSYLC  
KQGVNVNCGPIQYEPQSVEGIGGFQPLGPSDGQIAGAGHFPALDVQTV  
DRWKKVTLNNGGTNTFKWKL TAPHSTKEWKYYITKKGWNPKNPLTRS  
DLDLVPFYVKNDGGARP GTTVTHEANVPTDRSGYHLILAVWEIADTGN  
AFYQVIDVNLLNGLVSNFAFNNVVQTPTLF

WP\_000742280.1 *Bacillus cereus*

MKKNLSLQKMKKVILSGGVLLTGLLTFGFSEKASAHGYVESPASRSYLC  
KQGVNVNCGPIQYEPQSVEGIGGFQPLGPSDGQIAGAGHFPALDVQTV  
DRWKKVTLNNGGTNTFKWKL TAPHSTKEWKYYITKKGWNPKNPLTRS  
DLDLVPFYVKNDGGARP GTTVTHEANVPTDRSGYHLILAVWEIADTGN  
AFYQVIDVNLLNGLSSNFAFNNVVQTPTLF

WP\_097855297.1 *Bacillus toyonensis*

MKKTSLQKMKKVMLSGGILLTGLLTFGFSEKASAHGYVESPASRSYLC  
 KQGVNVCNCGPVQYEPQSVVEGIGGFPQLGPSDGQIAGAGHFALDAQSV  
 DRWKKITLNGGTNTFKWKL TAPHSTKEWKYYITKKDWNPNMPL TRSS  
 LDIVPFYVKNDGGVVRPGTTVTHEANVPTDRSGYHLILAVWEIADTGNA  
 FYQVIDVNLVNNGLNSNFAFNNAVQVPTLF

WP\_017149289.1 *Bacillus bingmayongensis*

RKSKHFQGFQKAMLSGVLFTGVLTFGFTEKASAHGYVESPASRSYLC  
 KQGVNTNCGPIQYEPQSVVEGPGSFPQLGPSDGQIAGAGHFDPDLVQTV  
 RWKKVPLSGGKNTFQWKL TAPHSTKEWKYYITKKDWDPNKPLSRSDL  
 DLVVPFYVKNDGGIRPGTTVIHEANVPTDRNGYHLILAVWEIADTGNAF  
 YQVIDVNLVNNGVTDSAHQSSYLPSSHLF

WP\_033676157.1 *Bacillus gaemokensis*

RSRRKLKNSIRYSLLCGMCMSVSLVSGFQAQKASAHGYVESPASRSYLC  
 KQGVNLCNCGPIQYEPQSVVEGPGFLFPQLGPSDGKIAGAGHFDPDLVQTV  
 DRWKKVTLGGKNTFQWKL TAPHSTKEWKYYITKKDWNPNKPLTRF  
 DLDLVPFYVKNDGGVVRPGTTVIHEANVPTDRSGYHLILAVWEIADTGN  
 AFYQVIDVNLVNNGLEGKMEFNNSNIHFPLRF

WP\_084157953.1 *Bacillus manliponensis*

RKGNRLKDSIRISLLCGACMIGLSTFSFAGKASAHGYVESPASRAYLCK  
 QGVNVCNGLVQYEPQSIEARGSFPQLGPSDGQIAGGGIFPELDAQSIDR  
 WEKVTLNGGKNTFQWKL TAPHSTREWKYYITKKDWDPNKPLTRSQLE  
 TIPFYQKNDGGVVRPGNTVVHEANVPTDRSGYHLILAVWEIADTPNAFY  
 QVIDVNLVNNGLNPVISSLHTQPSVFPY

WP\_089967265.1 *Lihuaxuella thermophila*

MAQRSF--

WCKWMVSCGMMLLVGATLVFAESASAHGYIESPASRAYLCKQGLNK  
 DCGQIRWEPQSVVEGPGSFPQSGPPDGQLAGTSRFPELNVQTADRWHKV  
 NIRGGNNTFQWYLTAPHATKEWKYYITRKGWNPDKPLARADLELFCH  
 YYDGGKRPPNTVTHTCNVPTDRSGYHVILGVWEIADTGNAFYQAMDV  
 NLVNGVSNVQVPSAHHKSSIGNY

WP\_006676405.1 *Paenibacillus dendritiformis*

IGSTLLSKVSPLFTAFLGLIVLGLASAIFADSASAHGYIESPASRAYQCKLG  
 MNTNCGQVQYEPQSVVEAKGNFPEGGPADGHIAGGGIFAPLDEQSADR  
 WNKVKMQGGTNTFQWHL TAPHATSEWKYYITKKDWDPNKPLTRADL  
 DPVPFCTIQDGGKPPATVTHECSVPTDRSGYHLILGVWEIADTGNAFY  
 QVIDVDLVNDGSGIELPSAPAQGDQVKH

WP\_087435284.1 *Paenibacillus apiarius*

IWNHLVSKVSPLFAAFGLTALGLATLIFADSASAHGYIESPTSRAVLCKQ  
 GLNKDCGQVQYEPQSVVEGKGSFPQGGPADGQIAGGGVFAELNEQTAE  
 RWHKVTLQGGKNTFKWYLTAPHATSEWKYYITKKDWDPNKPLTRAD  
 LDPVPFCSIDDGGKRPPNVTHECTVPTDRSGYHLILGVWEIADTGNAF  
 YQVIDVNLNMGGTGEQAPAAPGDGDQVKH

WP\_087445137.1 *Paenibacillus thiaminolyticus*

IGSTLLSKVSPFLTAFLGLIVLGLASAI FADSASAHGYIESPASRAYQCKLG  
MNTNCGQVQYEPQSVEAKGNFPVSGPADGHIAGGGIFAPLDEQSADR  
WNKVKMQGGTNTFQWHLTAPHATSEWKYYITKKDWDPNKPLTRADL  
DPVPFCTIQDGGKKPPATVTHECSVPTDRSGYHLILGVWEIADTGNAFY  
QVIDVDLVNDGSEIELPAAPGQGDVKH

WP\_036222403.1 *Lysinibacillus sphaericus*

MNTKFTKLSKKGLSAALLAAGIIGISTAPNAYAHGFVEKSPASRAALCTQ  
ALNLMCGSIMYEPQSLEAPKGFPGSPMDGKIASAGFGILDQQTDR  
WFKNTITGGPNTFTWKYTAPHLTSKWHYYITKRNWNPNKPLTRADLEP  
IGTVAHNGSAASTNLTHTINVPTDRSGYHVILAVWDVADTSNAFYNVI  
DVNLVNNDGNVDTEAPTQPGDKVEY

WP\_082332692.1 *Lysinibacillus contaminans*

MKLHIFNSKSLSVIFGALLMLVLTFFSSTASAHGFVSKPESRGLLCKTG  
ANINCGGVQYEPQSLEAPGNFPIGGPADGQIAGANTFPKLDEQSKYRWT  
KVPMKSGANTFEWTLTAAHATAKWDYYLTKQDWNPDQPLKRADLEL  
FCSINDGGKKPPFNVKHNCEVPERSGYQVILAVWSIADTPNAFYNVIDA  
NFDGTTIPPIDPGPIDPGDKVKY

WP\_036094696.1 *Listeria newyorkensis*

MKKFLGKSVLFFVAFALLFATFAPGASAHGYISKPESRAYLAKLGINQN  
AGAIQWEPQSVEATGNFPLGGPSDGTIAGGGKFPMDAQTDRWHHID  
LLGGQNNFTWTLTALHRTKEYKYYITKKGWNPNSLLTRGDLELLTTID  
AHNEVPSTTVNHQVPLPTDRNGYVVVLGVWEIADTGNAFYQAVDVNL  
INNGTMTLK

WP\_070239340.1 *Listeria monocytogenes*

MKKITKIGMFFAVFMLAVVLFETTASAHGYISKPASRVYLANKGINVG  
VGSAQYEPQSVEAPKGFASGPADGSIAGGGKYSLLDAQTANRWAKV  
DIESGPLTVEWTLTAPHRTSSWQYFITKKGWDPNKPLTRASLEPLTTIEA  
DGSVPNALTKQEINIPDDRSYVILGVWNIADTGNAFYQVIDANIINSS  
VAPAVDNEAPTGDKVIY

WP\_010772090.1 *Enterococcus caccae*

MKKKLLGLALMSTIILGGGLLSAEEASAHGYVEKPAARGYQGLDKNT  
KYGMVITNPQSLEFDKGFPQAGPADGQIASGGQITDMDSTGLNRWTKQ  
DINTGVNTFTWHYTAPHSTTKWHYYMTKVGWNPDKPLSRADFDLGE  
VKHDGSAASNKSHQITVPENRSGYHVILAVWDVADTTNAFYNVIDV  
NVKGGGEITPPVEETPAGDTVTF

WP\_069664391.1 *Enterococcus termitis*

MMKKLVGLTMMATICLAGAGVLFSDKANAHGYVESPVSRGYQGALD  
KNTKYGNVITNPQSLEAPKGFPEKGPADGRIASGGQIGDLSTGVDRW  
TKQEAKTGVNTFTWHYTAPHATSKWHYYITKNGWNPEKPLARENMEL  
IGEIKHDGSTASNKSHQVTIPSDHTGYHVVLAVWDVADTSNAFYNVI  
DLNLKSDGGTTPPVEETPAGEKVY

WP\_034688872.1 *Enterococcus mundtii*

MKKSTLIGLGFILAGIGSTLTSVEVA AHGYVSEPASRGYQGSLDKNTKY  
GAVINEPQSLEAPKGFPAAGPEDGQIASGADFLDQQTASLWTKQQLT  
AGANDFTWTFTANHSTTKWHYYMTKAGWDQNDVLTRDDLEFIGEVG  
NNGQLASTNPHTSINIPNDRLGYHVILAVWDVADTKNGFYNVIDVDVK  
GETVLADLQK

WP\_076633771.1 *Lactobacillus plantarum*

VKTKKNNVFRYLLVIIGMMVALLGFEAQASAHGFVTNPGGRAYLGST  
GLNTNIGSVMYEPQSIEAPKNTIDGKIASAGKFSQLDEQTANRWYKTPV  
KAGNLDVTWRLTARHKTSTWDYYITKPGWNPAPLKFSDFKKIASYN  
DNGAMPSEFMTHQVNIPSNEKGYQVLLSVWNIADTGNAFYQVSDINVQ

WP\_021731441.1 *Lactobacillus*

LSTKKNRILRYLFVIVGMMIAFLGSAHVQASAHGFVTNPGGRAYLGSTGL  
NTNIGSVMYEPQSIEAPKNTIFIDGKIASAGNFAQLDEQNANRWYKTPVR  
AGKLSVTWQLTARHKTSTWDYYLTKPGWNPAPLKFSDFKKIASYND  
NGAMPNEFVTHQVNIPADEKGYQILLSVWNIADTGNAFYQVSDLNVQ

WP\_055538846.1 *Streptomyces neyagawaensis*

PRTFTRKRAKWYAAGVGLATMGALVFSSGASGHGYTDLPVSRQKLCQ  
NGTVTNCGDIQWEPQSVEGPKGFPGSGPADGQICSAGRFGQLNSPTGG  
AWPTTRVTGGQNTFRWQFTAMHATTDKYYVTKPGWNQNHALARSD  
LNLTPFFTVPYNGQRPPSTLSHTGRLPSGLSGHHVILAVWTIADTGNAF  
YACSDVTF

WP\_055712380.1 *Streptomyces torulosus*

PRTFTRKRAKWYAAGVGLATMGALVLSSGASGHGYTDLPVSRQKLCQ  
NGTVTNCGDIQWEPQSVEGPKGFPGSGPADGQICSAGRFGQLNSPTGG  
AWPTTRVTGGQNTFRWQFTAMHATTAFTYYVTKPGWNQNHALARSD  
LNLTPFFTVPYNGQRPPSTLSHTGRLPSGLSGHHVILAVWTIADTGNAF  
YACSDVTF

WP\_005486591.1 *Streptomyces bottropensis*

MRHHARNRTKWYAAAVGLATTGAFVLSSGATGHGYTDLPVSRQKLC  
QNGSVTNCGDIQWEPQSVEGPKGFPGSGPADGRLCSGGRFNQLDASTG  
GAWPTTRVTGGQNTFRWQFTAMHATSDFKYYVTRAGWNQNHALTRS  
DLNLTPFFTVPYNGQRPPSTLSHTGRLPSGLSGHHVILAVWTIADTANA  
FYACSDVTF

WP\_033531196.1 *Streptomyces galbus*

MRKHTRSRTKWYAAAVGLATTGALVLSSGATGHGYTDLPVSRQKLCQ  
NGTVTNCGDIQWEPQSVEGPKGFPGSGPADGQICSGGRFNQLNASTGG  
AWPTTRVTGGQNTFRWQFTAMHATTDKYYVTKAGWNQNHALARSD  
LNLTPFFTVPYNGQRPPATLSHTGRLPSGLSGHHVIVAVWTIADTTNAF  
YACSDVTF--

WP\_046731057.1 *Streptomyces humi*

MRKRTKVSAAVVLGVATAGAFALSTGASGHGYTDLPISRQKLCANGTV  
TNCGDIQYEPQSVEGPKGFASGPADGQLCNGGRFAQLSSPTGGAWPT  
TRVTGGQNTFRWQFTAMHATTDKYYVTKQGWQNHALARSDLNTT  
PFLTPYNGQRPPATLSHSGTLPSGLSGHHVILAVWTIADTGNAFYACS  
DVTF

WP\_093654234.1 *Streptomyces wuyuanensis*

MRKRIGAAAMVGLAVAGTLLATGSASSHGTYDSPISRQKLCANGTVGN  
CGEIQWEPQSVGPKGFPGAGPADGKLCAGGRFAQLDDPRGGAWPTT  
RVSSGQNTFRWQFTAMHATTDKYYITRNGWNPSQPLTRAALDPQPFL  
TIPYNGQRPPGTLSSHGTLTLP-SKSGRHLILAVWTIADTPNAFYACSDVQF

WP\_026416933.1 *Actinomadura oligospora*

PGTRTFTPRKTTLLLA AVAGLGLPLLSAAPALAHGYTTSPPSRALLCKQ  
GVVRNCGPIQWEPQSTEGPKGFPSAGPADGTLCAAGRWAPLDDPRGG  
AWPARSLTSGASSFTWTLTAAHATTSEFRYFVTRDGWNPAQPLTRAQLD  
PTPFLQVDYGGRIPPYSVTHTGTLPV-  
KHGRHMILAVWTIADTANAFYQCSVDVDFG

WP\_017615731.1 *Nocardiosis salina*

MQNRVLRSSAAVAGSTALIFALMPAGTASAHGYVSDPPSRQAQCAAG  
VVECGPIQWEPQSVGPGSLMCSGGAFFSELDDDSYGWDVTPVGTTSL  
EWTITAAHSTAWEYFIDGDLVDSFDEGGAQPPSNFTHDVLDSGYSGE  
QTILARWNVADTDNSFYACIDVNVGAL

WP\_039991854.1 *Serratia odorifera*

MNATSRTLLSVGLLGAAMFGASHQASAHGYVESPASRSYQCKLQLNT  
QCGSVQYEPQSVGLKGFQSGPADGHASADTFFELDQQTPTRWKLNK  
NLHSGPNSFTWNLTA RHSTTSWRYFITRQGDASQPLTRAAFDLTPFC  
QFNDGGAIPAAKVTHQCNIPADRTGSHVILAVWDVADTGNAFYQAIDV  
NLSK

WP\_044552811.1 *Serratia liquefaciens*

MNNTSRTLMSLGLLSAALFGVSQAAA AHGYVETPASRAYQCKLQLNT  
QCGSVQYEPQSVGLKGFQAGPADGHASADTFFELDQQTPTRWNKI  
NLHTGANSFTWRLTA RHSTTSWRYFITKPNWDASQPLTRASFDLTPFCQ  
QNDGGAIPAAQVTHQCNIPADRSVSHVILAVWDVADTTNAFYQAIDVN  
LTK

WP\_054307289.1 *Serratia rubidaea*

MNTMTRTLMTLGLLSAATLGVSH TASAHGYVESPASRAYQCKQQLNT  
QCGSVQYEPQSVGLKGFQAGPPDGHIASADTFFELDQQTPTRWKLNK  
NLHTGENTFTWNLTA RHSTTSWRYFITKPGWDASQPLSRASFDLTPFCQ  
YDDGGAIPAAKVSHKCTIPADRSVSHVILAVWDVADTGNAFYQAIDVN  
LSN

WP\_085118064.1 *Serratia proteamaculans*

MNKTSRTLMSLGLLSAALFGVSQAAA AHGYVETPASRAYQCKLQLNT  
QCGSVQYEPQSVGPKDFPQAGPADGHASADTFFELDQQTPTRWNKI  
NLHTGPNSTWTLTA RHSTTSWRYFITRPNWDASQPLTRASFDLTPFCQ  
QNDGGATPAAQVTHQCNIPADRSVSHVILAVWDVADTTNAFYQAIDV  
NLSK

WP\_050539174.1 *Yersinia mollaretii*

MKYIRANILILTGTTLSSYFSSLAHAHGYIQSPPSRAYLCYQGINHYCG  
AVQYEPQSVGKYKNFPYSGPEDGRIASGGPFSA LDAQTPTRWQKTNVH

SGTMNLQWQLTATHSTTHWRYYLTKQGWNSSQPLTRASFDLVPFCQY  
NDNGRVPNTRVVHQCSLPLDRSGYHVILAAWDIADTNHAFYQVVDISF  
PH

WP\_051714045.1 *Shewanella*

VPKFAIPKLTQLSLVALALTAGSSLLSQTASAHGYVISPESRSYACKTGS  
NVNCGAIQWEPQSVEGSPGFESGPADGKIASAAAFSPLDEQSPSRWSK  
RDIKAGWNDFSQFTANHVTRNWRYYLTRQGWQDQNALSRASFDLA  
PFCVIDGGMVQPPKLVTHNCYVPEDRTGYHVILAVWEVGDTTNSFYNA  
IDVNLSSGAVVPGEWTDIGCKPWPY

WP\_099457584.1 *Shewanella xiamenensis*

VPKFAIPKLTQLSLVALALTAGSSLLSQTASAHGYVISPESRSYACKTGS  
NVNCDAIQWEPQSVEGSPGFESGPADGKIASAAAFSPLDEQSPSRWSK  
RDIKAGWNDFSQFTANHVTRNWRYYLTRQGWQDQNALSRASFDLA  
PFCVIDGGMVQPPKLVTHNCYVPEDRTGYHVILAVWEVGDTTNSFYNA  
IDVNLSSGA-VVPGEWTDIGCKPWPY

WP\_009837614.1 *Pseudoalteromonas tunicata*

MKKNLKLFLAMAPLATLVSLPFAQTAVAAGHYISKPESRGYLCRLTQNT  
NCGNVVYEPQSLEGPDRFPESGPADGHASAGAFSQLNAQTISRWTKRP  
IKAGPNEFTWFTANHSTRDWRYFITKTTWDPNSPLTRDQFEAVPFCEY  
SGHYKQPPRQVTHLCNVPADRNGYHIVLGVWDVGDGTMSFYNVVDL  
MIDNGDTSNVYWQDVGCKPWPY

WP\_082916329.1 *Pseudoalteromonas neustonica*

MNHLHKTLLAMSPALAMLLPVSNTASAHGYISKPESRGYLCRLRENA  
NCGNVVYEPQSLEGLDRFPESGPVDGHASAGGFGQLDSQSINRWTKR  
HIKAGPNEFSWTLTAAHSSRDWRYFITKKSWNPNPNSPLTRDQFEAVPFCE  
YQSYNKQPPRQLTHLCNVPSDRSGYHIVLGVWDVADTPMSFYNVVDV  
MIDNGDTSNVSWQDVGCKPWPY

WP\_072034004.1 *Rahnella aquatilis*

MKKYLMTPVLSLIFSGSLMLGQEASAHGYVSSPASRAYECNLQNNKNC  
GPVQYEPQSIIEGPNFPIGGPPDNRIPSGGQYHELDAQTGERWVKNSIKS  
GPITFTWTLTAQHSTKSWKYMTKPGWDINKPLTRDSFNLTPFCEFYD  
DGAVPPPVVNHSCNFPNGNIGYNVILAVWNIQDTSYAFYQAIDVDITK

WP\_042289422.1 *Citrobacter*

MKLSKIALAVATLTVASSALAHGYIESPASRAYMCKLQNVDCGSVQY  
EPQSVEKTSGFPTGAPPDGLASAGQYSQLDRQSLNAWTKSPMTAGPH  
QFVWHHTAPHKTTNWRYYITKQNWDPNKPLTRDQFDLTPFCTINGNG  
QAPAVTQSMNCNVP-ERTGYQVIYGVWEIADTTNSFYQAIDVDFGNSG-  
NVTPEDETPGVCKPFY

WP\_077227974.1 *Leclercia adecarboxylata*

MKLSKIALALATLTVASSALAHGYVESPASRAYMCKLQNVDCGTVQY  
EPQSVERTSGFPTGAPPDGLASAGQYSQLDRQSLNAWTKTPITAGKNT  
FTWYHTAPHKTVNWRWYITKQDWNPNKPLTRDQFESTPFCTVNGNGQ



APSPRQEMSCNVP-QRTGYQVIYAVWEIADTTNSFYQAIDVDFGNGG-  
NVTPDETPAVCKKAPY

WP\_045353104.1 *Enterobacter cloacae* complex

MKLSKIALTVATLTVASSALAHGYIESPASRAYMCKLQONIDCGSVQY  
EPQSVEKTSGFPTGAPPDGQLASAGNYSQLDKQSLNTWTKNPMTAGPH  
DFVWHHTAPHKTTNWRYYITKQNWDPNKPLTRDQFELTPFCTINGNG  
QAPAMTKSMTCNVP-ERTGYQVIYGVWEIADTSNSFYQAIDVDFGNGG-  
NVTPDETPAICKPFY

WP\_059288204.1 *Enterobacter hormaechei*

MKLSKIALAVTTLTVASSALAHGYIESPASRAYMCKLQONIDCGSVQY  
EPQSVEKTSGFPTGAPPDGQLASAGSYSQLDKQSLNAWTKNPMTAGPR  
EFVWHHTAPHKTTNWRYYITKQNWDPNKPLTRDQFELTPFCTINGNGQ  
APAMTKSMTCNVP-ERTGYQVIYGVWEIADTANSFYQAIDVDFGNGG-  
NVTPDDTPAVCRPVF

WP\_053064552.1 *Klebsiella oxytoca*

MQLKKLSIYTAALLFTSSALAHGYVAFPPSRA YQCNTGKNSDCGSVQW  
EPQSVEQASGFPEGAPPDGQLASAGNFSQLDSQSPTRWAKSAIKSGENN  
FIWHHSAPHKTTNWRYYITKQNWQNKPLTRSDFESKPFQIDGNGMT  
PAIEVTHSCNVP-  
ERTGYQVIYAVWEIADTANSFYQAIDVDFGGTGDDAENGLWTTCRPF  
PY

WP\_064352001.1 *Klebsiella*

MQLKKLSIYTAALLFTSSALAHGYVAFPPSRA YQCNTGKNSDCGSVQW  
EPQSVEQTSGFPEGAPPDGQLASAGNFSQLDSQSPTRWAKSAIKSGENN  
FIWHHSAPHRRTNWRYYITKQNWQNKPLTRSDFESKPFQIDGNGMT  
PAIEVTHSCNVP-  
ERTGYQVIYAVWEIADTANSFYQAIDVDFGGTGDDAENGLWTTCRPF  
PY

WP\_084204703.1 *Aeromonas popoffii*

MAAKIQLNHIATALALLASGGVLAHGYISQPESRNYLCKTGGSQCGA  
VQWEPQSVEGSPGFQSGPQDQIASAGN WSELNAQTSRWARREVQ  
AGPFAISWTFANHVTRNWRYYLTKQDWNPNQSLTRA AFDLTPFCV  
DGNMVQPPKQVTHRCTLPERTGYQLILGVWEVGDTSNSFYNLIDANFK  
GGTQPPLSWSQGGCRPFPS

WP\_079516857.1 *Kosakonia oryzae*

MELLMKLSKVFLAVTTLTCLMAGGALAHGYVTEPASRAALCTANQNKD  
CGAPQYEPQSVEGPDGFPAAGPADGHLASAGSMVNL DQQSASRWTKH  
PMKAGKNSFTWKFTA AHKTGSWKYYITKANWNP NQPLTRNSFEAQP  
CEVTGNGAIANTNPKHECDVP-  
ERDGYQVIMAAWDVSDTGATFYNVIDVDFGGNNPAPAPGDEEENCQK  
VSY

WP\_062702299.1 *Chryseobacterium indologenes*

MINRKFFFPVLLIMALLVPSFNLSAHGYVVSPASRGYQGSLDKATLYGT  
VINEPGSLEALKGFALGPADGKIASGSGNTLLDIQTADRWKKTNITAG  
VNTFIWKYLAYHATAKWHYYMTKPGWNPKNPLTRQDLELIGEVTHNG  
TPPQDNVPHHITVPANRTGYHVILAVWDVADTGNAFYNVIDVNVTSGT  
GVSTPPAVPTGGTRVY

WP\_084694528.1 *Chryseobacterium vrystaatense*

MIKLRIIFSALVLCCTLIFSSHLSAHGYVMSPASRGYQGSLDKTSLYGSV  
INEPGSLEAKKGFALGPADGMIASGSGNTVLDLQTADRWKKTNITTG  
VNTFIWKYLAYHATAKWHYYMTKPGWNPQNPLSRQSLELIGEVHNG  
TPPQDNTPHHITIPANRQGYHILAVWDVADTANAFYNVIDVNVQSTVT  
PTTPAVPTGLGKTVFY

WP\_090024402.1 *Chryseobacterium oleae*

MIKLRIFFSALLCILTFSSKLSAHGYVMSPASRGYQGSLDKATIYGSVIN  
EPGSLEAKKGFAPFGPADGMIASGSGNTILDIQTADRWKKTNVTTGVN  
TFIWKYLAYHATAKWHYYMTKPGWNPQNPLSRQNLELIGEVHNGTTP  
QDNTPHHITIPANRQGYHVILAVWDVADTANAFYNVIDVNVQSTVTPT  
QPATPTGLGKTVFH

WP\_082798703.1 *Chryseobacterium cucumeris*

MKTSKFFFALLMLAMLVPSLHLSAHGYVLSPASRGYQGSLDKAAIYG  
SVINEPGSLEAPKGFPAAGPADGKIASGSGDTLLDIQTADRWKKTNISTG  
VNAFIWKYSAYHATAKWHYYMTKQGWNPQNPLSRQDLELI--  
GTMHNGTTPQDNVSHQITVPANRTGYHILAVWDVADTTNAFYNVID  
VNVTSGTGVSAPATPTGLGKTVFH

WP\_089695525.1 *Chryseobacterium culicis*

MMTRKFFFQVFLMMSILISLIHLSAHGYVVSPASRGYQGSLDKASIYGS  
VINEPGSLEAPKGFASGPADGKIASGSGDTLLDIQTADRWKKTNITTGI  
NSFIWKYLAYHATAKWHYYMTKQGWDPNKPITRQDLELGTIAHNGTP  
PQDNVSHQITVPANRTGYHILAVWDVADTTNAFYNVIDVNVTSGTGV  
AAPAIPPTGLGKTVFH

WP\_083997416.1 *Chryseobacterium angstadtii*

SINRSYKKHLKIMIKRILFSLFLMLLFSSHLFAHGYVLSPASRGYQGSL  
DKATLYGSVINEPGSLEAKKGFAPFGPADGRIASGSGNTVLDLQTADR  
WKKTNITAGVNTFIWKYSAYHATAKWHYYMTKPGWDPNQPLKRQDL  
ELIGEIVHNGTTPQDNVPHQITVPNNRSGYHILAVWDIADTVNAFYNVI  
DVNVQTTGGPITAPATPTGLGKTVFH

## APPENDIX II

### ENDO 1,4 BETA Xln A

P18429 *Bacillus subtilis* (Query)

KNFLVGLSAALMSISLFSATASAASTDYWQNWTDGGGIVNAVNGSGG  
 NYSVNWSNTGNFVVGKGWTTGSPERTINYNAGVWAPNGNGYLTLYG  
 WTRSPLEIYYVVDWSWGTYRPTGTYKGTVKSDGGTYDIYTTTRYNAPSI  
 DGDRTTFTQYWSVRQSKRPTGSNATITFSNHVNAWKSHGMNLGSNWA  
 YQVMATEGYQSSGSSNVTW

XYL NODE 45 *ancestral enzyme*

KKLLAVLLAAAMSLSMFAVTASAAGTDYWQNWTDGGGTVNAVNGS  
 GGNYSVNWSNTGNFVVGKGWTTGSPNRVINYNAGVFAPSGNGYLTLY  
 GWTRNPLIEIYYVVDWSWGTYRPTGTYKGTVNSDGGTYDIYTTTRYNAPS  
 IDGDTQFTQYWSVRQSKRPTGSNATITFSNHVNAWASHGMNLGSNW  
 SYQVLATEGYQSSGSSNVTW

### C-LPMO

AAD27623.1 *Streptomyces viridosporus* (query)

HGVAMVPGSRTYLCQLDAITGTGALNPTNPACRDALNKSGSSALYNW  
 FAVLDSRAAGRPGYVPDGTLCAGDRSPYDFSAYNAARADWPRTHL  
 TSGATVKVQYSNWAHPGDFRVYLTKPGWSPTSPLGWNDLELIQTVT  
 NPPQQGSPGTNGGHYYWDLKLPSSGRSGDRLIFMQWVRSQENFFSCS  
 DI

LPMO NODE 50 *ancestral enzyme*

HGAMVFPGSRTYLCYQDGVGGGGALQPTNPACAAVAQGGTQPLYD  
 WFGVLRNSAAGRHRREIIPDGQLCSGGTRGPYDFSAYNLARTDWPTTQL  
 TAGATIQFRYNNWAPHPGTWYLYVTKDGWDPTRPLKWSDEPFDTVT  
 NPPLSNGPGTDDGHYYWDATLPNGKSGRHIIYSIWQRSDSPEAFYSCSD  
 V

**Ch-LPMO**

WP\_098855344.1 *Bacillus thuringiensis* (Query)

MKKNSLQKMKKVILSGGVLLTGLLTFGFSEKASAHGYVESPASRSYLC  
KQGVNVNCGPIQYEPQSVEGIGGFPQLGPSDGGIAGAGHFPALDVQTV  
DRWKKVTLNGGTNTFKWKLTAHSTKEWKYYITKKGWNPKNPLTRS  
DLDLVPFYVKNDGGARPGTTVTHEANVPTDRSGYHLILAVWEIADTGN  
AFYQVIDVNLLNGLVSNFAFNNVVQTPTLF

LPMO NODE 53 *ancestral enzyme*

VMKKMLMKSKKISIAVALLMAGLLTLLFASSASAHGYVSSPASRAYLC  
SLGKNTNCGSVQYEPQSVEAPKGFPAAGPADGQIASGGKFSQLDEQTA  
NRWTKTPIKAGANTFTWHFTAPHATTKWHYYITKQGWNPNKPLTRAD  
LELIPFCEIDDNGATPSTNVTHQVNVPSDRSGYHVILAVWDIADTGNAF  
YQVIDVNVGGGGATTAPANPTATGDKVTY

---

# List of Abbreviations

---

AcCNC: Nanocrystals prepared by sulfuric acid treatment

AFM: Atomic force microscopy

Anc C-LPMO: Ancestral cellulose lytic polysaccharide monoxygenase

Anc Ch-LPMO: Ancestral chitin lytic polysaccharide monoxygenase

Anc EG: Ancestral endoglucanase

Anc EG+CBM: Ancestral endoglucanase with carbohydrate binding module attached

Anc LPMO: Ancestral lytic polysaccharide monoxygenase

ANC XLN: Ancestral xylanase

*B. subtilis*: *Bacillus subtilis*

BC: Bacterial cellulose

BKP: bleached Kraft pulp

Bt: *Bacillus thuriangiensis*

CBH: Exoglucanase

CBM: Carbohydrate-Binding Module

CFCh: Chitin nanofibers

CI%: Crystallinity index

CNC: Cellulose nanocrystals

CNCh: Chitin nanocrystals

CNF: Cellulose nanofibers

CP/MAS  $^{13}\text{C}$  NMR: Cross-polarization magic angle spinning  $^{13}\text{C}$   
Nuclear Magnetic Resonance

DNA: Deoxyribonucleic acid

DNS: 3,5-dinitrosalicylic acid

DTG: Derivative of thermogravimetric curves

*E. coli*: *Escherichia coli*

EG: Endoglucanase

En CNCh: Enzymatic produces nanochitin

EnCNC: Enzymatic produced nanocrystals

FTIR: Fourier-transform infrared spectroscopy

IPTG: Isopropyl  $\beta$ -D-1-thiogalactopyranoside

IR: infrared

LPMO: Lytic polysaccharides monooxygenases

MW: molecular weight

OD: Optical density

Q: Query

*S. viridosporus*: *Streptomyces viridosporus*

TEA: Triethylamine

TEMPO: 2,2,6,6-tetramethylpiperidine-1-oxyl

TGA: Thermogravimetric analysis

UBKP: Unbleached Kraft pulp

XLN: xylanase

XRD: X-ray diffraction.





---

# Acknowledgements

---

I would like to finish this thesis mentioning all the people who have made it possible.

First of all, thank you Prof. Txema Pitarke for giving me the opportunity to accomplish my master and PhD thesis in nanoGUNE, developing my PhD in such a great place would not have been possible without your support.

I am especially grateful to my supervisor Raúl Pérez Jiménez for giving me the chance to join nanobiomechanics group and learn cutting edge science. Thank you for your support, confidence, advices and your sense of humor. Thanks also to my co-director David de Sancho, without your collaboration I would not have finished my thesis. Thank you.

My thanks to all the members (former and current) of nanobiomechanics group. Thank you Aitor for showing me ASR and Marie Fertin for performing my first experiments with me. I would like to specially thank Alvaro and Jorg for their unconditional support from the beginning, nunca olvidaré aquellas tardes que terminaban con una caña en mano. My most special thanks to Leire, eskerrikasko emandako guztiagatik. But, my hurt is with Borja and Antonio; Borja, contigo he aprendido lo más bonito de la ciencia, no ponerle límites a la imaginación y el trabajo en equipo, sabes que has sido mi mayor pilar, y puedo decir con orgullo que no solo en el trabajo, si no en la vida también. Gracias a ti Antonio, tu luz me ha iluminado en muchas ocasiones. Gracias a los dos, por tanto.

---

No quiero olvidarme de las maravillosas personas que nanogune me ha dado. Nestor y Javi, por los que empezamos y terminaremos juntos! Nos queda mucho por recorrer. Milesker Andoni, beti prest, laguntzeko edo parrandarako. Teresa, siempre con una sonrisa y buenos consejos. Pero especialmente gracias a ti Sarai; Milesker txiki, nere aizpa bezela izateagatik, zure adiskidetasuna ezinbestekoa izan da neretzako.

Un especial agradecimiento a mis compañeros de Madrid: Berni, Xabi y Patri.vosotros sois el claro ejemplo de como se puede ser competitivo y buena persona al mismo tiempo.

Nanogunetik kanpo dauden pertsona gertukoenak ere oso presente ditut. Maria, zure eskua eman zenidan eta zientziarekiko grina erakutsi zenidalako, ez iezadazu inoiz askatu. Milesker Janire, Helena, Martin eta Mikel izan ginelako, garelako eta izango garelako. Eskerrikasko nere lagunei, zuen terapia orduak ez dute preziorik! Milesker Eneko, egunik zatarrena alaitzeko dezun abilezeiagatik.

Azkenik, nere familia eskertzea gustatuko litzaidake. Aita eta Ama, eman didazuen guztiagatik, zuek gabe hau ez zen posible izango. Eskerrikasko Amaia, euki daitekeen aizpa hoberena zeralako. Milesker Marta, Luis eta Maier, neri hegoak emateagatik. Baita zuei ere Belen eta Lulu, milesker beti-beti hor zaudetelako. Eta milesker zuri Itzal, tesia iteko zein bizitzeko euki daitekeen bidelagunik onena zea, milesker nere bizitza maitasunez betetzeagatik.

Amaia, Ana, Itzal eta Iñigori. Izateagatik..

